INFORMATION TO USERS

This manuscript has been reproduced from the microfilm master. UMI films the text directly from the original or copy submitted. Thus, some thesis and dissertation copies are in typewriter face, while others may be from any type of computer printer.

The quality of this reproduction is dependent upon the quality of the copy submitted. Broken or indistinct print, colored or poor quality illustrations and photographs, print bleedthrough, substandard margins, and improper alignment can adversely affect reproduction.

In the unlikely event that the author did not send UMI a complete manuscript and there are missing pages, these will be noted. Also, if unauthorized copyright material had to be removed, a note will indicate the deletion.

Oversize materials (e.g., maps, drawings, charts) are reproduced by sectioning the original, beginning at the upper left-hand corner and continuing from left to right in equal sections with small overlaps. Each original is also photographed in one exposure and is included in reduced form at the back of the book.

Photographs included in the original manuscript have been reproduced xerographically in this copy. Higher quality 6" x 9" black and white photographic prints are available for any photographs or illustrations appearing in this copy for an additional charge. Contact UMI directly to order.

UMI

A Bell & Howell Information Company
300 North Zeeb Road, Ann Arbor MI 48106-1346 USA
313/761-4700 800/521-0600

Glutamate Receptor Plasticity in the Hippocampus: Implications for Age-Related Memory and Learning Deficits

by

Adam H. Gazzaley

A dissertation submitted to the Graduate Faculty in Biomedical Sciences in partial fulfillment of the requirements for the degree of Doctor of Philosophy, The City University of New York

1997

This manuscript has been read and accepted by the Graduate Faculty in Biomedical Sciences in satisfaction of the dissertation requirement for the degree of Doctor of Philosophy.

Date 11/12/96

James L. Roberts, Ph. D.
Examining Committee Chair

Date 11/12/96

Terry A. Krulwich, Ph.D.
Executive Officer

John H. Morrison, Ph.D.

George W. Huntley, Ph. D.

David R. Colman, Ph. D.

R. Suzanne Zukin, Ph. D.

Supervisory Committee

The City University of New York

Abstract

Glutamate Receptor Plasticity in the Hippocampus: Implications for Age-Related Memory and Learning Deficits

by

Adam H. Gazzaley

Advisor: John H. Morrison, PhD

Memory and learning deficits that negatively impact on quality of life are a common occurrence in our aged population. The studies described in this thesis were designed to further our understanding of cellular and molecular alterations occurring in conditions that are associated with age-related memory and learning deficits. Based on the established importance of glutamate receptors and the hippocampus in memory and learning processes, we first investigated potential differences in glutamate receptor immunofluorescence within the hippocampus of juvenile, adult, and aged macaque monkeys. Second, to explore the influence of fluctuations in estrogen levels, comparable to those that occur during menopause, on NMDARs, we compared both NMDAR1 immunofluorescence and mRNA *in situ* hybridization intensity within different hippocampal regions between ovariectomized rats and ovariectomized rats treated with estradiol and progesterone. Third, to investigate the effects of altering a key afferent input on NMDARs, which we hypothesize occurs to some degree during aging, we evaluated NMDAR1 immunofluorescence and mRNA *in situ* hybridization intensity in rat dentate gyrus following synaptic reorganization induced by unilateral transection of the perforant path input from the entorhinal cortex. The results of these studies reveal that glutamate receptor plasticity is associated with all three conditions. In the first study, we demonstrated a circuit-specific decrease in NMDAR1 immunofluorescence within the dendrites of the dentate gyrus. The second study revealed that estrogen

serves to maintain NMDAR1 immunofluorescence intensity levels within both the dentate gyrus and the CA1 field of the hippocampus, possibly via post-transcriptional regulation of the NMDAR1 subunit protein. Lastly, the third study demonstrated that both NMDAR1 protein and mRNA levels are modifiable by changes in afferent input, and additionally demonstrated that NMDAR1 mRNA is one of a limited population of mRNAs that is transported into dendrites. In conclusion, the data presented in this thesis suggest that alterations in the distribution of NMDAR1 protein, which may have been precipitated by fluctuations in estrogen levels and an alteration in afferent input, occurs in the hippocampus during aging and may be associated with age-related memory and learning impairment.

Dedication

For their never ending love and support
This work is dedicated to my family

Acknowledgments

I am very grateful for the assistance of the following people: Drs. George Huntley, Deanna Benson, Nancy Weiland, Bruce McEwen, Steven Siegel, Jeffrey Kordower and Elliott Mufson for their collaborative efforts as coauthors in the studies described in this thesis; William Janssen for an education in laboratory technical skills; Roxanne Moosher for technical help with confocal microscopy; and Yiling Hu for extensive assistance with *in situ* hybridization; and the members of my committee for their time and guidance. I would also like to thank The National Academy of Sciences and The Society for Neuroscience for allowing me to include published articles in Chapters 4 and 5 of this thesis.

I wish to extend a special thanks to Brett Morrison, Drs. George Huntley, Deanna Benson, Patrick Hof and James Roberts for continuous support, thought-provoking conversations and creating a stimulating and enjoyable work environment.

I am indebted to Karen Lasley and Brian Cohen for helping me maintain a positive mental and emotional state throughout the duration of this thesis work.

Lastly, my deepest thanks goes to my mentor and friend Dr. John Morrison, for providing the best possible scientific training, granting me the freedom necessary to develop independent thinking and for showing me how rewarding and enjoyable science can be.

Preface

Focus on age-related health decline has been intensifying in recent years in both the clinical and basic sciences. This is largely due to a significant increase in the average age in our society. Currently, the fastest growing segment of the population is the age group that is over 85 years old (Amenta et al., 1991). By the year 2030 a projected 21% of the population in the United States will be over 65 years old, a substantial increase from 10% in 1975 (Brody, 1992). Medical science has done an extraordinary job of increasing the average human life expectancy, however, the medical and scientific community must accept the burden of their successful efforts. The aging process is associated with a diverse collection of health concerns, and one of the most troubling to many is the loss of cognitive abilities. Aside from the devastating effects of Alzheimer's disease (AD), which affect approximately 20% of individuals in their mid-eighties, 70% of eighty year old people suffer memory loss and other cognitive deficits associated with normal aging that negatively impact on their quality of life.

Given modern medicine's success in increasing the length of life, we must now focus on improving its quality throughout an individual's lifetime. We feel that this can be most effectively accomplished by enriching our understanding of the changes that occur in the normal aging brain. This goal is addressed in this thesis by studies aimed at isolating glutamate receptor alterations in both aged brains and experimentally manipulated non-aged brains. Hopefully information attained in this pursuit will be useful for the future development of pharmacological interventions aimed at averting or correcting functional compromise that occurs during aging.

Contents

---

[1] Gazzaley, A.H., Siegel, S.J., Kordower, J.H., Mufson, E.J., Sladek, J.R. and Morrison, J.H. (1996) Circuit-specific alterations of N-methyl-D-aspartate receptor subunit 1 in the dentate gyrus of aged monkeys. *Proceedings of the National Academy of Science USA* 93:3121-3125

[2] Gazzaley, A.H., Weiland, N.G., McEwen, B.S. and Morrison, J.H. (1996) Differential regulation of NMDAR1 mRNA and protein by estradiol in the rat hippocampus. *Journal of Neuroscience* (In Press)

[3] Gazzaley, A.H., Benson, D.L., Huntley G.W. and Morrison J.H. (1996) Differential subcellular regulation of NMDAR1 protein and mRNA in dendrites of dentate gyrus granule cells following perforant path transection. *Journal of Neuroscience* (Submitted)

List of Illustrations

Abbreviations

AAMI	age-associated memory impairment
AchR	acetylcholine receptor
AD	Alzheimer's disease
AMPA	α-amino-3-hydroxy-5-methyl-4-isoxazole propionic acid
BSA	bovine serum albumin
CA	cornu ammonis
CA1-sr	CA1 stratum radiatum
CLSM	confocal laser scanning microscopy
CO	cytochrome oxidase
DAB	3,3'-diaminobenzidine tetrahydrochloride
DNMS	delayed-nonmatching-to-sample
DTT	dithiothreitol
ECL	entorhinal cortex lesion
EM	electron microscopy
FITC	fluorescein isothiocyanate
GABA	γ-aminobutyric acid
GFAP	glial fibrillary acidic protein
GCL	granule cell layer
GluR	glutamate receptor
IgG	γ type immunoglobulin
IML	inner one-third of the molecular layer
LTP	long-term potentiation
mAB	monoclonal antibody
MRI	magnetic resonance imaging
mRNA	messenger ribonucleic acid
MAP2	microtubule associated protein 2
NMDA	N-methyl-D-aspartate
NMDAR1	N-methyl-D-aspartate receptor subunit 1
OML	outer two-thirds of the molecular layer
OVX	ovariectomized rats
OVX+E	ovariectomized rats treated with estradiol
OVX+E+P	ovariectomized rats treated with estradiol plus progesterone
RNA	ribonucleic acid

Chapter 1

Introduction

The primary objective of this thesis is to increase our understanding of cellular and molecular alterations that are associated with age-related memory and learning deficits. This is accomplished by three independent studies employing non-human animal models (Chapters 4, 5 and 6). The first study (Chapter 4) focuses on identifying alterations that occur in aged monkeys. Both aged humans and aged non-human primates experience memory deficits associated with normal aging (Poon, 1985; Rapp and Amaral, 1991). Given the important role of both glutamate receptors (GluRs) (Collingridge, 1987; Maren et al., 1993) and the hippocampus (Alvarez et al., 1995; Gage et al., 1984) in learning and memory formation, we investigated potential differences in glutamate receptor distribution and immunofluorescence intensity within the hippocampus of juvenile, adult, and aged macaque monkeys (Chapter 4).

The experimental studies described in Chapters 5 and 6 were designed to explore the influence of factors that may be involved in the generation of age-related cognitive deficits on NMDAR1 protein and mRNA regulation in the hippocampus. The study described in Chapter 5 addresses the issue that the study in Chapter 4 was performed exclusively on aged females. Estrogen increases the number of NMDA receptor binding sites and induces physiological changes consistent with a functional enhancement of NMDA receptors in rat hippocampus (Weiland, 1992; Wong and Moss, 1992). It is thus possible that the NMDAR1 alteration revealed in the aged monkeys was gender-specific and associated with menopause, which results in a dramatic reduction in circulating estrogen levels during aging. Furthermore, decreases in estrogen levels may be associated with age-related memory and learning deficits, since estrogen has been revealed to have an important role in cognitive function (Philips and Sherwin, 1992a; Philips and Sherwin, 1992b; Singh et al., 1994). Therefore, in Chapter 5 we investigate cellular and molecular

mechanisms of estradiol-induced NMDAR regulation in the hippocampus by comparing intensity levels of NMDAR1 immunofluorescence and NMDAR1 mRNA hybridization within different hippocampal regions in ovariectomized rats and ovariectomized rats treated with estradiol and progesterone.

The focus of the third study relates to our findings in Chapter 4, which revealed that aged monkeys, as compared to young adult and juvenile monkeys, experience a decrease in NMDAR1 immunofluorescence intensity within the distal segments of granule cell dendrites (i.e., the segments that receive the perforant path input from the entorhinal cortex), in comparison with more proximal dendritic segment. Other investigations have identified pathological changes in the entorhinal cortex of aged primates (Hof and Morrison, 1994; Mufson et al., 1994), and physiological alterations of the perforant path in aged rodents (Barnes, 1994). Based on these findings, we hypothesized that intradendritic levels of NMDAR1 are dynamic, and modifiable by alterations in the afferent condition of the perforant path. To explore this hypothesis, the third study (Chapter 6) investigates changes in both NMDAR1 immunofluorescence and NMDAR1 mRNA hybridization intensity in rat dentate gyrus following synaptic reorganization induced by unilateral transection of the perforant path input from the entorhinal cortex. Given that a key feature of Alzheimer's disease is devastation of the perforant path due to a severe loss of the neurons of origin in the entorhinal cortex (Hyman et al., 1984; Lippa et al., 1992), understanding compensatory changes in NMDAR1 levels or distribution following perturbations of the perforant path may also be crucial for understanding mechanisms of memory loss associated with neurodegenerative processes.

In addition to exploring alterations associated with age-related memory and learning deficits, another focus of this thesis is to increase our understanding of the mechanisms involved in GluR plasticity. Several studies have previously revealed alterations in GluR ligand binding sites induced by a variety of different conditions, including, aging, hormonal manipulations, and lesions (Ulas et al., 1990; Weiland, 1992; Wenk and Walker,

1991). In an attempt to discover cellular and molecular mechanisms that may be the basis of these functional binding alterations and resulting physiological and behavioral changes, we have used quantitative immunocytochemical and *in-situ* hybridization techniques to investigate changes in NMDAR1 subunit protein and mRNA within retained anatomical structures.

Chapter 2

Background

The purpose of this section is to present background information on common themes that are addressed throughout this proposal, as well as to discuss in more detail the inspiration and the rationale for focusing on particular species, anatomical structures and neurochemical markers.

Normal Human Brain Aging

For the context of this thesis, terms such as "aging", "age-related" and "age-associated" will be used to refer to events occurring during the post-maturational period of an animal's life. It will not be used to signify all references to aging processes of the brain, which by some definitions also include brain development and maturation.

Normal brain aging refers to the events that occur in the brain of an aged animal that are not associated with pathological conditions related to a disease process. Just as the brain has been observed to undergo extensive changes during development, there are a large number of changes that occur in the brain as it ages that might be considered part of a natural process. There is an extensive literature of structural and neurochemical changes in the aging human brain that are not associated with disease-related pathological conditions, such as Alzheimer's disease and Parkinson's disease. Some of these changes are thought to result in a progressive decline in the functional ability of the brain. In humans, cognitive decline occurs frequently during the normal aging process and affects such features as visuospatial abilities, conceptualization, general intelligence and memory (Albert, 1990). Memory deficits, which have been termed age-associated memory impairment (AAMI) appear early, in the mid-fifties, and occur in 55% of individuals in their sixties (Reinikainen et al., 1990). The major effect on memory function appears to be in the transfer of primary memory (short-term), into secondary

memory (long-term), which results in the inability to retain new information over time (Albert, 1990; Craik, 1977; Petersen et al., 1992; Poon, 1985).

An important feature of the functional impairments observed in normal aging is their variability. Not all aged individuals experience cognitive decline, and those that do may only experience deficits in certain abilities (Rapp and Amaral, 1992). These observations have led to the subclassification of normal aging into "usual aging" which refers to individuals that experience age-related functional decline, and "successful" aging reserved for those that do not (Rowe and Kahn, 1987).

Animal Models

The decision to use animal models to study aging, as opposed to humans, was based on several considerations. First, we must consider why we do not study human subjects and human brain tissue if what we are essentially interested in is the effects of aging on the human brain. One reason is that the fixation of the human brain is less than optimal because humans, unlike laboratory animals, cannot be transcardially perfused with fixative. Rather, human brains when used for research purposes are immersed in fixative after removal from the skull. Thus, there is an intervening post-mortem time delay before the brain is submerged in the fixative. Depending on the duration of this delay the quality of the tissue will be detrimentally affected. Although these factors do not make human tissue useless for all anatomical studies, they do result in a reduction in the quality of immunocytochemical labeling for glutamate receptor subunits, which is the principal experimental procedure used in this thesis. This may be do to the fact that the receptors are membrane bound and poor fixation affects the integrity of the cell membrane. Additionally, the availability of control, non-aged human tissue of an appropritate age, with complete clinical documentation and a postmortem time interval of less than 4 hours is difficult to obtain. Another drawback of performing these studies

on human brains is that experimental manipulations such as lesions, physiological recordings and tract tracing are only performed on experimental animals. Thus, it is not be possible to directly correlate age-related findings with experimental manipulations in the same species. Considering the vast supply of scientific literature available on the animal models used in this thesis, it was logical to initiate our investigation on these well-established models.

The next consideration is whether or not animal models of normal aging in humans are valid to use. The fact that animals age and eventually die is not justification in itself because aging consequences may be species specific. For example, humans are the only species that experience certain age-related disorders such as Alzheimer's disease. However, behavioral studies on both aged non-human primates and rodents have revealed that they both exhibit cognitive deficits associated with normal aging. Aged monkeys experience recognition memory deficits, as documented by the delayed-nonmatching-to-sample recognition (DNMS) memory task (Rapp and Amaral, 1991), and studies of aged rats in the Morris water maze have demonstrated their inability to form as effective spatial representations of their environment as young rats (Gage et al., 1984; Gallagher and Burwell, 1989). Considering the vast difference in baseline cognitive abilities between humans, monkeys and rats the age-related memory deficits experienced by monkeys and rodents appear to be similar to human memory impairments (Craik, 1977; Flicker et al., 1984; Perlmutter et al., 1981) Additionally, these aged animals also experience both structural and neurochemical changes similar to aged humans. Thus, the use of aged laboratory animals to study normal aging appears to be justified and has become a very common research theme.

Therefore, we have chosen to use animal models in this thesis because the advantages of their use overcome the disadvantages associated with the use of human brains. Our laboratory has successfully obtained high quality GluR immunocytochemical staining in the hippocampus and cortex of both monkeys and rats, however efforts do continue

to optimize staining in human tissue. In this thesis, we have successfully extended observations made in aged monkeys (Chapter 4) to two experimental models in the rodent (Chapter 5 and 6), which have impacted on our interpretation of the aging results. We now plan to duplicate these experimental paradigms in the aged monkeys to form direct intra-species comparisons, an experimental plan that could not have been duplicated in humans. The obvious disadvantage of the use of animal models is that extrapolation of observations to humans rely upon the assumption that the same chemical and structural changes occur between different species. It is for this reason that the initial aging study was performed in non-human primates, a species in which we feel more secure with such extrapolations. Even if some conclusions in this thesis are not entirely applicable to human aging, we feel that we have still made important contributions to the understanding of basic cellular mechanisms of GluR plasticity.

Hippocampal Formation

The hippocampal formation, located in the medial temporal lobe, consists of a number of defined subregions; the dentate gyrus, the hippocampus proper (Cornu Ammonis subfields- CA1, CA2, CA3, CA4), the subicular complex and the entorhinal cortex (Amaral et al., 1987). The decision to focus our anatomical evaluation on the hippocampal formation was based on three major reasons. First, the role of the hippocampal formation in learning and memory has been very well established. Our current understanding of this crucial role of the hippocampal formation is based primarily on numerous localized lesion studies in the monkey (Alvarez et al., 1995; Meunier et al., 1993; Zola et al., 1989; Zola et al., 1992) and the rat (Gage et al., 1984; Gallagher and Burwell, 1989), as well both post-mortem (Zola et al., 1986) and magenetic resonance imaging (MRI) studies of naturally occurring cases of human amnesia (Press et al., 1989). Aside from these in vivo studies, cellular models of learning such as long-

term potentiation (LTP), which was first documented in the perforant path circuit (Bliss and Lømo, 1973), and kindling have been readily observed, and are most frequently studied within hippocampal circuits. The extensive documentation of hippocampal involvement in memory processes suggests it is an appropriate anatomical structure in which to investigate mechanisms of age-related memory impairment.

The second reason for focusing on the hippocampal formation in this thesis is that memory and learning deficits experienced by aged animals are very similar to deficits that are induced by damaging the hippocampal formation. Memory studies performed on monkeys, such as the DNMS memory task, have revealed that aged monkeys (Rapp and Amaral, 1991) and monkeys that received bilateral lesions of hippocampal formation structures (Alvarez et al., 1995; Zola et al., 1989) exhibit memory deficits that resemble one another. Additionally, rats with bilateral hippocampal lesions perform poorly on spatial memory tasks such as the Morris water maze (Morris et al., 1982). A similar impairment in aged rats in the acquisition of spatial information has been observed that parallels these deficits in the lesioned rats (Gage et al., 1984; Gallagher and Burwell, 1989).

A third reason to focus on the hippocampal formation is that many hippocampal alterations have been documented to occur in aged animals. Alzheimer's disease (AD), which results in devastating memory loss, is associated with severe structural damage in the hippocampal formation (Hyman et al., 1986; Hyman et al., 1984; Van Hoesen and Hyman, 1990). Synaptic loss seems to be disproportionately large within the hippocampus, extensively involving the input from the entorhinal cortex (Cabalka et al., 1992; Honer et al., 1992). Aside from hippocampal involvement in AD, there have been several discoveries of hippocampal alterations during normal aging in humans. The hippocampal formation, particularly the entorhinal cortex, is often a site of neurofibrillary tangle accumulation in non-demented elderly adults (Bouras et al., 1994; Hof and Morrison, 1994; Price et al., 1991). Furthermore, MRI studies on elderly

individuals have suggested that hippocampal atrophy occurs during normal aging, and correlates with poorer performance on tests of secondary memory acquisition (Golomb et al., 1993; Golomb et al., 1994). Additionally, use of a recently developed non-biased quantitative method, the optical disector, has revealed a selective cell loss of subicular and hilar neurons within the hippocampus of normal, aged humans (West, 1993). These observations in the human hippocampal formation, and other studies revealing physiological (Barnes, 1994) and synaptic changes (Geinisman et al., 1992) in the aged rat, suggest the hippocampus to be an optimal site to investigate age-related structural and chemical alterations that can be linked to functional deficits.

Dentate Gyrus Anatomy

The dentate gyrus, a region in the hippocampal formation, is composed of three layers; the granule cell layer, the molecular layer, and the polymorphic cell layer. The granule cells are the principal projection neurons of the dentate gyrus and their cell bodies are organized in the granule cell layer, a very compact collection of cells which curves to form three blades in the monkey (medial, central and lateral) and two blades in the rat (suprapyramidal and infrapyramidal) (Amaral and Witter, 1989; Rosene and Van Hoesen, 1987). The granule cells are small (~7 μm), round cells with a very thin cytoplasmic rim and either a single or several spiny apical dendrites extending in a conical fashion into the molecular layer (Clairborne et al., 1990; Frotscher et al., 1988) (Fig. 2.1). The axons of the granule cells extend from the basal pole and traverse the hilus (where they

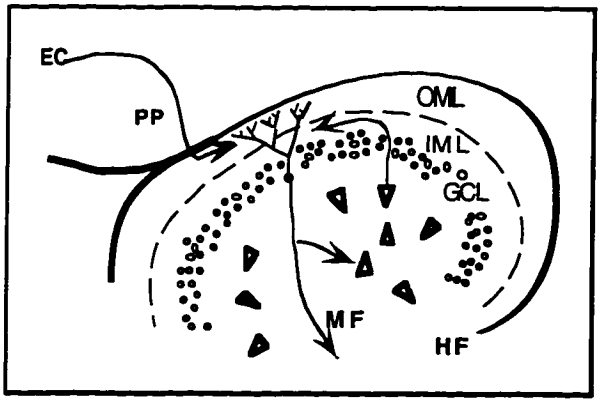

Figure 2.1 Schematic of dentate gyrus anatomy. Details in text.

give off collaterals) as the mossy fiber projection, to terminate in the stratum lucidum of CA3 (Amaral and Witter, 1989). The molecular layer is a relatively cell sparse region consisting mostly of the dendrites of the granule cells that extend to the obliterated hippocampal fissure (Fig. 2.1). The majority of the granule cells input is received in the molecular layer. Aside from granule cell dendrites and an extensive web of axonal fibers, the molecular layer also contains GABAergic interneurons (Halasy and Somogyi, 1993) and neuroglia. The polymorphic cell layer, part of the hilar region, is located on the basal side of the granule cells and is populated by a variety of different neuronal cell types, the polymorphic hilar neurons (Amaral, 1978; Frotscher et al., 1991).

One striking feature of the dentate gyrus is the segregated distribution of the excitatory afferents in a proximo-distal pattern across the extent of the dendritic field within the molecular layer. The outer-two thirds of the molecular layer (OML) receives an excitatory input (Lambert and Jones, 1990) almost entirely from the ipsilateral entorhinal cortex via the perforant path (Steward, 1976; Witter et al., 1989), while the inner one-third of the molecular layer (IML) receives a commissural and associational projection from the hippocampal polymorphic hilar cells (Berger et al., 1980) (Fig. 2.1). There is also evidence of a minor projection from the contralateral entorhinal cortex to the OML (Goldwitz et al., 1975; Steward et al., 1976). Perforant path axons emanating from layer II of the entorhinal cortex travel in the underlying white matter, through the angular bundle, and enter the molecular layer through two different paths. They either directly cross the obliterated hippocampal fissure after perforating the pyramidal cell layer of the subiculum, or travel within the molecular layer of the subiculum and the CA fields, where some fibers terminate and others enter the dentate gyrus molecular layer at the suprapyramidal tip (Witter, 1989). The perforant path in both rats and monkeys are topographically organized such that the lateral entorhinal cortex projects to the caudal dentate gyrus (septal in rats and cats) and the medial entorhinal cortex projects to the rostral dentate gyrus (temporal in rats and cats) (Ruth

et al., 1982; Witter and Groenewegen, 1984; Witter et al., 1989).

Since this proposal utilizes both monkeys and rats as experimental subjects, it is important to clarify some anatomical differences that exist between these two species in reference to the anatomy of the dentate gyrus. The only difference observed between the granule cells of rodents and primates is the presence of occasional basal dendrites within monkeys and humans, which extend into the hilar region and occasionally into the molecular layer (Frotscher et al., 1988; Seress and Mrzljak, 1987). In respect to connectivity, two main differences have been observed. First, the extensive commissural projection from the hilar neurons to the contralateral IML is much more limited in primates than in rats, and is restricted to the uncal region. Additionally, the crossed projection from the entorhinal cortex to the contralateral dentate gyrus exists in an even more limited fashion in monkeys than in rats. This sparse projection is solely from the caudal part of the medial entorhinal cortex to the caudal region of the dentate gyrus (Amaral et al., 1984). Secondly, the laminar termination of the perforant path within the OML differs between rats and monkeys. The rat demonstrates a distinct pattern of bilaminate termination within the OML such that the medial entorhinal cortex terminates in the inner half of the OML and the lateral entorhinal cortex terminates in the outer half of the OML (Steward, 1976). In the monkey, projections from all regions of the entorhinal cortex terminate diffusely throughout the OML, although the rostral entorhinal cortex preferentially projects to the outer half of the OML and the caudal entorhinal cortex projects more heavily to the inner half of the OML (Witter and Amaral, 1991).

Glutamate Receptors

Glutamate receptors (GluRs) are the primary mediators of excitatory neurotransmission in the central nervous system (Nakanishi, 1992). GluRs, like many other neurotransmitter receptors, can be divided into two main subdivisions, ionotropic

and metabotropic receptors. The metabotropic receptors are coupled to G-proteins and upon glutamate binding, activate second messenger systems within the cell (Sugiyama et al., 1987). The ionotropic receptors are ligand-gated cationic channels that are divided into three subclasses based on their selective activation by different pharmacological agonists; NMDA, AMPA (α-amino-3-hydroxy-5-methyl-4-isoxazole propionic acid) and kainate (review; Hollmann and Heinemann, 1994). Through the use of molecular cloning techniques, such as expression cloning, the characterization of GluRs revealed an extraordinary diversity of receptor subunits (Bettler et al., 1990; Boulter et al., 1990; Hollmann et al., 1989; Keinanen et al., 1990; Moriyoshi et al., 1991; Nakanishi et al., 1990) that are grouped within the different subclasses based on their sequence homology and agonist selectivity; NMDA (NMDAR1, NMDAR2A-D), AMPA (GluR1-4), kainate (GluR5-7, KA1,2). The results of physiological studies of subunits expressed in *Xenopus* oocytes suggest that these subunits combine to form functional heteromeric complexes (Boulter et al., 1990; Keinanen et al., 1990; Monyer et al., 1992; Nakanishi et al., 1990). It has also been suggested that combinations of the different subunits within a subclass leads to functional diversity of the GluRs. Additional functional diversity is obtained via alternative RNA splicing of the NMDAR (review; Zukin and Bennett, 1995) and the AMPA receptor subunits (Sommer et al., 1990).

The decision to focus the neurochemical element of this thesis on GluRs was based on their well documented role in learning and memory formation. First, NMDARs have been revealed to have an important role in the induction of LTP, a synaptic model of learning and memory formation (Bliss and Collingridge, 1993; Bliss and Lømo, 1973; Collingridge, 1987; Collingridge and Bliss, 1987). This is primarily attributed to the unique property of the NMDAR in being voltage-activated, due to a voltage-dependent channel blockade by Mg^{2+}, as well as ligand-gated (Nakanishi, 1992). Thus, the receptor acts as a coincidence detector, so that following both the removal of the Mg^{2+} block by sufficient depolarization and the binding of glutamate to the receptor complex the channel

becomes highly permeable to Ca^{2+}, a molecule critically involved in neuronal plasticity (Bliss and Collingridge, 1993). Secondly, a more direct role for NMDA receptors in learning has been revealed through pharmacological studies in rats, which demonstrated that administration of an NMDAR antagonist results in selective learning impairment (Morris et al., 1986). Additionally, non-NMDA GluRs have also been implicated in LTP (Maren et al., 1993). Another feature that makes the study of GluRs optimum within the context of this thesis is their prevalent localization within hippocampal circuits as demonstrated by physiological, autoradiographical and immunocytochemical methodology (Andreasen et al., 1988; Andreasen et al., 1989; Cotman et al., 1987; Lambert and Jones, 1990; Siegel et al., 1994; Siegel et al., 1995).

Receptor Plasticity

Neurotransmitter receptors function at a pivotal point for the control of synaptic transmission in the nervous system. Alterations in the activity, concentration and intracellular placement of receptors can modulate signal propagation within neurons. The ability of a structure to shift between different states is known as plasticity (Klein et al., 1989). The early studies of receptor plasticity consisted primarily of investigations of alterations in acetylcholine receptors (AchR) induced within the myotubule during development and following changes in muscle activity or denervation. It was demonstrated in this system that AchR clustering at synaptic sites during development is dependent upon the presence of motor neuron axonal input (Frank and Fischbach, 1979; Schuetze and Role, 1987). It was also revealed that following muscle fiber denervation a condition known as denervation supersensitivity occurs, which results in an increased number of AchR binding sites (Miledi and Potter, 1971) and increased mRNA levels (Merlie et al., 1984) in the denervated muscle fibers several days after nerve lesion. A similar increase in AchR binding sites occurs following alterations in

activity without denervation of the muscle (Fambrough, 1979; Lømo and Rosenthal, 1972).

Receptor plasticity has also been described in the CNS for other receptor systems. For example, the number of GluR binding sites are responsive to various experimentally induced conditions, such as; aging, hormonal and pharmacological manipulations, lesions, kindling and LTP (Bessho et al., 1994; Geddes et al., 1985; Lahtinen et al., 1993; Magnusson and Cotman, 1993; Maren et al., 1993; Thomas et al., 1994a; Ulas et al., 1990; Weiland, 1992; Wenk and Walker, 1991; Williams et al., 1992). However, studies that have investigated cellular and molecular mechanisms of this plasticity, such as alterations in receptor subunit protein and mRNA levels as well as subcellular distribution are limited. This endeavor represents one of the principal focuses of this thesis, and the rationale for the use of the specific experimental procedures discussed in Chapter 3.

Chapter 3

Experimental Design

Immunocytochemistry

Immunocytochemistry, the technique used in this thesis to localize GluR subunits within neuronal structures in tissue sections, is based on principles developed more than 50 years ago, which demonstrated that antibodies specific to an antigen can be linked to a histochemical marker without impacting on the ability of the antibody to bind to the antigen (Marrack, 1934). Fluorescein conjugated antibodies, which were used as fluorescent markers in the studies described in this thesis, were first used as histochemical markers to localize antigens in tissue sections in the 1940s (Coons et al., 1942). Although immunocytochemistry was initially applied to neurobiology in the late 1960s, when it was used to localize dopamine β–hydroxylase in peripheral sympathetic neurons (Geffen et al., 1969), it was not used to localize GluR subunit proteins within tissue sections until the early 1990s. It was the application of molecular cloning techniques, such as expression cloning, first successfully applied to the GluR system by Hollmann et. al (Hollmann et al., 1989) that permitted the cloning of functional members of the glutamate receptor family and the subsequent development of subunit specific antibodies. Prior to the cloning of GluR subunits, GluR localization studies were limited to autoradiographic studies using radiolabeled ligands to receptor complex binding sites (Monaghan and Cotman, 1982; Monaghan et al., 1983).

Immunocytochemistry was used in this thesis, because unlike radioligand binding studies, individual receptor subunits can be identified and can be localized to cellular and subcellular compartments. The staining was performed on tissue sections rather than homogenized tissue, or Western blots, because we were interested in evaluating staining alterations between different conditions within preserved anatomical structures.

Thus, through the uses of the proposed methodology, we can obtain information related to the cellular mechanisms of GluR plasticity in response to different conditions. The main disadvantage of using immunocytochemistry in these studies is that the results are not necessarily reflective of changes in functional receptor complexes. Therefore, throughout this thesis correlations will be made with radioligand binding, physiology and behavioral studies.

Quantitative Evaluation of Immunufluorescence Intensity

To objectively evaluate differences in immunufluorescence intensity between regions from different experimental groups, rigid criteria must be followed for tissue preparation, tissue processing, microscopic evaluation and analysis design. Foremost, it is essential that all tissue that is being compared be treated identically in all phases of the analysis. Below is a list of factors, and their rationale, that we developed and followed as precisely as possible to assure comparability between regions from different experimental groups in the quantitiative immunofluorescence evaluations described in this thesis. Details of these methods are described in Chapters 4, 5 and 6; Experimental Procedures.

Tissue Preparation and Processing

1) All tissue was exposed to fixative for the same duration of time.

2) Sections were cut to approximately the same thickness, using the same vibratome setting.

3) Immunofluorescence was used rather than a 3,3'-diaminobenzidine tetrahydrochloride (DAB) reaction. The consistency of the staining between runs was improved by this decision because immunofluorescence does not involve the use of a precipitation reaction, which is considerably more dependent upon such factors as time and temperature. Additionally, the use of a fluorescent marker was optimal for confocal microscopic evaluation.

4) The immunostaining procedure was conducted with same antibody concentration of

solutions, time of incubation and temperature of incubation. If absolute values were being compared, all tissue was processed in the same experimental run. When this was not possible, comparisons were made between ratios from regions on individual tissue sections to control for potential experimental differences between runs.

5) An antibody concentration was used that resulted in the lowest possible background levels (as evaluated by nuclear staining), while still yielding intense, specific cellular staining.

6) A sufficient quantity of solution per well was used so that sections were completely submerged.

7) Only one tissue section was placed in each well to prevent sections from sticking together, which would result in uneven staining.

8) While incubating in an antibody solution, sections were shaken vigorously to prevent sticking to sides of the well or floating to the surface. Additionally, the sections were flipped occasionally to ensure even staining on both sides.

Confocal Microscopy

1) Confocal microscopy was chosen for this analysis as opposed to conventional microscopy for two main reasons. First, it ensures that "out-of-focus" elements that may artifactually alter intensity levels does not enter into intensity measurement. This eliminated the confounding effect induced by differences in section thickness or degree of antibody penetration. Second, it yields high magnification, high resoultion images. This allowed for the accurate subtraction of unlabeled portions of the field by image anlysis software, permitting us to determine the intensity within cellular structures.

2) All confocal parameters were kept constant throughout an experiment and between antibodies. Parameters include: lasers, filters, laser power, pinhole size and electronic zoom. Analyses was performed in as short a time period as possible since the laser power decreases over time.

3) The only feature that varied between antibodies was the contrast/brightness settings, because a single setting would not yield a suitable image for all antibodies used. The contrast/ brightness setting was established prior to beginning the analysis by randomly testing sections at different settings until a setting was found that yielded a high resolution images for both bright and dim sections, without regions above the maximal pixel intensity of 255. This setting remained constant throughout the analyses for each antibody.

4) The same 63X oil objective was used for the entire analysis.

5) The collection of confocal images and the thresholding procedure was performed without knowledge of which experimental group the section was from.

6) The field analyzed was positioned in the same region of the microscopic field to eliminate the confounding effect of any uneveness in laser field illumination.

7) Due to fluorescence quenching only one optical section was scanned for each region analyzed.

8) A predetermined z-axis distance from the surface of the tissue section that was adhered to the glass slide was selected for the single optical section. This was necessary since the immunofluorescence intensity varies throughout the depth of penetration.

9) A region was analyzed only once, and was not returned to at a later time, due to fluorescence quenching.

Analysis Design

1) A sufficient number of animals, sections and fields were selected to perform a statistical analysis.

2) The same anatomical region was compared between groups. This includes both the rostral-caudal position in the brain, as well as the location on each section.

3) High magnification fields to be analyzed (63X) were selected randomly, at a low magnification (16X).

In-situ hybridization

In-situ hybridization was performed in parallel with the immunocytochemistry experiments described in Chapters 5 and 6 to obtain information on changes in NMDAR1 gene expression following hormonal manipulation and perforant path transection. This technique, which was first described almost thirty years ago (Gall and Pardue, 1969), is based on the hybridization of nucleic acid probes, such as radiolabeled oligonucleotides (Chapter 5) or cRNA (Chapter 6) probes, with a specific nucleic acid sequence found in a tissue section. *In-situ* hybridization was chosen for these experiments because, unlike other methods of measuring RNA levels such as Northern blots and dot blots that require cell lysis, *in-situ* hybridization can be performed on intact tissue. Thus, information concerning changes in discrete cell groups, as well as alterations in subcellular distribution, can be obtained using this technique. Details regarding the quantitiative analysis of hybridization intensity is available in Chapters 4 and 5; Experimental Procedures.

Chapter 4

Circuit-specific Alterations of N-methyl-D-aspartate Receptor Subunit 1 in the Dentate Gyrus of Aged Monkeys

Abstract

Age-associated memory impairment occurs frequently in primates. Based on the established importance of both the perforant path and *N*-methyl-D-aspartate (NMDA) receptors in memory formation, we investigated the glutamate receptor distribution and immunofluorescence intensity within the dentate gyrus of juvenile, adult, and aged macaque monkeys with the combined use of subunit specific antibodies and quantitative confocal laser scanning microscopy. Here we demonstrate that aged monkeys, as compared to adult monkeys, exhibit a 30.6% decrease in the ratio of NMDA receptor subunit 1 (NMDAR1) immunofluorescence intensity within the distal dendrites of the dentate gyrus granule cells, which receive the perforant path input from the entorhinal cortex, relative to the proximal dendrites, which receive an intrinsic excitatory input from the dentate hilus. The intradendritic alteration in NMDAR1 immunofluorescence occurs without a similar alteration of non-NMDA receptor subunits. Further analyses employing synaptophysin as a reflection of total synaptic density and microtubule-associated protein 2 as a dendritic structural marker, demonstrated no significant difference in staining intensity or area across the molecular layer in aged animals as compared to the younger animals. These findings suggest that, in aged monkeys, a circuit-specific alteration in the intradendritic concentration of NMDAR1 occurs without concomitant gross structural changes in dendritic morphology or a significant change in the total synaptic density across the molecular layer. This alteration in the NMDA receptor-mediated input to the hippocampus from the entorhinal cortex may represent a molecular/cellular substrate for age-associated memory impairments.

Introduction

Memory loss is a consistent feature of Alzheimer's disease (AD), and has been linked to severe structural alterations in the perforant path (Cabalka et al., 1992; Flood et al., 1987; Hyman et al., 1984), an excitatory projection of the entorhinal cortex to the hippocampal dentate gyrus (Lambert and Jones, 1990). Both human (Poon, 1985) and non-human primates (Rapp and Amaral, 1991) also frequently experience age-related memory loss in the absence of overt AD symptoms. However, while certain pathological profiles seen in AD (e.g. amyloid plaques) are present in normal primate aging (Mufson et al., 1994), similar dramatic structural deterioration of the perforant path does not seem to occur (Flood et al., 1987; Tigges et al., 1995; West et al., 1993). This suggests that rather subtle molecular changes in structurally intact neural circuits crucial for memory processes may mediate age-associated memory impairment. The important role of both the perforant path and *N*-methyl-D-aspartate (NMDA) receptors in memory processing (Meunier et al., 1993; Morris et al., 1986) and long term potentiation (LTP) (Bliss and Collingridge, 1993; Bliss and Lømo, 1973), a cellular model for learning, has been extensively documented. Recently, the NMDA receptor distribution within the adult primate hippocampus, has been investigated with immunohistohemical methods (Siegel et al., 1994), and has confirmed both autoradiographic (Cotman et al., 1987) and physiological (Lambert and Jones, 1990) results which reveal a significant NMDA receptor presence at the perforant path termination zone in the outer molecular layer (OML) of the dentate gyrus. However, there is no information available as to the integrity of the NMDA receptor complex within the dentate gyrus of the aged primate. This is investigated in the present study by using a monoclonal antibody specific to NMDAR1 (14). NMDAR1 is an obligatory subunit of the NMDA receptor complex and was therefore used as a marker of all NMDA receptors (Monyer et al., 1992).

Autoradiographic ligand binding studies have suggested that NMDA receptors, as

well as non-NMDA glutamate receptors (GluRs), are affected by the normal aging process (Magnusson and Cotman, 1993; Nicoletti et al., 1995). However, many such analyses were performed on rodents, which differ from primates in certain elements of hippocampal circuitry (Witter and Amaral, 1991), and possibly in their anatomical alterations associated with aging (Barnes and McNaughton, 1980; Geinisman et al., 1987; Tigges et al., 1995; West et al., 1993)]. Furthermore, autoradiographic ligand binding techniques lack dendritic resolution and receptor subunit specificity, which precludes the identification and localization of subcellular subunit changes, as well as the determination of the degree to which receptor alterations are accompanied by structural degeneration. In this study, we employed confocal laser scanning microscopy (CLSM) to clearly resolve individual immunofluorescent dendrites and quantitative techniques with a broad array of immunohistochemical probes to determine whether receptor changes are due to alterations in receptor concentration within the dendrites or are the result of dendritic structural reorganization.

In addition to NMDA GluRs, there is growing evidence of the involvement of non-NMDA GluRs in learning and memory associated processes such as LTP (Maren et al., 1993). Non-NMDA GluRs have also been demonstrated by immunocytochemical techniques to be present postsynaptically in the OML of the dentate gyrus (Siegel et al., 1995). To investigate the possibility of concurrent changes in these receptors, quantitative CLSM was performed on tissue immunolabled with antibodies to both AMPA (α-amino-3-hydroxy-5-methyl-4-isoxazole propionic acid) receptor subunits 2/3 (GluR2/3) (Wenthold et al., 1992), and kainate receptor subunits 5/6/7 (GluR5/6/7) (Huntley et al., 1993).

Experimental Procedures

Animals and Tissue Processing

Eighteen monkeys, consisting of one male and two female juvenile rhesus monkeys (1 - 2 years old) (*Macaca mulatta),* one adult female and three male rhesus monkeys, five adult male cynomolgus monkeys (5 - 9 years old) (*Macaca fascicularis)* and six aged female rhesus monkeys (24 - 32 years old), were employed in this study. The aged animals used in this study were between 24 and 32 years old. Only 10-25% of rhesus monkeys raised in captivity can be expected to live beyond 25 years. Monkeys, older than 20 years of age are generally considered to be aged while monkeys between the ages of 5-10 years old are placed in the adult category and are often used as a control group in aged studies (Peters, 1991). In this study we employed an additional juvenile group of 1-2 year old rhesus monkeys. All monkeys received care and treatment in accordance with institutional and NIH guidelines. The animals used in the quantitative analysis were raised in captivity and housed in single cages for the most of their lives. All aged monkeys used in this study were retired breeders and were not involved previously in any pharmacological or invasive studies. Monthly serological tests, annual physical exams, and necroscopy analyses failed to discern any age-related changes that covaried with the findings obtained in this study. The aged monkeys could not be behaviorally tested due to age-related physical impairments such as cataracts and arthritis which make testing difficult but are unlikely to directly impact on hippocampal GluRs. The animals were deeply anesthetized with ketamine hydrochloride (25 mg/kg, i.m.) and Nembutal (30 mg/kg, i.v.) and perfused transcardially with ice-cold 1% paraformaldehyde in 0.1 M phosphate-buffered saline (PBS) for 1 minute, followed by 10 - 14 minutes of cold 4% paraformaldehyde in PBS (0.125% glutaraldehyde was added to the perfusate for the cynomolgus monkeys). The brains were immediately removed, cut into 5-6 mm blocks in a coronal plane, and postfixed in cold 4%

paraformaldehyde in PBS for 6 hours. The blocks were cut on a vibratome at a setting of 50 mm.

Immunocytochemistry

Four closely associated but non-adjacent hippocampal sections, at the level of the lateral geniculate nucleus, were incubated with each of the five primary antibodies used in this study at the appropriate dilutions in PBS with 0.5 mg/ml bovine serum albumin, for 48 hours. Only sections incubated in the primary antibody for microtubule-associated protein 2 (MAP2) contained 0.3% Triton X-100. Sections were then washed three times in PBS, transferred to biotinylated anti-mouse IgG H&L (except for sections treated with primary antibody to GluR 2/3 which were transferred to biotinylated anti-rabbit IgG H&L) for 2 hours, washed again in PBS and transferred to FITC-conjugated Avidin for 1 hour. Sections were then mounted, and coverslipped with Vectashield (Vector Laboratories) to reduce fluorescence quenching.

CLSM and Quantitative Evaluation

Quantitative CLSM analysis was performed on the most recently perfused rhesus monkeys of the three age groups to assure a comparably high quality of immunocytochemical staining essential for this analysis (juvenile, n=3; adult, n=3 and aged, n=4). Two sections from each animal were selected for analysis with a Zeiss LSM 410 inverted confocal microscope. On all sections analyzed, FITC was excited by an Argon/Krypton laser at 488 nm that was attenuated by a 90% neutral density filter, reflected to the specimen with an FT488/568 dichroic mirror and imaged with a Zeiss Plan-Neofluar 63x/1.25 N.A. oil immersion objective. A confocal aperture was set with a digital pinhole size of 17. A suitable contrast/brightness setting that yielded a high resolution image for both bright and dim sections, without regions above the maximal pixel intensity of 255, was determined for each antibody.

To control for inherent bias, the area in each section where the lamination effect

was maximally observed was selected for quantitative sampling in every animal from all three age groups. For each section, six fields within the IML (dendritic field immediately distal to the granule cell layer) and OML (midpoint between the granule cell layer border and the hippocampal fissure) were randomly chosen in the selected area. Thus, 24 fields were sampled from each animal for each antibody used in the quantitative analysis. Each field was scanned one time at a predetermined z-axis distance into the tissue with a two line average for a total scan time of 4.52 s and an electronic zoom factor of 4.5 (which increases the resolution to 0.0881 mm/pixel and magnification to 283.5 X), resulting in scanned regions of identical area (2039 μm^2). Each digitized image consisted of a 512 X 512 X 8- bit pixel array in which every pixel was assigned a gray level intensity value ranging from 0 to 255. Subtraction of background immunofluorescence was accomplished with a photometric offset (Zeiss Inc.) to establish a pixel intensity threshold below which a pixel would have no contribution to the average pixel intensity or area of the field. The offset was accomplished by viewing the image at a display magnification of 2 X and increasing the thresholding value until the blue-colored display, designating the thresholded area, abutted the dendrites (Fig. 4.1). The average pixel intensity and area of the portion of the field above threshold was calculated, thus representing the immunofluorescence intensity and area of the granule cell dendritic shafts only.

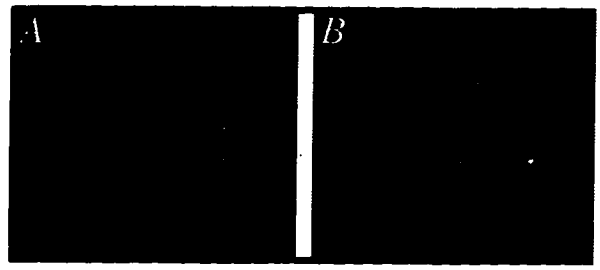

Figure 4.1 A CLSM image of NMDAR1 immunolabeled granule cell dendrites without (A), and with (B), intensity thresholding denoted by a gray overlay between the dendrites.

The OML/IML ratio of the intensity and area measurements were then computed for each animal by dividing the mean of the 12 OML values by the mean of the 12 IML values. The mean ratio value for each age group was then obtained from these individual ratios. The OML/IML ratio was used, as opposed to absolute comparisons, to control for any methodological variability in staining intensity that existed between the sections.

RESULTS

NMDAR1 Immunofluorescence

In juvenile and adult monkeys, NMDAR1 immunofluorescence was present within the pyramidal cell bodies and throughout the dendritic arbor of the subiculum and all fields of Ammon's horn, as described previously (Siegel et al., 1994). The receptor distribution and intensity within these regions, as well as within both temporal and prefrontal neocortical areas, were indistinguishable from that observed in the aged monkeys, based upon non-quantitative microscopic analysis. A similar examination of the dentate gyrus of juvenile and adult monkeys revealed somatic granule cell labeling with a relatively homogeneous distribution of immunofluorescence throughout the dendritic extent of the molecular layer (Fig. 4.2 *A,B,C*). In contrast, the molecular layer of all the aged monkeys in this study exhibited a striking reduction in the immunofluorescence intensity in the OML compared to the IML (Fig. 4.2 *D,E,F*). By visual inspection, certain areas of the dentate gyrus, within a given section, exhibited this lamination pattern to a greater degree than other areas. However, this partial heterogeneity in the pattern had no consistent regional distribution in the dentate gyrus.

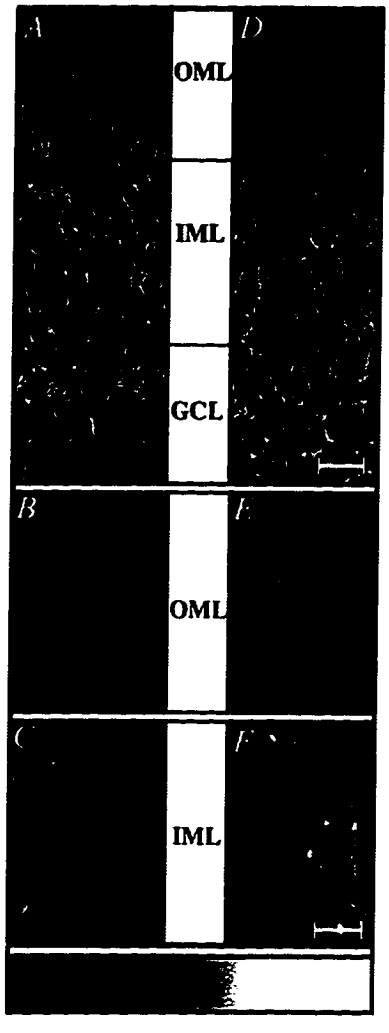

Figure 4.2 CLSM images of NMDAR1 immunofluorescence in the dentate gyrus of young (*A, B, C*) and aged (*D, E, F*) monkeys. *B* and *E*, higher magnification of OML. *C* and *F*, higher magnification of the IML. Scale bars: *A,D* 25 μm; *B,C,E,F*, 10 μm.

Quantitative CLSM analysis of the areas of maximal lamination, revealed that the OML/IML dendritic intensity ratios of the juvenile and adult monkeys were not significantly different from each other, but were significantly different from those of the aged monkeys

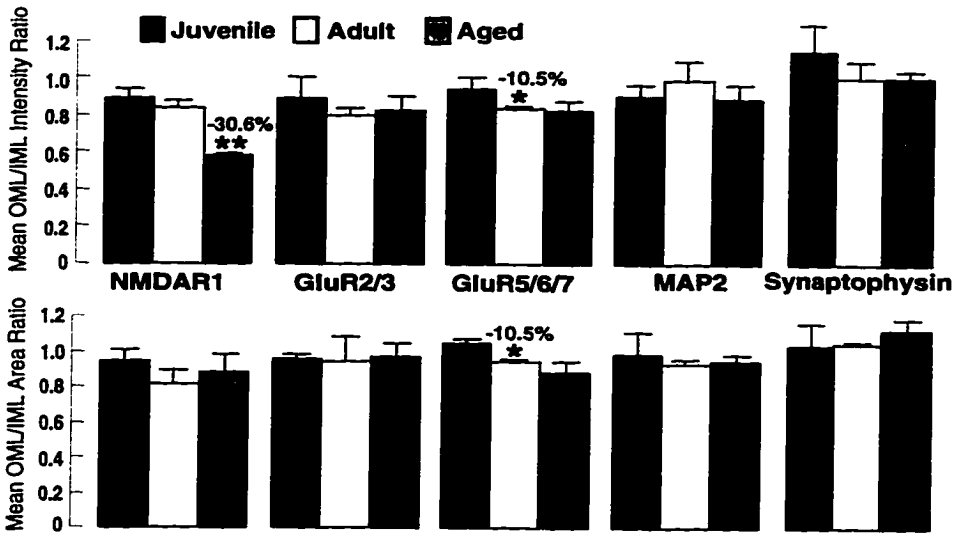

Figure 4.3 Quantitative CLSM analyses demonstrating the OML/IML ratio for fluorescence intensity and area of the dendritic segments for all five antibodies analyzed in each age group. The OML/IML ratios represent the means of the intensity and area measurements for each OML image divided by the means for each IML image (36 OML values/36 IML values for the juveniles and adults, 48 OML values/48 IML values for the aged). Note that the only statistical % difference in intensity, or area, when comparing adult to aged, is the decrease in the fluorescence intensity ratio of the OML/IML for NMDAR1 labeling (-30.6%). In addition, a small but statistically significant % decrease is evident for GluR5/6/7 intensity and area ratios when comparing juveniles to adults (-10.5%). Error bars represent 1 s.d.
* $P < .05$, ** $P < .0001$ (Unpaired Student's t-test).

(34.4% and 30.6%, respectively), which exhibited a markedly lower intensity of immunofluorescence within the dendritic segments of the OML compared to the IML (Fig. 4.3). This decrease in the OML/IML intensity ratio was observed in all of the aged monkeys in this study.

Non-NMDA Receptor Immunofluorescence

In contrast to the NMDAR1 result, we observed a relatively homogeneous staining intensity, with antibodies to GluR5/6/7 and GluR2/3, throughout the molecular layer in animals of all age groups (Fig. 4.4 *A,B,C,D*), comparable to the recent observation of uniform molecular layer labeling with an antibody to GluR2/3 in aged humans (Hyman et al., 1994). Quantitative analysis demonstrated no statistically significant difference between the aged and adult monkeys for either antibody (Fig. 4.3). This suggests that the intradendritic change in GluR concentration from adulthood to old age was NMDA

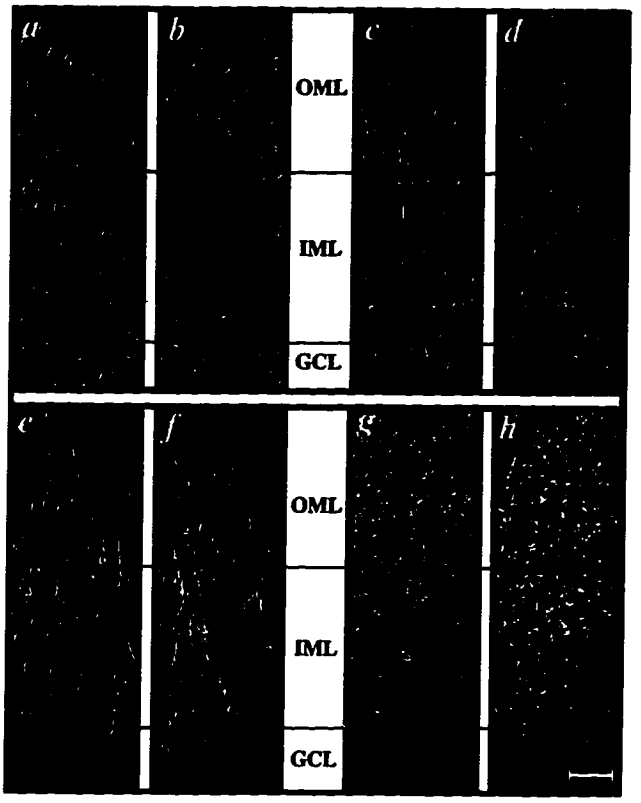

Figure 4.4 Confocal images demonstrating GluR2/3 (*A,B*), GluR5/6/7 (*C,D*), MAP2 (*E,F*), and synaptophysin (*G,H*) immunofluorescence in the dentate gyrus of a young, (*A,C,E,G*) and aged (*B,D,F,H*) rhesus monkeys. Note that the fluorescence intensity is fairly uniform throughout the dendritic extent of the molecular layer (OML vs. IML) for all four antibodies in both the adult and aged monkeys. IML, inner molecular layer; OML, outer molecular layer; GCL, granule cell layer. Scale bars: *H* 25 μm. Same magnification for all images.

receptor specific, although a larger sample size may have revealed subtle shifts in non-NMDA GluRs. A small, but statistically significant difference between the juveniles and adults for GluR5/6/7 labeling (Fig. 4.3) was also observed. This may represent a developmental shift in the kainate subunit pattern, comparable to morphological alterations that occur during the development of the primate granule cell dendrites (Duffy and Rakic, 1983).

Dendritic Area

In addition to determining the immunofluorescence intensity, we investigated whether there was a loss of dendritic area in the OML relative to the IML in aged monkeys (Fig. 4.1). Analyses of the adult and aged animals demonstrated no significant difference in immunofluorescent dendritic area across the molecular layer for any of the GluR subtypes examined (Fig. 4.3). To explore further the possibility of structural alterations, we immunolabeled hippocampal sections with a monoclonal antibody to the soma/dendrite-

specific cytoskeletal protein, MAP2 (Huber and Matus, 1984). Qualitative (Fig. 4.4 *E,F)* and quantitative examination revealed no significant age-associated differences in either dendritic immunofluorescence intensity or area across the molecular layer (Fig. 4.3).

Synaptic Density

In order to investigate whether the NMDAR1 alteration was associated with a change in synaptic density across the laminae of the dentate gyrus, hippocampal sections were incubated with a monoclonal antibody to synaptophysin (Wiedenmann and Franke, 1985) (Fig. 4.4*G,H*), an integral membrane glycoprotein of synaptic vesicles that has been used extensively as a reflection of total synaptic density (Masliah et al., 1993). Quantitative analyses determined that there was no significant age-associated difference in the OML/IML ratio of either the synaptophysin immunofluorescence intensity or area (Fig. 4.3), suggesting the preservation of total synaptic density in the OML relative to the IML.

DISCUSSION

In the present study we demonstrated a change in NMDAR1 immunofluorescence intensity at the intradendritic level by using confocal laser scanning microscopy (CLSM) and gray level intensity quantification. Previous investigations have demonstrated that immunoreactive intensity is a reflection of protein concentration (Good et al., 1992), suggesting that our results reveal a relative decrease in the cytoplasmic pool of NMDAR1 within the distal segments of the granule cell dendrites that comprise the perforant path terminal zone (OML). Both immunofluorescence area data for the GluRs and MAP2 suggest that the relative decrease in NMDAR1 concentration within the distal granule cell dendrites occurs without concomitant major dendritic structural alterations (Fig. 4.5), which is in contrast to the severe dendritic pruning of the granule cells that occurs

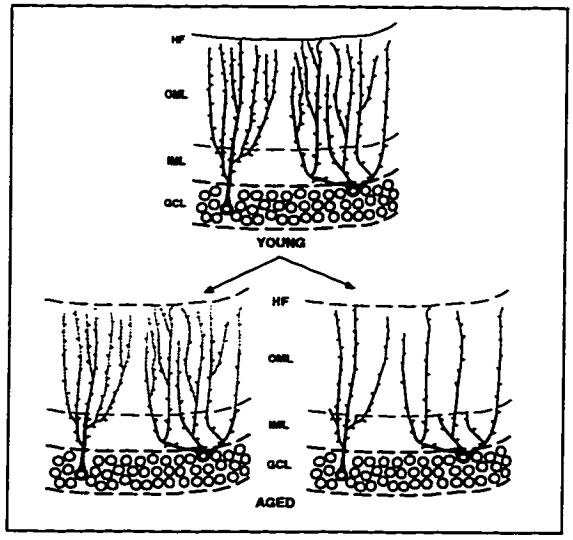

Figure 4.5: Schematic showing two possible interpretations of the data discussed in the text on age-related changes in NMDAR1 immunofluorescence. The lower left panel designates the scenario supported by our data. The results suggest that a decrease in NMDAR1 levels occurs within the dendritic segments of the OML relative to the IML in the aged rhesus monkey (lower left panel) as compared to the adult monkey (upper panel) in the absence of a significant loss of dendritic area within defined fields of the OML vs. IML (lower right panel).

in AD (Flood et al., 1987). We have also demonstrated by quantitative measures that the receptor change was NMDA receptor specific, even though all three classes of GluRs are colocalized within these dendrites (Siegel et al., 1995). This suggests that the intradendritic parcellation of a neurotransmitter receptor is specifically modifiable in an age-related and circuit-specific manner.

Both entorhinal lesion experiments in animals and post-mortem analyses of AD brains have revealed a dramatic decrease in synaptophysin immunoreactivity within the dentate gyrus OML (Cabalka et al., 1992). In this study, however, quantitative analysis revealed no change in the total synaptic density across the molecular layer. In addition, a recent quantitative study demonstrated that there was no loss of total synapses in the OML of the aged primate dentate gyrus (Tigges et al., 1995) or age-related loss of neurons in layer II of the primate entorhinal cortex (West et al., 1993), in sharp contrast to the extensive neuronal loss in this region in AD (Hyman et al., 1984). It should be noted that these reports do not parallel the observed loss of synapses in both the middle molecular layer (MML) and IML of aged rats (Geinisman et al., 1992), and physiological findings consistent with a reduction in the number of perforant path axons in aged rats (Barnes and McNaughton, 1980). These data may reflect species differences between rodents and primates in the effects of aging on these neural circuits. Nevertheless, it appears unlikely that the receptor alterations we observed in the molecular layer of the aged monkeys result from a

degeneration of the perforant path with concomitant deafferentation of the dentate gyrus, although the presence of functional changes in the perforant path that are not reflected anatomically (Barnes, 1994) cannot be ruled out as contributing factors to the receptor alterations. In addition, given that all the aged animals in this study were female, age-related changes in estrogen levels cannot be excluded as a potential contributing factor.

The combined use of subunit-specific GluR antibodies with quantitative CLSM analysis has provided a particularly high level of molecular and anatomical resolution in the present analysis, enabling us to demonstrate NMDAR1 subunit-specific changes in receptor concentration within segments of granule cell dendrites that correspond to the laminar segregation of inputs. Although we have not quantitatively ruled out subtle receptor changes in other hippocampal or neocortical regions, we have established that the segregated inputs to the dentate gyrus are differentially affected by aging. Given the crucial role that both the perforant path and NMDA receptors have in learning and memory, we hypothesize that the present findings provide a molecular/cellular substrate that may contribute to age-associated memory impairment, in contrast to the structural disconnections of hippocampal circuits that are a hallmark of AD pathology (Cabalka et al., 1992; Hyman et al., 1984). It will be of great interest to test this hypothesis in human and non-human primate populations with longitudinal behavioral assessment by correlating subtle circuit-specific molecular changes in the absence of overt neuron and synapse loss with age-related cognitive decline.

Chapter 5

Differential Regulation of NMDAR1 mRNA and Protein by Estradiol in the Rat Hippocampus

Abstract

Estradiol treatment increases the number of NMDA receptor binding sites and changes evoked synaptic currents in a manner consistent with a steroid induced functional enhancement of NMDA receptors in rat hippocampus. In this study, we investigate the cellular mechanisms of estradiol induced NMDA receptor regulation at the protein and mRNA levels in ovariectomized rats treated with ovarian steroids using immunocytochemical and *in situ* hybridization techniques. Confocal laser scanning microscopy was used to quantify alterations in immunofluorescence intensity levels of NMDAR1 subunit proteins within neuronal somata and dendrites of discrete hippocampal fields, while in parallel, *in situ* hybridization was used to examine NMDAR1 mRNA levels in corresponding hippocampal regions. The data indicate that estradiol treatment in ovariectomized rats significantly increases immunofluorescence intensity levels in comparison with non-steroid treated ovariectomized rats within the somata and dendrites of CA1 pyramidal cells and to a lesser extent within the granule cell somata of the dentate gyrus. In contrast, such alterations in immunofluorescence intensity occur without concomitant changes in mRNA hybridization levels. Thus, these data suggest that estradiol modulates NMDA receptor function via post-transcriptional regulation of the NMDAR1 subunit protein. The increase in immunofluorescence intensity may reflect an increase in the concentration of the subunit protein, which could account for estrogen induced changes in pharmacological and physiological properties of the NMDA receptor.

Introduction

Ovarian steroids affect brain regions and behaviors that are not directly associated with reproductive functions (McEwen et al., 1995). However, the mechanisms by which these effects are produced have not yet been determined. *N*-methyl-D-aspartate receptors (NMDARs), a subtype of ionotropic glutamate receptors (Moriyoshi et al., 1991), are implicated as mediators of effects of estradiol on morphological plasticity and related physiological and cognitive processes in the brain. For example, in the CA1 field of rat hippocampus estradiol treatment following ovariectomy increases dendritic spine density (Gould et al., 1990) and synapses (Woolley and McEwen, 1992) on pyramidal cells via a mechanism dependent on NMDAR activation (Woolley and McEwen, 1994). Additionally, intracellular recordings reveal that estradiol treatment increases the duration of EPSP's in a subpopulation of CA1 neurons, an alteration suggestive of an increased NMDAR contribution (Wong and Moss, 1992). Less direct evidence of NMDAR involvement in estrogen induced neural modifications includes estrogen's role in facilitating seizure induction (Backstrom, 1976; Buterbaugh and Hudson, 1991; Terasawa and Timiras, 1968) and memory and learning enhancement (Luine, 1994; Parnavelas et al., 1974; Philips and Sherwin, 1992a; Philips and Sherwin, 1992b; Singh et al., 1994) in both humans and experimental animals. This connection is based on the NMDAR's important role in seizure-triggering mechanisms (Gilbert, 1988; Sato et al., 1989) and memory and learning (Bliss and Collingridge, 1993; Morris et al., 1986).

Few studies have directly addressed the mechanisms underlying estrogen regulation of NMDARs. Autoradiographic analysis has revealed that NMDAR agonist binding sites are increased in the dendritic layer of CA1 in response to estradiol treatment in ovariectomized rats (Weiland, 1992). However, since an alteration in receptor stoichiometry or regulation by modulatory ligands can alter ligand binding, these results do not determine if steroidal treatment induced an increase in NMDA receptor subunit

protein levels in these neurons. Additionally, no studies have investigated the effect of ovarian hormone treatment on NMDAR subunit mRNA levels in hippocampal neurons. Therefore, the focus of this study is to elucidate the cellular mechanisms by which hippocampal NMDARs are regulated by ovarian steroids. Through the use of quantitative confocal laser scanning microscopy (CLSM), we have recently demonstrated that the immunocytochemically localized cytoplasmic pool of the NMDAR subunit 1 (NMDAR1), an obligatory subunit of the NMDAR complex (Monyer et al., 1992; Nakanishi, 1992), is modifiable in hippocampal neurons during aging (see Chapter 4) (Gazzaley et al., 1996a) and in response to deafferentation (see Chapter 6) (Gazzaley et al., 1996a). These data suggest that alterations in cytoplasmic receptor protein levels is a component of the neuronal response strategy to various conditions. To investigate the role of estradiol and progesterone in regulating NMDARs at the protein level, we performed a CLSM evaluation of NMDAR1 immunofluorescence intensity in the somata and dendrites of the dentate gyrus, CA1 and CA3 hippocampal fields of ovariectomized rats and ovariectomized rats treated with estradiol and estradiol plus progesterone. A CLSM analysis was selected for this study because it is performed on structurally intact tissue and permitted the evaluation of discrete cell groups and intracellular compartments, which would not have been possible by biochemical methods such as a western blot analysis of homogenized tissue extracts. Additionally, to determine whether changes observed at the protein level reflect changes at the level of gene transcription we examined NMDAR1 mRNA levels by quantitative *in situ* hybridization analysis in the same hippocampal regions.

Experimental Procedures

Animal and Tissue Processing

Forty three young adult Sprague-Dawley rats (Charles River, Wilmington, MA),

weighing approximately 250 g, were maintained in a temperature and light controlled environment with a light (14 hr): dark (10 hr) cycle (lights on at 0500 hr). Animals were treated in accordance with the principles and procedures of the NIH Guide for the Care and Use of Laboratory Animals, and all surgeries were performed under Metofane anesthesia. Sixteen rats were used in the immunocytochemical analysis. All sixteen rats were ovariectomized for one week at which time ten rats received Silastic capsules containing 180 μg of 17-β estradiol/sesame oil and the remaining six were sham operated. Two days later at 1000 hr, five of the estradiol-treated animals were injected subcutaneously with progesterone (1 mg. in 0.3 ml oil/rat) and all remaining animals were injected with oil. This procedure resulted in the following groups of ovariectomized rats: 6 sham plus oil (OVX), 5 estradiol plus oil (OVX+E) and 5 estradiol plus progesterone (OVX+E+P). Five hours after progesterone or oil injection (1500 hr), the animals were deeply anesthetized with Metophane and transcardially perfused with cold 1% paraformaldehyde in 0.1 M phosphate-buffered saline (PBS) followed by cold 4% paraformaldehyde in PBS. The brains were removed, postfixed in 4% paraformaldehyde and sectioned at 40 μm on a vibratome (OTS 3000, Electron Microscopy Sciences, Fort Washington, PA). The sections were stored in PBS with 0.1% sodium azide at 4°C.

Twenty seven rats were used for the *in situ* hybridization study. All rats were ovariectomized for 1 week and then adrenalectomized. Eighteen rats were then treated with Silastic capsules containing 180 μg of 17-β estradiol/sesame oil while the other nine where sham operated. Two days later at 1000 h, the animals were either injected subcutaneously with progesterone (1 mg. in 0.3 ml oil/rat) or oil resulting in the following groups of ovariectomized rats: 9 sham plus oil (OVX), 9 estradiol plus oil (OVX+E) and 9 estradiol plus progesterone (OVX+E+P). The animals were killed by decapitation five hours after progesterone or oil injection (1500 hr), and the brains were removed, frozen on dry ice and stored at -70°C.

In situ Hybridization

In situ hybridization was performed using previously published sequences of oligonucleotides (Oligos Etc., Inc., Wilsonville, OR) complementary to rat cDNA encoding subunit residues between putative transmembrane domains I and II, encoding amino acids 566-580 and recognizing all published splice variants (Monyer et al., 1992). A search of GenBank database indicated that there is no significant homology between any of these sequences and known mammalian gene sequences. Oligonucleotides were 3 ' end labeled with terminal transferase (Boehringer Mannheim, Indianapolis, IN) using a 2:1 molar ratio of [α-^{35}S] dATP:cDNA (1200-1400 Ci/mmol; New England Nuclear, Boston, MA). Unincorporated nucleotides were removed using NucTrap push columns (Stratagene Cloning Systems, La Jolla, CA). Hybridization was performed as previously described (Orchinik et al., 1994). Briefly, sections were fixed in 4% paraformaldehyde, acetylated, hybridized with saturating concentrations of labeled oligonucleotides overnight at 42°C, washed to a final stringency of 0.1X SSC (1X = 0.15 M NaCl and 0.015M sodium citrate) at 55°C for 1 hr, dehydrated and exposed to Hyperfilm-βmax (Amersham Corp., Arlington Heights, IL) for 24 hrs.

Quantitative *In Situ* Hybridization Analysis

The films were analyzed by measuring the optical density of specific regions of the hippocampus using an automated paint function which covered the region of interest (Imaging Research, Inc., St. Catherines, Ontario, Canada). Bilateral measurements were taken from 4 sections per animal, 9 animals per group in the principal cell layer of CA1, CA3 and the suprapyramidal layer of the dentate gyrus. Background was measured from the corpus callosum and subtracted from the total optical density.

Immunocytochemistry

Three non-adjacent sections from the rostral hippocampus of each rat were incubated with monoclonal antibodies to both the NMDAR1 subunit (54.1; (Siegel et al., 1994)

and microtubule-associated protein 2 (MAP2) (Huber and Matus, 1984) at a concentration of 4.6 µg/ml and 2.5 µg/ml respectively, in PBS for 48 hours. Sections were then washed three times in PBS, transferred to biotinylated anti-mouse IgG H&L (Vector Laboratories, Burlingame, CA) for 2 hours, washed again in PBS and transferred to FITC-conjugated Avidin (Vector Laboratories, Burlingame, CA) for 1 hour. Sections were then mounted, and coverslipped with Vectashield (Vector Laboratories, Burlingame, CA) to reduce fluorescence quenching.

CLSM and Quantitative Immunocytochemical Evaluation

Quantitative CLSM analysis was performed on three sections from each rat brain, for each of the two antibodies, with a Zeiss LSM 410 inverted confocal microscope. The investigator was blinded throughout the evaluation as to which sections were from which experimental group. The quantitative analysis performed in this study was adapted from a previous study which quantified relative differences in immunofluorescence intensity levels (see Chapter 4) (Gazzaley et al., 1996b). The confocal parameters were established at the beginning of the study and remained constant throughout. An Argon/ Krypton laser was used to excite FITC at 488 nm. A 90% neutral density filter was used to attenuate the light and a confocal aperture pinhole setting of 17 was set digitally. The image was visualized with a Zeiss Plan-Neofluar 63x/1.25 N.A. oil immersion objective. For each antibody, a contrast/brightness setting was selected that yielded a high resolution image for both bright and dim sections without exceeding a maximal pixel intensity of 255. For the NMDAR1 analysis, a separate contrast/brightness setting was established for somata and dendrites due to a considerable intensity difference between them that prevented the use of a single setting. All of the settings were kept constant throughout the analysis to yield unbiased measurements for each set of comparisons.

For the study of somatic immunofluorescence intensity, six fields were randomly

selected on each section within a centrally located region of the suprapyramidal blade of the dentate gyrus granule cell layer and the middle portion of the CA1 and CA3 pyramidal cell layer. The dendritic immunofluorescence intensity study consisted of six randomly selected dendritic fields, on each section, from the middle molecular layer of the dentate gyrus and the stratum radiatum of CA1 adjacent to the somatic regions analyzed in the somatic immunofluorescence analysis. All dendritic fields scanned were the same size (3832 μm^2) and were all selected at a distance of approximately 70μm from the principal cell layers. Each field was scanned only once, in order to reduce fluorescence quenching, and at the same predetermined z-axis distance from the surface of the section. Scanning was performed with a two line average for a total scan time of 4.52 s and an electronic zoom factor of 3.28 which increased the resolution to 0.0081 μm/pixel. Each digitized image consisted of a 512 X 512 X 8- bit pixel array in which every pixel was assigned a gray level intensity value ranging from 0 to 255. An image analysis program (Zeiss, Inc., Thornwood, NY) was used to determine the average pixel intensity of each field. To remove the negative contribution of unlabeled portions of the field to the average field intensity (i.e. nuclei, and unlabeled regions between soma and dendrites), a photometric offset was used to establish a pixel intensity threshold below which a pixel would have no contribution to the average pixel intensity of the field. The threshold was set by viewing the image at a display magnification of 2 X and manually increasing the thresholding value until a blue-colored display,

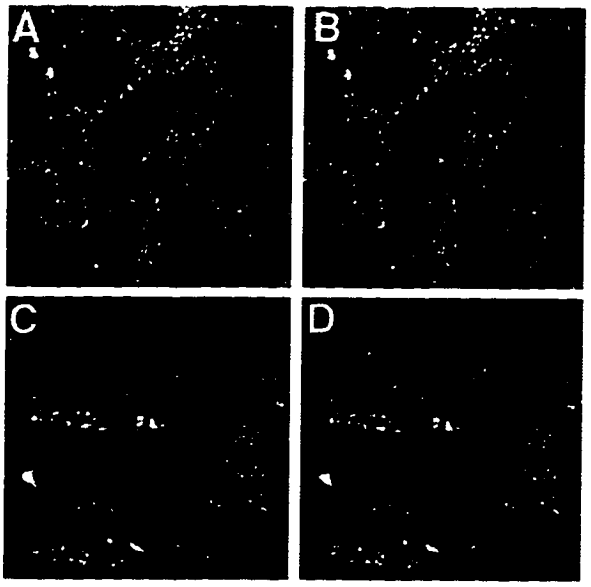

Figure 5.1 Confocal images of NMDAR1 immunolabeled CA1 pyramidal cell somata (A and B) and dendrites (B and C) before (A and C) and after (B and D) intensity thresholding as indicated by the gray-color overlay within the nuclei and between the dendrites.

designating the thresholded area, completely occupied the unstained nuclei and abutted upon somatic and dendritic profiles (Fig. 5.1). Thus, the average pixel intensity of the portion of the field above threshold represents the immunofluorescence intensity within either the dendritic segments or the somata of the principal cell layers.

Data Analysis

For the CLSM immunocytochemical analysis, an intensity value was computed for each animal, in each of the three regions, by determining the mean of the 24 individual field values (six field values obtained from each of three sections). For both the immunocytochemical and *in situ* hybridization analysis, a mean value for each group was obtained from the individual values determined for each animal, in CA1, CA3 and the dentate gyrus. Percent difference was determined by comparing the steroid-treated ovariectomized rats to the non-treated ovariectomized rats (i.e., ((OVX+E)- (OVX))/ (OVX) or ((OVX+E+P)- (OVX))/ (OVX)). All the data were analyzed with a one-way analysis of variance (ANOVA), at a significance level of <0.05, and a Sheffe's post-hoc test.

Results

NMDAR1: Somatic Immunofluorescence Intensity

NMDAR1 immunolabeling was evaluated in three groups of rats; ovariectomized rats (OVX) and ovariectomized rats that had been treated with either estradiol (OVX+E) or estradiol plus progesterone (OVX+E+P). This steroid treatment paradigm has been used previously by Weiland and Orchinik (1995) and results in serum estrogen levels of about 20 pg/ml and progesterone levels of 60 ng/ml, which mimic preovulatory hormone levels. Non-ovariectomized rats were not used in this study since estrogen levels fluctuate throughout the estrous cycle. In animals from all three groups, NMDAR1 immunofluorescence was present within the cell bodies and dendrites of the hippocampal

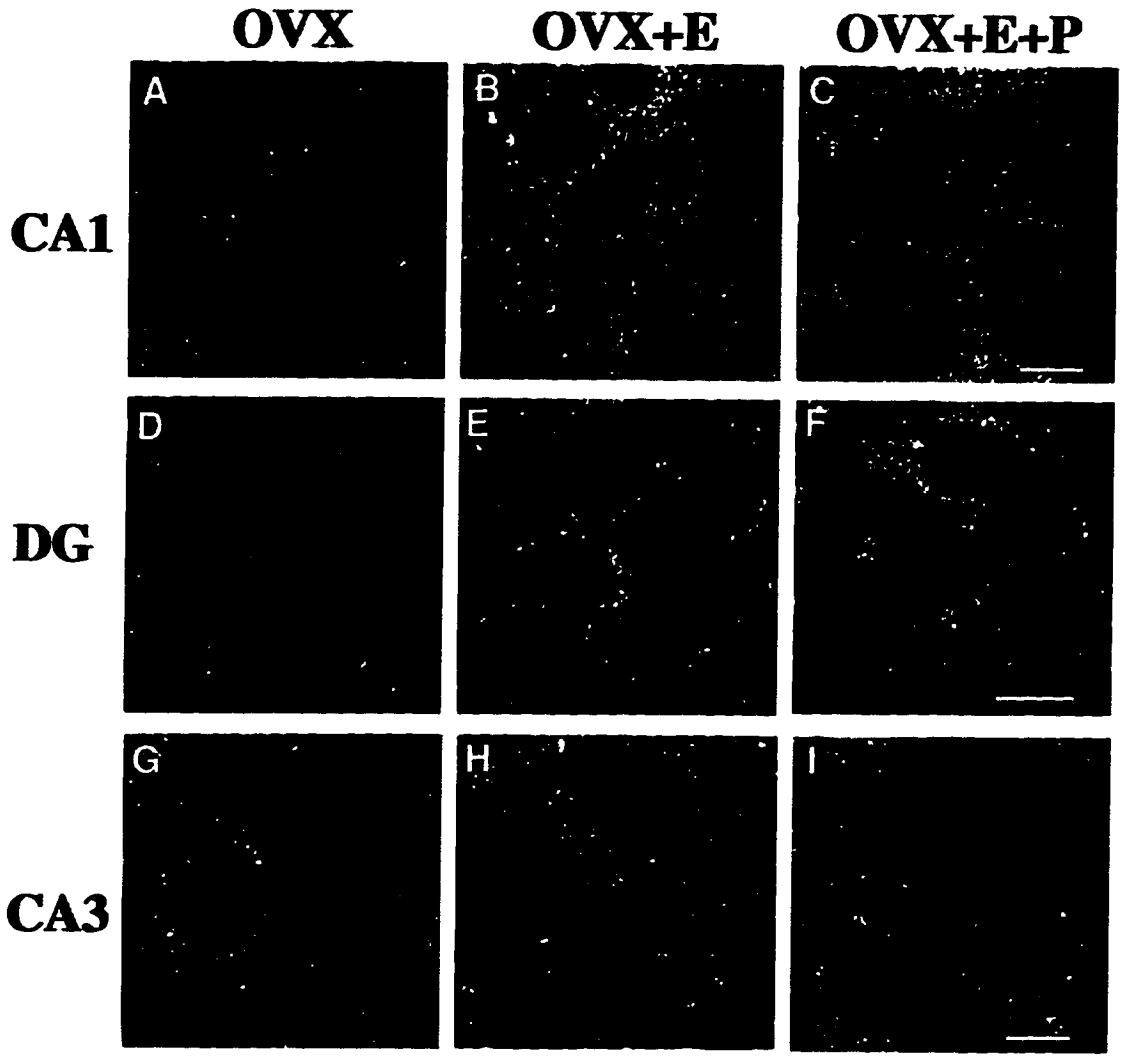

Figure 5.2 Examples of CLSM images of NMDAR1 immunolabeled somata in CA1 (A-C), the dentate gyrus (D-F) and CA3 (G-I) of OVX (A,D,G), OVX+E (B,E,H), and OVX+E+P (C,F,I) rats. Note the presence of punctate staining within the cytoplasm surrounding the unlabeled nuclei (see discussion). When comparing the CA1 fields, an increase in the somatic intensity of staining is evident in the OVX+E and OVX+E+P rats (B and C) as compared to the OVX rats (A). This increase in the steroid-treated ovariectomized rats is also apparent in the dentate gyrus (E & F compared to D), although to a lesser extent. There is no obvious difference in intensity levels between the three groups in the CA3 field (G,H,I). DG, dentate gyrus; OVX, ovariectomized rats; OVX+E, estradiol-treated ovariectomized rats; OVX+E+P estradiol plus progesterone-treated ovariectomized rats. Scale bars:10μm.

principal neurons, a general pattern consistent with earlier descriptions of NMDAR1 immunolabeling in the male rat hippocampus (Petralia et al., 1994). Confocal images of pyramidal cells within the CA1 and CA3 subfields and granule cells of the dentate gyrus revealed a patchy intracellular distribution of immunofluorescence throughout the somatic and dendritic cytoplasm, while nuclei contained no labeling (FIG. 5.2 and

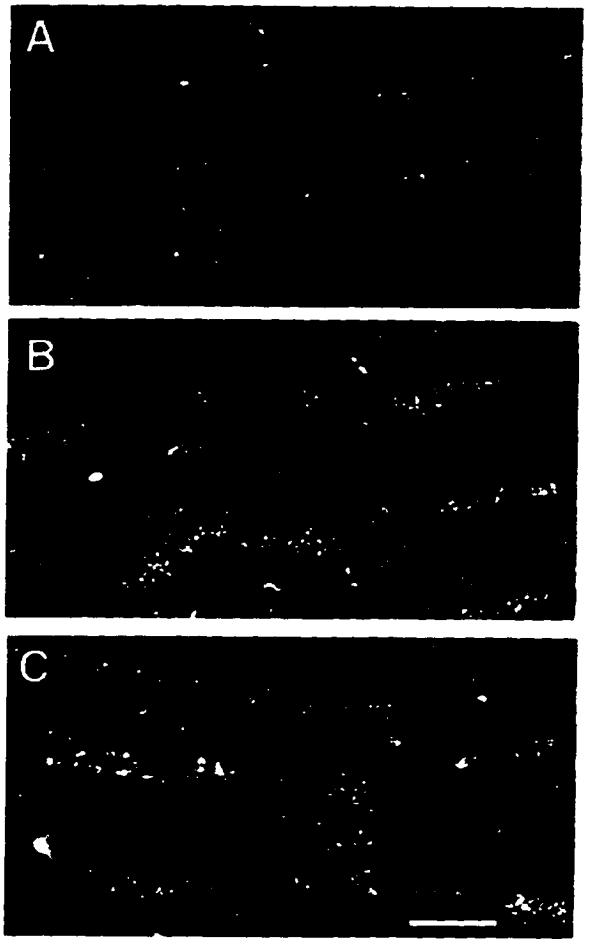

Figure 5.3 Examples of CLSM images of NMDAR1 immunolabeled dendrites in the CA1 subfield of an OVX rat (A), an OVX+E rat (B), and an OVX+E+P rat (C). Note the presence of punctate staining within the cytoplasm of the dendritic segments (see discussion) and the increased intensity of staining within the CA1 dendrites of the steroid-treated ovariectomized rats (B and C) rats compared to the non-steroid treated ovariectomized rats (A). Scale bar: 10μm.

5.3). There were no observable qualitative differences in overall distribution and intracellular pattern of immunolabeling between OVX rats and steroid-treated ovariectomized rats.

Immunofluorescence intensity levels of the cytoplasmic pool of receptors within the somata of the CA1 and CA3 pyramidal cell layers and the dentate gyrus granule cell layer were obtained by CLSM quantitative analysis. All statistical comparisons were made between the three groups, within a given hippocampal subfield. In the CA1 subfield of either the OVX+E or OVX+E+P group, quantitative data revealed a significant intensity increase within the pyramidal cell somata of 52.2% in comparison with the OVX group (Fig. 5.2 a,b,c; Fig.5.4a). No difference in intensity levels were evident between the two steroid-treatment groups.

In the dentate gyrus, a smaller, but statistically significant intensity increase was observed within the somata of the granule cells in OVX+E (31.3%) and OVX+E+P (33.5%) rats relative to the OVX rats (Fig. 5.2 d,e,f; Fig. 5.4a). This intensity increase was of a significantly lower magnitude than that recorded in the CA1 field, as determined by a statistical comparison of the CA1/ DG ratio between the three groups, which revealed a significant increase in the ratio in the steroid-treatment groups as compared to OVX

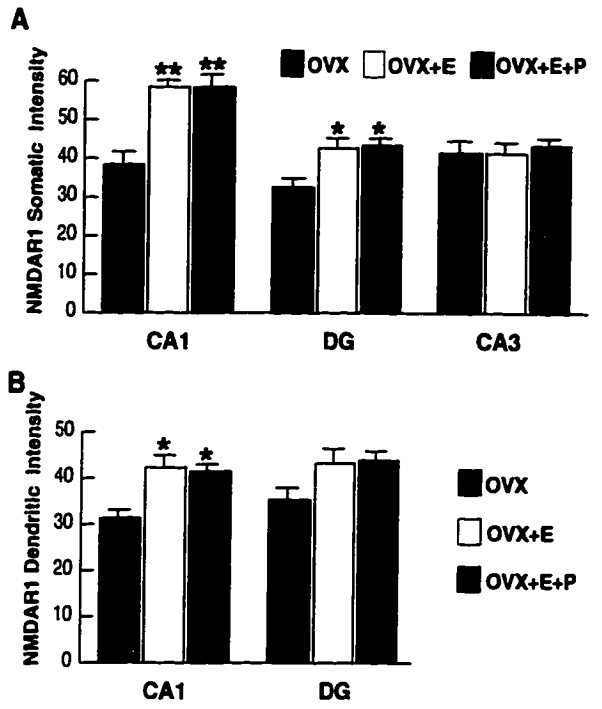

Figure 5.4 Bar graphs depicting NMDAR1 immunofluorescence intensity measurements in the somata (A) and dendrites (B) of the CA1, dentate gyrus (DG) and CA3 fields of the hippocampus. For somatic intensity measurements (A) there is a significant increase in both CA1 and the dentate gyrus when comparing OVX+E and OVX+E+P rats to OVX rats. Based upon the results of the somatic intensity measurements (A), the CA1 and the DG dendritic fields were quantified (B). In (B) note that there are significant increases only in the dendritic intensity measurements of steroid-treated rats as compared to the OVX rats in the CA1 subfield, although there is a trend toward increase in the dentate gyrus. Values represent means ± SEM for 6 OVX rats and 5 OVX+E and OVX+E+P rats (24 measurements per rat). * $p<0.05$, ** $p<0.0001$ compared with OVX group; (ANOVA and Sheffe's test).

group. As in the CA1 subfield, there was no significant difference between the OVX+E and the OVX+E+P groups.

Quantitative analysis of the somata of the CA3 pyramidal cells revealed no difference in immunofluorescence intensity levels between the three groups (Fig. 5.2 g,h,i; Fig. 5.4 a).

NMDAR1: Dendritic Immunofluorescence Intensity

To investigate the cytoplasmic pool of the NMDAR1 subunit protein within the dendrites of the two regions where a somatic intensity increase was observed, we analyzed fields of dendritic segments in the CA1 stratum radiatum and the dentate gyrus molecular layer. Quantitative analysis revealed a statistically significant increase in intensity within the dendritic segments of the CA1 field when comparing both the OVX+E and the OVX+E+P group to the OVX group (35% and 32%, respectively) (Fig. 5.3 a,b,c; Fig. 5.4b). There was no significant intensity difference between the two steroid-treated groups in the CA1 dendrites. Analysis of the dentate gyrus dendritic fields revealed no significant difference between the three groups but there was a trend

toward an increase in both steroid-treated groups compared to the OVX group (Fig. 5.4b).

MAP2: Somatic Immunofluorescence Intensity

To access whether the NMDAR1 intensity change may have been the result of a more general increase in protein production, an identical quantitative analysis was performed following immunocytochemical staining with a monoclonal antibody to MAP2. MAP2 was selected because it is localized specifically within the soma and dendrites of all principal cells in the hippocampus and there are no reports of estradiol-induced changes in MAP2 cytoplasmic concentration. Quantitative and qualitative analysis revealed no significant differences in immunofluorescence intensity or distribution between the three groups in the somata of any hippocampal field analyzed (Fig. 5.5 a-i; Fig. 5.6).

NMDAR1 mRNA Labeling

To determine whether a change in immunofluorescence intensity levels of the NMDAR1 protein corresponded to an alteration in gene transcription, *in situ* hybridization analysis of NMDAR1 mRNA levels was performed. Hybridization signal was localized within the somata of the dentate gyrus granule cells and the pyramidal cells of the CA fields (Fig 5.7), and no overt differences were observed in the overall distribution of hippocampal mRNA labeling in comparison to that previously described in the rat brain (Moriyoshi et al., 1991). Densitometric analysis of the films determined that there was no significant difference in silver grain intensity in the principal cell layers of CA1, CA3 and the dentate gyrus across the three groups (Fig. 5.8).

Discussion

In the present study, quantitative confocal microscopic evaluation of NMDAR1

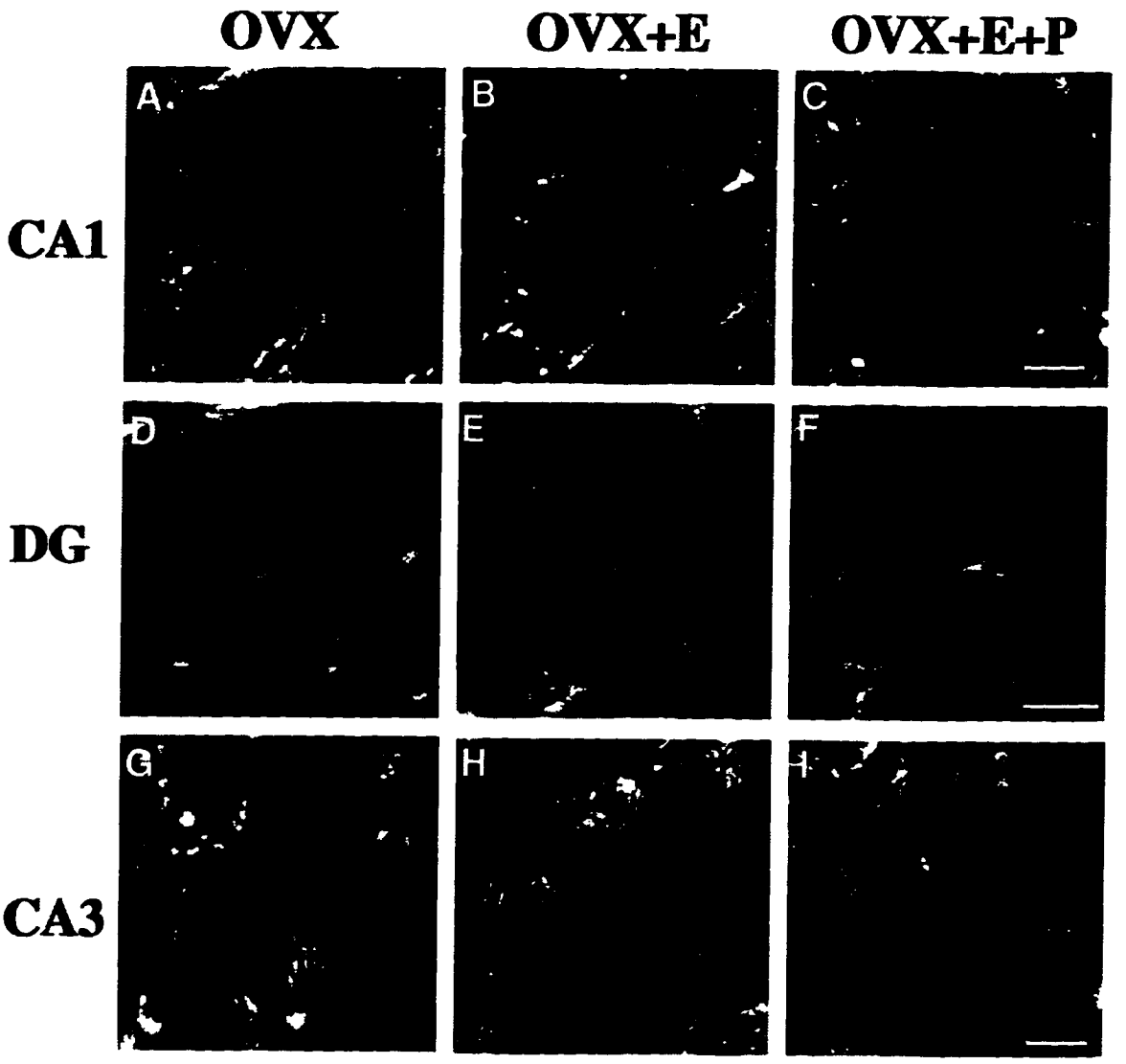

Figure 5.5 Examples of CLSM images of MAP2 immunolabeled somata in CA1 (A-C), the dentate gyrus (D-F) and CA3 (G-I) of OVX rats (A,D,G), OVX+E rats (B,E,H), and OVX+E+P rats (C,F,I). Note that there is no obvious differences in intensity levels when comparing between the different experimental groups within any hippocampal subfield.. Scale bars: 10μm.

immunofluorescence intensity revealed that both estradiol and estradiol plus progesterone-treatment in ovariectomized rats induced a significant intensity increase within the somata and dendrites of CA1 pyramidal cells in comparison with non-steroid treated ovariectomized rats. A smaller, though statistically significant, increase was also observed within the somata of the dentate gyrus granule cells of steroid-treated animals in comparison with non-treated ovariectomized animals, but not within their

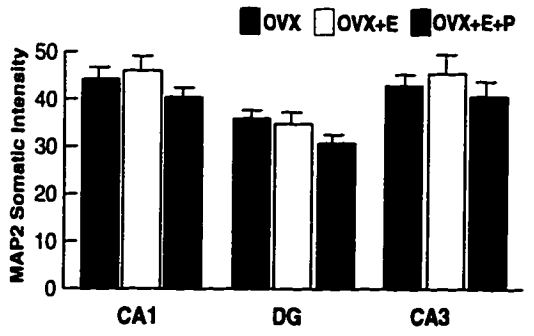

Figure 5.6 Bar graphs depicting MAP2 immunofluorescence intensity measurements in the somata of the CA1, dentate gyrus and CA3 fields of the hippocampus. Quantitative analysis revealed no statistically significant differences between the three groups when comparing within a hippocampal field. Values represent means ± SEM for 6 OVX rats, 5 OVX+E and OVX+E+P rats (24 measurements per rat).

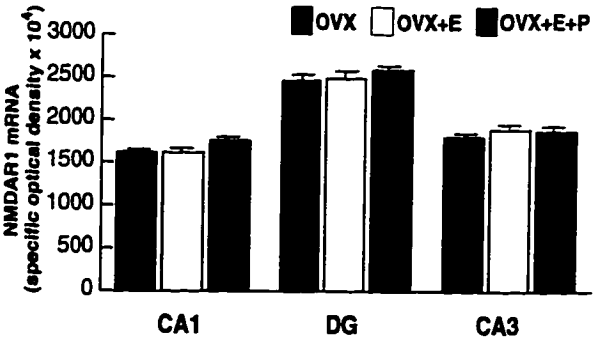

Figure 5.8 Bar graphs depicting the quantification of NMDAR1 mRNA labeling in the CA1, dentate gyrus, and CA3 subfields of the hippocampus. There were no statistically significant differences in optical density measurements in any of the subfields between the three groups. Values represent means ± SEM for 9 OVX rats, 9 OVX+E and 9 OVX+E+P rats.

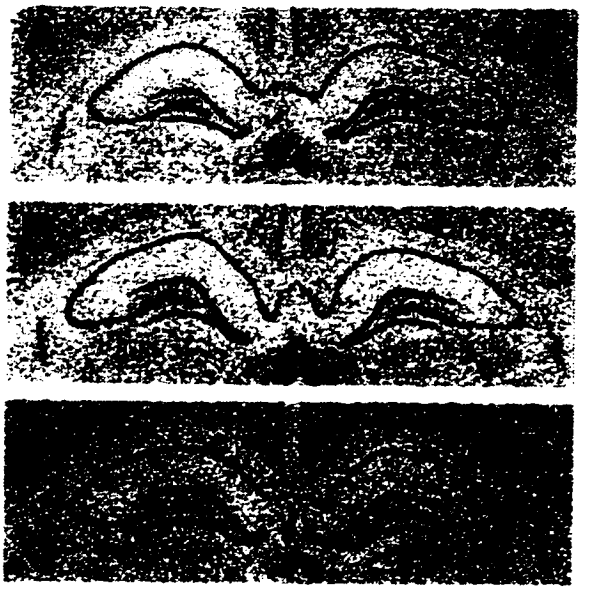

Figure 5.7 Photomicrographs of film autoradiograms show NMDAR1 mRNA hybridization in the hippocampus of an (A) OVX rat, an (B) OVX+E rat and (C) an OVX+E+P rat. Note that there is no overt difference in hybridization distribution or intensity in the hippocampal subfields between rats from different treatment groups.

dendrites. Since there was a trend toward an intensity increase in the granule cell dendrites, the absence of a significant change may have been the result of an inability to detect small intensity increases due to a degree of variability inherent in this technique. Additionally, there were no detectable differences in intensity levels within CA3 pyramidal cell somata of animals from all three groups. *In situ* hybridization analysis revealed no accompanying detectable alterations in NMDAR1 mRNA levels in any hippocampal subfield in steroid-treated rats as compared to OVX rats.

Interpretation of NMDAR1 Immunofluorescence Intensity Data

The use of confocal microscopy yields high resolution, cross-sectional images of neurons, which when coupled with gray-level intensity quantification and a photometic offset enabled us to obtain intensity measurements within major cellular compartments. Several factors contribute to the validity of the immunofluorescence intensity results as representing significant alterations between non-treated ovariectomized rats and steroid-treated ovariectomized rats. First, methodological variability was reduced by rigidly controlling tissue processing, immunofluorescent staining, confocal parameters and analysis design. As a result, variability was minimized and intensity changes that were both consistent and of a substantial magnitude yielded statistically significant results. Additionally, the positive findings were regionally specific and occurred with greatest magnitude in CA1, the hippocampal field where estrogen induced morphological changes have been observed (Gould et al., 1990; Woolley and McEwen, 1992; Woolley and McEwen, 1994; Woolley et al., 1990). Our results also correlate with an increased number of NMDAR agonist binding sites (Weiland, 1992) and a suggested functional increase in NMDAR-mediated synaptic activity (Wong and Moss, 1992) in the CA1 neurons following estradiol treatment. Lastly, no intensity differences were observed in any hippocampal field following an identical analysis with a monoclonal antibody to MAP2, arguing against a more general increase in protein production.

Immunoelectron microscopic descriptions of the ultrastructural distribution of the NMDAR1 subunit aids in the interpretation of our results. Similar to our qualitative CLSM observations, electron microscopic descriptions of rat hippocampal neurons revealed a patchy distribution of NMDAR1 immunocytochemical deposition throughout the somatodendritic cytoplasm (Petralia et al., 1994). In the somata and dendrites these patches were associated with bundles of microtubules and the surface of mitochondria, as well as with rough endoplasmic reticulum, golgi apparatus and the nuclear envelope in somata (Petralia et al., 1994). The association of concentrations of NMDAR1 subunits

with these subcellular structures suggests that the cytoplasmic patches represent the synthesis, processing and transport pools of the protein. Previous CLSM investigations have demonstrated that immunoreactive intensity can reflect protein concentration (Dodge et al., 1993; Good et al., 1992), suggesting that our data may also represent alterations in protein concentration within these cytoplasmic pools. Given both an increase in NMDA agonist binding sites at the membrane (Weiland, 1992) and an increase in synaptic activity consistent with an enhancement of the NMDAR (Wong and Moss, 1992), alterations in the cytoplasmic pool of receptors appear to be reflected at the synaptic level.

Mechanism of Estrogen Regulation of the NMDAR

Consideration of both the immunofluorescence intensity and *in situ* hybridization data together suggest that alterations in NMDAR1 immunofluorescence are the result of post-transcriptional regulation of the NMDAR1 protein. Reasonable possibilities of post-transcriptional regulation include an increase in rate of protein translation and/or post-translational modifications such as an alteration in the rate of protein degradation. Given the association of NMDAR1 protein with microtubules in the dendrites, intensity increases in the CA1 dendrites may be the result of increased dendritic transport. It is possible that the *in situ* hybridization technique is not sensitive enough to detect subtle changes in mRNA levels, however, post-transcriptional control of NMDAR1 protein expression has previously been demonstrated in PC12 cells where NMDAR1 mRNA is transcribed but not translated (Sucher et al., 1993). Additionally, two examples of post-transcriptional regulation of the NMDAR1 subunit has been recently documented. Both cultured cortical neurons that were chronically treated with an NMDAR antagonist (Follesa and Ticku, 1996) and the hippocampus of rats treated chronically with ethanol (Follesa and Ticku, 1995; Trevisan et al., 1994), exhibited increased levels of NMDAR1 protein with no detectable change in NMDAR1 mRNA levels.

The mechanism of regulation suggested by these results is somewhat different from the classical cellular mechanism of steroid hormone regulation of gene transcription. This is indicated by previous observations which suggest that estrogen regulation of NMDARs may be mediated by transsynaptic interactions (Weiland, 1992; Woolley and McEwen, 1993; Woolley and McEwen, 1994). Indeed, putative intracellular estrogen receptors identified by autoradiography (Loy et al., 1988) and immunocytochemistry (Don Carlos et al., 1991; Weiland et al., 1996) are never found in CA pyramidal neurons but rather are found in interneurons in the CA1, subiculum and dentate gyrus subfields. Interestingly, very few such estrogen-sensitive interneurons are found in the CA3 region (Loy et al., 1988), where we could find no estrogen effect on NMDAR1 immunofluorescence intensity in the present study. An estrogen mediated increase in the expression of NMDARs and an increase in the density of excitatory spine synapses on CA1 pyramidal neurons that occur in an NMDA-dependent manner (Woolley and McEwen, 1994) may thus be reflections of the same underlying mechanism. This mechanism may involve a transsynaptic control of the excitability of pyramidal neurons via estrogen receptors in inhibitory interneurons, or it may reflect actions of estrogen more directly on the excitability of pyramidal neurons themselves by an as of yet undefined membrane mechanism. In either case, estrogen-induced changes in neuronal excitability may increase functional demands on the pyramidal neurons, leading to increased post-transcriptional expression of NMDAR1.

A more detailed characterization of estrogen induced NMDAR protein regulation remains to be elucidated. The subcellular distribution of the NMDAR1 subunit has been demonstrated to be controlled by specific amino acid sequences that are located within a C terminal exon that is subject to alternative splicing (Ehlers et al., 1995). The antibody used in this study detects all NMDAR1 splice variants. Future studies using splice variant specific antibodies are necessary to determine if estrogen induced regulation is NMDAR1 splice variant specific. Additionally, a possible stoichiometric

change in the NMDAR complex in CA1 is suggested by disparate results obtained using different agonist versus antagonist NMDAR binding ligands (Weiland, 1992). A stoichiometric change may also account for our determination of a subtle intensity increase in the dentate gyrus, while autoradiographic analysis revealed no change in NMDA agonist binding and a sight decrease in NMDA noncompetitive antagonist binding in the dentate gyrus (Weiland, 1992). The NMDAR is a heteromeric complex of several subunits, most likely consisting of an NMDAR1 subunit and one or more of four different NMDAR2 subunits that affect function and ligand binding characteristic (Hollmann and Heinemann, 1994; Monyer et al., 1992). Differential regulation of NMDAR subunits will be investigated following the development of antibodies specific for NMDAR2 subunits.

Functional Significance

Estradiol has an important role in cognitive function in experimental animals (Luine, 1994; Singh et al., 1994) and in maintaining certain memory functions in surgically postmenopausal women given estradiol replacement therapy, which are compromised in women not given estradiol (Philips and Sherwin, 1992b). Additionally, in some women, specific memory functions were found to covary with sex steroid plasma concentrations across the menstrual cycle (Philips and Sherwin, 1992a). Considering the well established role of the hippocampus (Alvarez et al., 1995; Zola et al., 1986) and NMDARs (Bliss and Collingridge, 1993; Morris et al., 1982) in learning and memory formation, estrogen may affect memory by maintaining dendritic spines (Gould et al., 1990), excitatory synapses (Woolley and McEwen, 1992) and NMDARs in specific hippocampal neuronal populations via mechanisms suggested in this study. We have previously characterized an intradendritic alteration in NMDAR1 immunofluorescence intensity within the dentate gyrus of aged female monkeys that revealed a decrease in intensity within dendritic segments of the outer molecular layer relative to dendritic

segments of the inner molecular layer (see Chapter 4) (Gazzaley et al., 1996b). Given our present findings of estrogen's role in regulating NMDAR1 immunofluorescence in the dentate gyrus following ovariectomy, it is possible that an age-related estrogen decrease in the aged female monkeys may have contributed to the NMDAR1 alterations observed previously.

In addition to increasing the duration of EPSP's in CA1 neurons in a manner suggestive of NMDAR enhancement, estrogen treatment also induced repetitive firing in some CA1 neurons that resembled epileptic bursting responses (Wong and Moss, 1992). These findings are consistent with other studies which revealed that estradiol replacement facilitates the induction of kindled seizures (Buterbaugh and Hudson, 1991) and decreases the threshold for seizure induction (Terasawa and Timiras, 1968) in the hippocampus of ovariectomized rats. Additionally, an increased incidence of seizures were observed in women with catamenial epilepsy that correlated with fluctuations in estrogen levels across the menstrual cycle (Backstrom, 1976). Based on the NMDAR's important role in seizure induction in experimental animals (Gilbert, 1988; Sato et al., 1989), estrogen may induce seizure activity by regulation of the NMDAR via modification of the NMDAR1 protein. Although there is no direct evidence for the link between estrogen induced NMDAR regulation and behavioral changes, it is reasonable that post-transcriptional NMDAR1 regulation has functional implications for learning and memory formation, age-related cognitive decline, and seizure induction.

Chapter 6

Differential Subcellular Regulation of NMDAR1 Protein and mRNA in Dendrites of Dentate Gyrus Granule Cells Following Perforant Path Transection

Abstract

Unilateral lesion of the excitatory perforant path results in the acute deafferentation of a segregated zone on the distal dendrites of hippocampal dentate gyrus granule cells (i.e. outer molecular layer), followed by sprouting, reactive synaptogenesis and a return of physiological and behavioral function. To investigate cellular mechanisms underlying NMDA receptor plasticity in response to such extensive synaptic reorganization, we quantitatively evaluated changes in intensity levels of NMDAR1 immunofluorescence and NMDAR1 mRNA hybridization within subcellular compartments of dentate gyrus granule cells 2, 5, and 9 days following perforant path lesions. There were no significant changes in either measure at 2 days post-lesion. However, at 5 and 9 days post-lesion, during the period of axonal sprouting and synaptogenesis, there was an increase in NMDAR1 immunolabeling that was restricted to the dendritic segments of the denervated outer molecular layer and the granule cell somata. In contrast, NMDAR1 mRNA levels at 5 and 9 days post-lesion increased throughout the full extent of the molecular layer, including both denervated and non-denervated segments of granule cell dendrites. These findings reveal that NMDAR1 mRNA is one of a limited population of mRNAs that is transported into dendrites, and further suggests that in response to terminal proliferation and sprouting, increased mRNA transport occurs throughout the full dendritic extent, while increased local protein synthesis is restricted to denervated regions of the dendrites whose afferent activity is perturbed. These results begin to elucidate the dynamic post-synaptic subcellular regulation of receptor subunits associated with synaptic plasticity following denervation.

Introduction

Plasticity of neurotransmitter receptor number or distribution is a key component of the compensatory neuronal response to denervation and changes in afferent activity (Klein et al., 1989). Although classically associated with the peripheral nervous system (Frank et al., 1975; Lømo and Rosenthal, 1972) plasticity of this kind has also been demonstrated in the CNS. For example, glutamate receptors (GluRs), which mediate most fast excitatory neurotransmission in the CNS, are responsive to various experimental perturbations in afferent activity. In several regions, including neocortex, hippocampus and cerebellum, the number of GluR binding sites and/or levels of GluR subunit mRNAs are influenced by exposure to pharmacological agents (Bessho et al., 1994; Williams et al., 1992), the induction of long-term potentiation (LTP) (Maren et al., 1993; Thomas et al., 1994a), the induction of seizure activity (Friedman et al., 1994; Gold et al., 1996; Kamphuis et al., 1994) and deafferentation (Geddes et al., 1985; Ulas et al., 1990). One subtype of ionotropic GluR, the *N*-methyl-D-aspartate receptor (NMDAR), is thought to play a key role in synaptic plasticity, particularly that associated with the establishment of connectivity during development (Shatz, 1990), and the induction of LTP, a synaptic model of learning and memory (Bliss and Collingridge, 1993; Bliss and Lømo, 1973). Additionally, alterations in the number of NMDAR binding sites occur during aging (Tamura et al., 1991; Wenk and Walker, 1991). We have recently shown that in aged monkeys, a decrease in the immunofluorescence intensity of the obligatory subunit NMDAR1 is evident within the segments of granule cell dendrites that receive the perforant path input from the entorhinal cortex, in comparison with more proximal dendritic segments that do not receive this input (see Chapter 4) (Gazzaley et al., 1996b). Based on this finding, we hypothesized that intradendritic levels of NMDAR1 are dynamic, and modifiable by alterations in the afferent activity of the perforant path.

To explore this hypothesis, we focus in the present study on the dynamic regulation

of NMDAR1 in rat dentate gyrus following synaptic reorganization induced by unilateral transection of the perforant path input from the entorhinal cortex. The perforant path input to the dentate gyrus selectively terminates on the ipsilateral distal two-thirds of the granule cell dendrites, which corresponds to the outer molecular layer (OML) (Steward, 1976). Two-four days following unilateral lesion of the entorhinal cortex, a 90% loss of synapses is confined almost exclusively to the OML (Matthews et al., 1976a; Steward and Vinsant, 1983), thus allowing investigation of receptor changes during terminal degeneration on spatially restricted segments of dendrites. This model also allows the study of receptor changes during a period of terminal proliferation (sprouting) and reactive synaptogenesis. Following denervation, terminal proliferation begins in the OML 4-6 days post-lesion (Lynch et al., 1977; Steward and Vinsant, 1983), and is characterized by sprouting of excitatory afferents from commissural/associational pathways (Zimmer, 1973) and the contralateral entorhinal cortex (Steward et al., 1974), along with some degree of physiological and behavioral recovery (Loesche and Steward, 1977; Reeves and Smith, 1987; Reeves and Steward, 1988). This is followed by a period of new synapse formation that begins 8-10 days post-lesion (Steward and Vinsant, 1983) and eventually results in the restoration of approximately 80% of the synapses (Matthews et al., 1976b).

Functionally, the perforant path input to the dentate gyrus provides the major conduit for information flow from the neocortex into the hippocampus and is thus a crucial component in memory processing (Skelton and McNamara, 1992; Vnek et al., 1995). This is underscored by observations that the entorhinal cortex is extremely vulnerable to pathological changes during aging (Bouras et al., 1994; Hof and Morrison, 1994; Price et al., 1991) and is devastated in Alzheimer's disease by a severe loss of the neurons of origin of the perforant path (Hyman et al., 1984; Lippa et al., 1992). Thus, understanding compensatory changes in NMDAR1 levels or distribution following perturbations of the perforant path may be crucial for understanding mechanisms of

memory loss associated with aging and disease. Although previous studies evaluating GluR plasticity following unilateral entorhinal cortex lesion have used autoradiographic techniques to assess alterations in various GluR ligand binding sites (Geddes et al., 1985; Ulas et al., 1990), such studies do not reveal details of the cellular and molecular mechanisms that may be the basis of physiological and behavioral recovery. The specific goals of this study, therefore, are to characterize temporal and spatial aspects of the regulation and localization of NMDAR1 protein and mRNA in the dentate gyrus following unilateral transection of the perforant path.

Experimental Procedures

Animals, Surgery and Tissue Processing

A total of thirty-eight male Sprague-Dawley rats weighing approximately 500 g were used in this study. Of these, 24 animals received a unilateral transection of the angular bundle; 5 were sham-lesioned and 9 control animals were not operated upon. All animals were cared for and treated in strict accordance with institutional and NIH guidelines. Animals were anesthetized with 30% chloral hydrate and placed into a Kopf stereotaxic frame. Stereotaxic transections of the perforant path (angular bundle) were made with an extendable Scouten wire knife (Kopf Inc., Tujunga, CA) as described previously (Laping et al., 1994; Schauwecker et al., 1996). The retracted knife was inserted into the brain 1 mm anterior and 6.3 mm lateral to lambda, to a level 5 mm ventral from the surface. The knife was extended 2.5 mm medially, raised 4 mm, and then retracted. This procedure was repeated at a position 1 mm anterior and 5.3 mm lateral to lambda. Five rats received sham-lesions at identical coordinates. In these animals, the wire shank was lowered to the same depth as above, but the retracted blade was not extended. For all operated animals, the craniotomy was covered with Gel-foam and the skin and fascia sutured. The lesioned rats were perfused transcardially at 2

(n=9), 5 (n=9), and 9 (n=6) days after surgery, and the shams (n=5) were perfused at 5 days post-surgery. All animals were deeply anesthetized with 30% chloral hydrate and perfused transcardially first with ice-cold 1% paraformaldehyde in 0.1 M phosphate-buffered saline (PBS) for 1 minute, followed by 10 minutes of cold 4% paraformaldehyde in PBS. The brains were immediately removed, blocked and postfixed in cold 4% paraformaldehyde in PBS for 6 hours. Sections from the rostral hippocampus were then cut in a coronal plane on a vibratome at a setting of 50 μm for immunocytochemistry. The rest of the block was cryoprotected in 20% sucrose solution and frozen. 40 μm-thick sections were cut from the remaining rostral hippocampus on a sliding microtome and stored in 4% paraformaldehyde in PBS at 4°C for *in-situ* hybridization. A caudal block from each animal containing the entorhinal cortex was sectioned in a horizontal plane for cresyl violet staining of the lesion site.

Hippocampal Cultures

Hippocampi were dissected from 18 day-old, fetal Sprague Dawley rats, and cell cultures were prepared as described previously (Goslin and Banker, 1991). Cells were plated at a density of 50,000 cells per 60 mm plastic petri dish on poly-L-lysine coated glass coverslips, and co-cultured with a monolayer of cortical astroglia in a sandwich-type configuration where neurons and glia are separated by small paraffin dots. 5μM cytosine arabinoside was added to inhibit proliferation of glial cells. Cultures were maintained for up to 4 weeks in MEM containing N_2 supplements, 1 mM sodium pyruvate and 0.1% ovalbumin.

Immunocytochemistry and Histochemistry

One series of sections through the rostral hippocampus of each rat was incubated for 48 hrs with a monoclonal antibody (mAB) to NMDAR1 (54.1; 1:250; (Siegel et al., 1994). A second series was incubated for 48 hrs with a mAB to synaptophysin (1:10; (Wiedenmann and Franke, 1985). All sections were then washed three times in PBS,

transferred to a solution containing biotinylated anti-mouse IgG H&L (1:200; Vector Laboratories, Burlingame, CA) for 2 hours, washed again in PBS and transferred to a solution of FITC-conjugated Avidin (1:200; Vector Laboratories, Burlingame, CA) for 1 hour. Double label immunocytochemistry was performed by incubating sections in a solution containing a cocktail of mAB 54.1 (1:250), and a polyclonal antibody to GFAP (1:25; Promeda, Foster City, CA), for 48 hours. Following three washes, the sections were incubated with biotinylated anti-mouse IgG H&L and Texas-red conjugated anti-rabbit IgG H&L for 2 hours, then washed and incubated with FITC-conjugated Avidin for 1 hour. Sections were mounted, and coverslipped with Vectashield (Vector Laboratories, Burlingame, CA) to reduce fluorescence quenching. Histochemical staining for CO activity was carried out on a third series of sections according to a previously described protocol (Wong-Riley, 1979). A fourth series of sections through the lesion site were stained with cresyl violet.

In-situ Hybridization and Quantitative Analysis

Sections were hybridized with [^{35}S]-labeled sense and antisense cRNA probes that were transcribed from PBS(KS+) containing a cDNA corresponding to the second cytoplasmic loop of the cloned rat NMDAR1 cDNA sequence (Moriyoshi et al., 1991) (Gift of Dr. S. Sealfon), using T3 and T7 RNA polymerase. In RNase protection assays, antisense NMDAR1 recognizes a single mRNA of the predicted size (Gore et al., 1996). *In-situ* hybridization was carried out as described previously (Benson et al., 1992). Briefly, sections were pretreated with 1 µg/ml proteinase K in 0.1M Tris, 0.25% acetic anhydride in 0.1M triethanolamine, and washed in saline sodium citrate 2X (SSC). Sections were preincubated in hybridization buffer (10% dextran sulfate, 50% deionized formamide, 50X Denhardt's solution, 0.3 mg/ml herring sperm DNA, 0.15 mg/ml wheat germ tRNA and 20 mM dithiothreitol (DTT)) for 1 hr. at 60°C, then transferred to hybridization solution containing an additional 20 mM DTT and 10,000 cpm/µl of [^{35}S]-

labeled antisense or sense riboprobes for 24 hrs. at 60°C. Sections were washed in 4XSSC with 5mM DTT, treated in 20 µg/ml ribonuclease A for 30 min. at 60°C, then washed in decreasing concentrations of SSC solutions (2X, 0.5X, 0.1X) with 5mM DTT for 30 min. each at 60°C. Sections were mounted and exposed to β max hyperfilm (Amersham) for 3 to 7 days. Slides were then dipped in Kodak NTB-2 emulsion, diluted 1:1, exposed at 4°C and developed using Kodak D19. The sections were counterstained with cresyl violet.

In situ hybridization of neuronal cultures was carried out as described previously (Kleiman et al., 1990), with [^{35}S]-labeled sense and antisense cRNA probes corresponding to the NMDAR1 cDNA sequence, as described above, as well as with sense and antisense rat ß-actin riboprobes that were transcribed from pGEM3Z containing a Sau3A/EcoR1 fragment complementary to 387 base pairs of the 5' end of rat ß-actin cDNA (gift of Dr. J. L. Roberts). Cells were fixed in 4% paraformaldehyde/4% sucrose in phosphate buffered saline (PBS) and stored in 70% EtOH. Cells were washed briefly in PBS containing 5mM $MgCl_2$, followed by 0.2M Tris/ 0.1M glycine (pH 7.4), then pre-incubated for 1 hour at 42°C in hybridization buffer consisting of 50% deionized formamide, 0.3M NaCl, 20mM Tris (pH 8.0), 5mM EDTA, 1X Denhardt's solution, 10% dextran sulfate and 10mM dithiothreitol. Each coverslip was incubated overnight at 55°C in 100µl of hybridization buffer containing 10mg/ml tRNA and 4 X10^6cpm of probe. Following hybridization, coverslips were rinsed in 2XSSC/10mM ß-mercaptoethanol (BME)/1mM EDTA, treated with RNAse A (2µg/ml in 500 mM NaCl/ 10 mM Tris (pH8)) for 30 mins, RT, washed in 2XSSC/10mM BME/1mM EDTA, then washed for 2 hr at 55°C in 0.1XSSC/10mM BME/1mM EDTA. Coverslips were rinsed in 0.5XSSC, dehydrated through graded alcohols and allowed to dry. For autoradiography, coverslips were mounted on slides and dipped in Kodak NTB2 emulsion and allowed to expose for 2-4 weeks at 4°C whereupon they were developed in Kodak D19 developer.

The autoradiographic films of the tissue sections were analyzed by measuring the optical density of hybridization in the OML, IML and the CA1-sr field using an automated paint function which covered the region of interest (Imaging Research, Inc., St. Catherines, Ontario, Canada). Measurements were taken from the contralateral and ipsilateral sides from 4 sections per animal, 3-4 animals per group. Optical density analysis of film autoradiograms was identical to that previously described (see Chapter 5) (Gazzaley et al., 1996c). For each animal, an intensity value for each of the three regions (IML,OML, CA1-sr), from both the ipsilateral and contralateral sides, was calculated as the mean of a single value obtained on each of the four sections. A mean value for each of the five groups, from each region, was obtained from the individual animal values. Within group, side-to-side comparisons were analyzed with paired Student's t-Tests, at a significance level of <0.05, and across group comparisons were analyzed with a one-way analysis of variance (ANOVA), and a Sheffé's post-hoc test, at a significance level of <0.05.

Confocal Microscopy and Quantitative Immunofluorescence Analysis

Quantification of NMDAR1 immunofluorescence intensity was performed according to a previously published method (see Experimental Procedures, Chapter 4 and 5) (Gazzaley et al., 1996b; Gazzaley et al., 1996c). Briefly, a Zeiss LSM 410 inverted confocal microscope was used to obtain high magnification fields of regions within the dentate gyrus from five animals per group and 3 sections per animal, from both the ipsilateral and contralateral sides. All confocal parameters, including brightness and contrast, were kept constant throughout the study. For each section, five fields within the granule cell layer (GCL), the IML (dendritic field immediately distal to the GCL) and the OML (midpoint between the GCL border and the hippocampal fissure) were randomly chosen within a centrally located region of the suprapyramidal blade of the dentate gyrus. Each field was scanned only once, in order to reduce fluorescence

quenching, and at the same predetermined z-axis distance from the surface of the section. An image analysis program (Zeiss, Inc., Thornwood, NY) was used to determine the average pixel intensity within the field, in which the contribution of unlabeled portions of the field were removed by a visually established pixel intensity threshold (Fig. 4.1 and 5.1). Thus, the average pixel intensity of the portion of the field above threshold represented the immunofluorescence intensity within either the cellular processes of the molecular layer, or the granule cell bodies. For each animal an intensity value was then computed, from each of the three regions (GCL, IML, OML), from both ipsilateral and contralateral sides, by determining the mean of the 15 individual field values (five field values obtained from each of three sections). A mean value in all five groups, from each region, was obtained from the individual values determined for each animal. Within group, side-to-side comparisons were analyzed with paired Student's t-Tests, at a significance level of <0.05, and across group comparisons were analyzed with a one-way analysis of variance (ANOVA), and a Sheffé's post-hoc test, at a significance level of <0.05.

Results

Perforant Path Transections

To denervate the OML of the dentate gyrus, we performed knife cut transections of the angular bundle. This transection effectively lesions the perforant path arising from both the lateral and medial entorhinal cortex (Fig. 6.1A). The extent of the lesion in all animals was determined by evaluating horizontal sections of the entorhinal cortex stained with cresyl violet (Fig. 6.1A) and coronal sections of the dentate gyrus histochemically stained for cytochrome oxidase (CO) (Fig 6.1B,C) or processed immunocytochemically for synaptophysin (Fig. 6.2). Previous studies have revealed that CO staining exhibits a prominent decrease in intensity in the OML as early as 16 hrs post-lesion (Borowsky

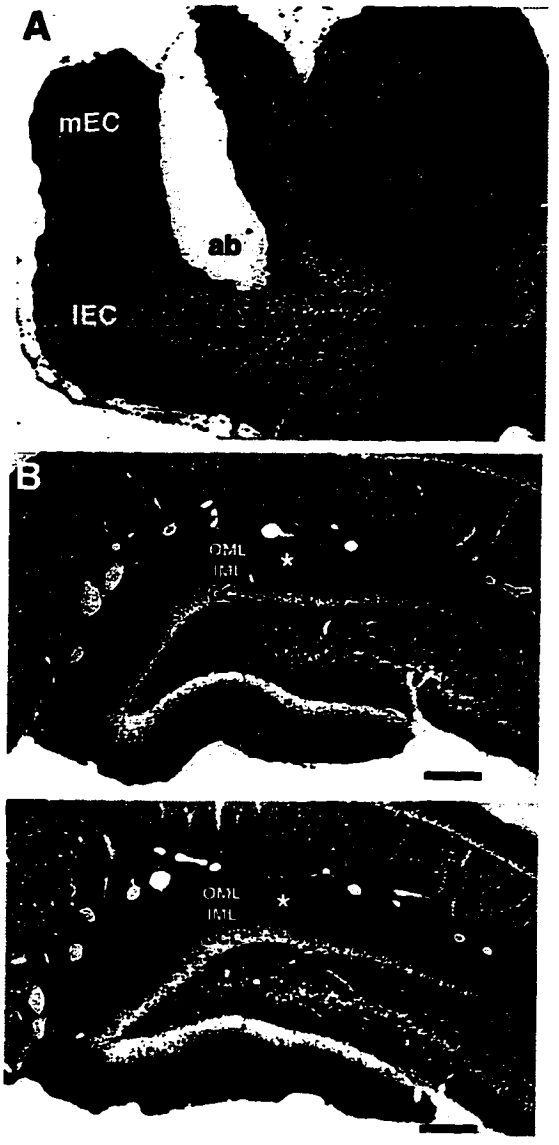

Figure 6.1 Photomicrographs of representative sections through the entorhinal cortex (A) and dentate gyrus (B,C) of a rat examined 5 days post-lesion. A) Horizontal Nissl-stained section showing the extent of the lesion of the angular bundle (ab), which transects the perforant path arising from both the medial (mEC) and lateral (lEC) entorhinal cortex. B,C) Coronal cytochrome-oxidase stained sections through the ipsilateral (B) and contralateral (C) sides. Note the decreased intensity of staining in the OML (asterisks) on the side ipsilateral to the lesion (B) in comparison with that of the OML of the contralateral side (C). Other abbreviations in this and subsequent figures: OML, outer molecular layer; IML, inner molecular layer; GCL, granule cell layer. Scale bars: A, 500 μm; B,C, 250 μm.

and Collins, 1989) and the density of terminals containing synaptophysin, an integral membrane glycoprotein of synaptic vesicles, decreases within the OML as early as 2 days post-lesion (Masliah et al., 1991). A time course of the NMDAR changes was established by perfusing animals at 2, 5 and 9 days post-lesion. Two days corresponds to the time of maximal deafferentation (Matthews et al., 1976a), five days to the onset of terminal proliferation (Steward and Vinsant, 1983), and nine days to onset of new synapse formation (Steward and Vinsant, 1983). In all animals used in this study, the extent of the transection and the effects on the dentate gyrus as determined by CO and synaptophysin staining were consistent. The ipsilateral (lesioned) dentate gyrus of rats evaluated at 2, 5 and 9 days post-lesion exhibited massive synapse loss in the OML, as revealed by a decrease in the number of synaptophysin-positive puncta (Fig. 6.2G,K,O), and a prominent decrease in the intensity of CO staining in this lamina (Figure 6.1B, asterisk). In contrast, the patterns of synaptophysin and CO staining in the contralateral (unlesioned) dentate gyrus of all

animals were indistinguishable from those in the dentate gyrus of unoperated and sham-lesioned control animals (Fig 6.2A,E,I,M).

Qualitative Evaluation of NMDAR1 Immunofluorescence

NMDAR1 immunofluorescence in the dentate gyri of unoperated and sham-lesioned controls was intense in the granule cell somata and their dendrites throughout the entire extent of the molecular layer, while nuclei were unstained (Fig. 6.2B,D). The intensity of immunofluorescence was slightly elevated in the inner molecular layer (IML) relative to the OML (Fig. 6.2B,D). These observations are consistent with previous descriptions of NMDAR1 immunostaining in the rat dentate gyrus (Petralia et al., 1994). In animals sacrificed 2 days post-lesion, the intensity of staining across the ipsilateral molecular layer (Figure 2H) appeared identical to that observed in the contralateral molecular layer (Fig. 6.2F) or in comparison with the molecular layer of the control animals (Fig. 6.2B,D). However, at both 5 and 9 days post-lesion, there was an overt increase in the staining intensity of processes in the ipsilateral OML relative to the ipsilateral IML (Fig. 6.2L,P). The immunofluorescence intensity at 5 and 9 days post-lesion across the contralateral molecular layer (Fig. 6.2J,N) did not appear different from the pattern in control animals (Fig. 6.2B,D). To verify the qualitative impressions of NMDAR1 immunofluorescence intensity changes, we performed a series of quantitative evaluations of the same animals.

Quantitative Evaluation of NMDAR1 Immunofluorescence: Within-Group Comparisons of Ipsilateral vs. Contralateral Regions

Given previous evidence that shrinkage occurs within the denervated region of the molecular layer (Caceres and Steward, 1983), the impression of an intensity increase in the OML could be the result of either an increase in the density of dendrites with normal staining, or an actual increase in the staining intensity within individual dendrites. To distinguish between these two possibilities, we determined quantitatively the average

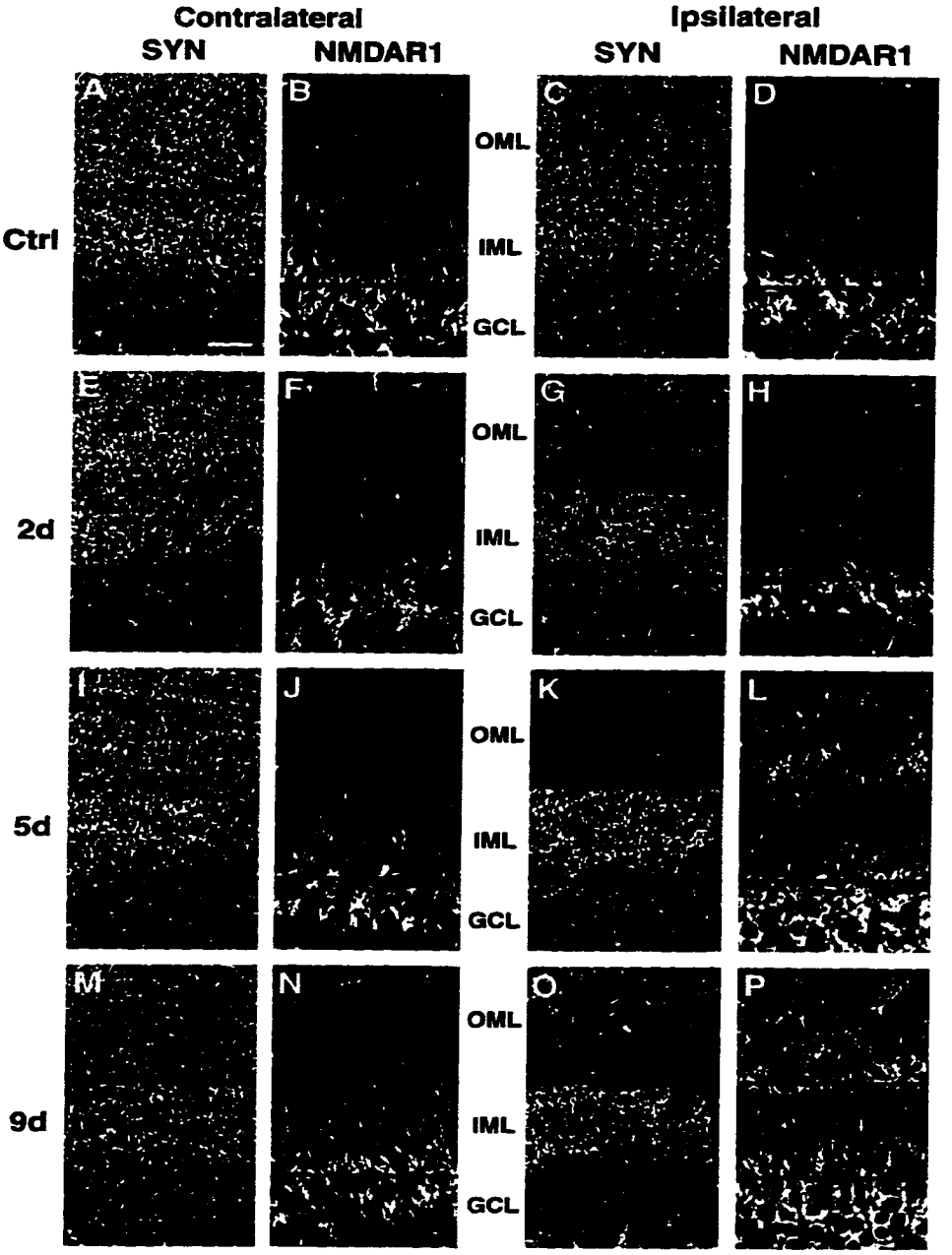

Figure 6.2 Digitized confocal microscopic images of NMDAR1 (B,D,F,H,J,L,N,P) and synaptophysin (SYN; A,C,E,G,I,K,M,O) immunofluorescence in the dentate gyri of an unoperated control animal (Ctrl, A-D) and animals examined 2 (E-H), 5 (I-L) and 9 (M-P) days post-lesion. The series on the left represent fields from the non-lesioned, contralateral side; the series on the right represent fields from the lesioned, ipsilateral side. Note that the pattern of synaptophysin-positive puncta is uniform across the entire molecular layer (OML and IML) in both sides of the control animal (A and C), and in the contralateral side of the 2 day (E), 5 day (I) and 9 day (M) animals. In contrast, an overt decrease in synaptophysin immunofluorescence is evident in the OML compared to the IML on the ipsilateral side in the 2 day (G), 5 day (K) and 9 day (O) animals. NMDAR1 immunofluorescence is relatively uniform throughout the entire molecular layer (OML and IML) in the control animal (B and D) and the contralateral side of all the lesioned animals (F, J, N). In the 2 day post-lesion animal, a similar, homogeneous pattern is evident across the molecular layer on the ipsilateral side (H). In contrast, an overt increase in the immunofluorescence intensity of the OML compared to the IML is apparent in the ipsilateral side of the animals 5 (L) and 9 days (P) post-lesion. Scale bar: 30μm

immunofluorescence intensity within individual cellular profiles using high magnification confocal images of the IML and OML. The intensity values obtained are thus independent of area, and the negative contribution of unlabeled portions of the field was subtracted by establishing a pixel intensity threshold (see Experimental Procedures, Chapter 4 and 5) (Gazzaley et al., 1996b; Gazzaley et al., 1996c). Within group comparisons of comparable regions in the ipsilateral vs. contralateral dentate gyrus were performed since the contralateral OML receives a very limited crossed projection from the opposite entorhinal cortex (Steward et al., 1976), and is thus only subtly deafferented by this lesion (Davis et al., 1988). A series of paired Student's t-tests of the ipsilateral OML vs. the contralateral OML revealed no difference between sides in either control group (sham and unoperated groups), or the group of animals 2 days post-lesion, although in the 2 day post-lesion animals there was a trend toward an increase in the ipsilateral side. In contrast, statistically significant increases in the staining intensity of the ipsilateral OML was evident at both 5 and 9 days post-lesion in comparison to the respective contralateral OML. Such changes were specific to the denervated OML, since comparisons of the ipsilateral IML vs. the contralateral IML in control groups and all of the lesioned groups demonstrated no significant differences in intensity levels. Comparisons of the immunofluorescence intensity within granule cell somata revealed an increase in the ipsilateral side relative to the contralateral side at 5 and 9 days post-lesion, but no differences at the earlier time point or in control groups. Thus, the only significant differences in the intensity of NMDAR1 immunofluorescence between sides was an intensity increase in the OML and granule cell bodies at 5 and 9 days post-lesion in the denervated ipsilateral side.

To verify the change in the ipsilateral OML, we compared the ratios of the intensity of the OML/IML between the ipsilateral and contralateral sides for all groups. The staining intensity value of the IML serves as a non-varying denominator because ipsilateral vs. contralateral comparisons revealed no significant differences in IML

intensity levels between the sides in any group. In agreement with comparisons of the absolute intensity values (see above), comparisons of the OML/IML ratios revealed a significant increase in the ipsilateral OML/IML ratio compared to the contralateral OML/IML ratio at 5 and 9 days post-lesion, while no change was observed in either control group or the 2 days post-lesion group (Fig. 6.3).

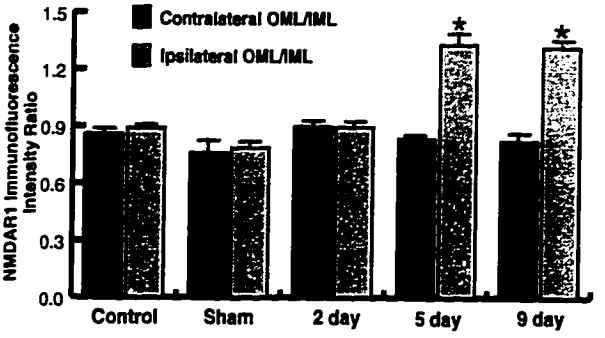

Figure 6.3 Bar graphs comparing ratios of NMDAR1 immunofluorescence intensity values of the OML/IML in unoperated (Control), sham, 2 day, 5 day, and 9 day post-lesion groups. Statistical comparisons were performed both within-groups (ipsilateral vs. contralateral sides; Student's unpaired t-test) and across-groups (ANOVA and Sheffé's test). Statistical analyses revealed that ipsilateral OML/IML ratios of both the 5 and 9 day group were significantly increased (asterisks; $p<0.05$) compared to either the corresponding contralateral OML/IML ratios (within-group comparisons), or each of the ipsilateral ratios from the control, sham and 2 day groups (across-group comparisons). There were no other statistically significant differences, either between contralateral and ipsilateral sides, or for either side compared across the groups. Values represent the mean ± SEM of 5 rats per group (30 measurements per rat).

Quantitative Evaluation of NMDAR1 Immunofluorescence: Across-Group Comparisons

In order to compare the NMDAR1 immunofluorescence intensity in the OML between lesioned and control groups and between the lesioned groups at different time-points following lesion, the ratios of the intensity of the OML/IML were used. Statistical analyses (ANOVA and post-hoc Sheff's test) of the ipsilateral OML/IML intensity ratios demonstrated that both the 5 and 9 day groups were significantly increased compared to either control group or the 2 day group, but were not significantly different from one another (Fig. 6.3). The OML/IML ratios of the control groups and the 2 day post-lesion

group were also not significantly different from each other (Fig. 6.3). Such changes were specific for the lesioned side, since comparisons of the contralateral OML/IML ratios revealed no differences across any of the groups. Thus, the immunofluorescence intensity in the ipsilateral OML of the 5 and 9 day post-lesion groups is not only elevated in comparison to the contralateral OML (see above), but also relative to the OML of the control groups, while no significant differences are detectable in the 2 day post-lesion group in either within-group (ipsilateral vs. contralateral) or across-group comparisons (Fig. 6.3). These quantitative data are thus consistent with the qualitative observations reported above, and demonstrate that the visual impression of an intensity increase in the denervated OML arises from an actual increase in the staining intensity within individual cellular profiles.

Determining the Contribution of NMDAR1 Immunoreactive Astrocytes to Immunofluorescence Intensity Measurements

The cellular profiles evaluated in the quantitative analyses of the molecular layer were almost entirely granule cell dendrites. However, astrocytes are also present in the molecular layer, and have been demonstrated to hypertrophy in the OML of the denervated dentate gyrus in response to an entorhinal cortex lesion (Jensen et al., 1994). To evaluate the presence of NMDAR1 in astrocytes of the dentate gyrus, as well as their potential contribution to intensity changes, we simultaneously immunolabeled sections from control and lesioned brains using antibodies to NMDAR1 and glial fibrillary acidic protein (GFAP). Confocal microscopy revealed that astrocytes were immunoreactive for NMDAR1 within the molecular layer of both sides of all animals. Qualitative CLSM evaluation of the contralateral OML of lesioned animals and the OML of control animals revealed that the intensity of NMDAR1 immunofluorescence within GFAP-labeled astrocytes was either equivalent to, or greater than the intensity of the surrounding dendritic profiles (Fig. 6.4A,B). However, NMDAR1 immunofluorescence intensity within astrocytes in the ipsilateral OML of lesioned animals was sometimes equivalent,

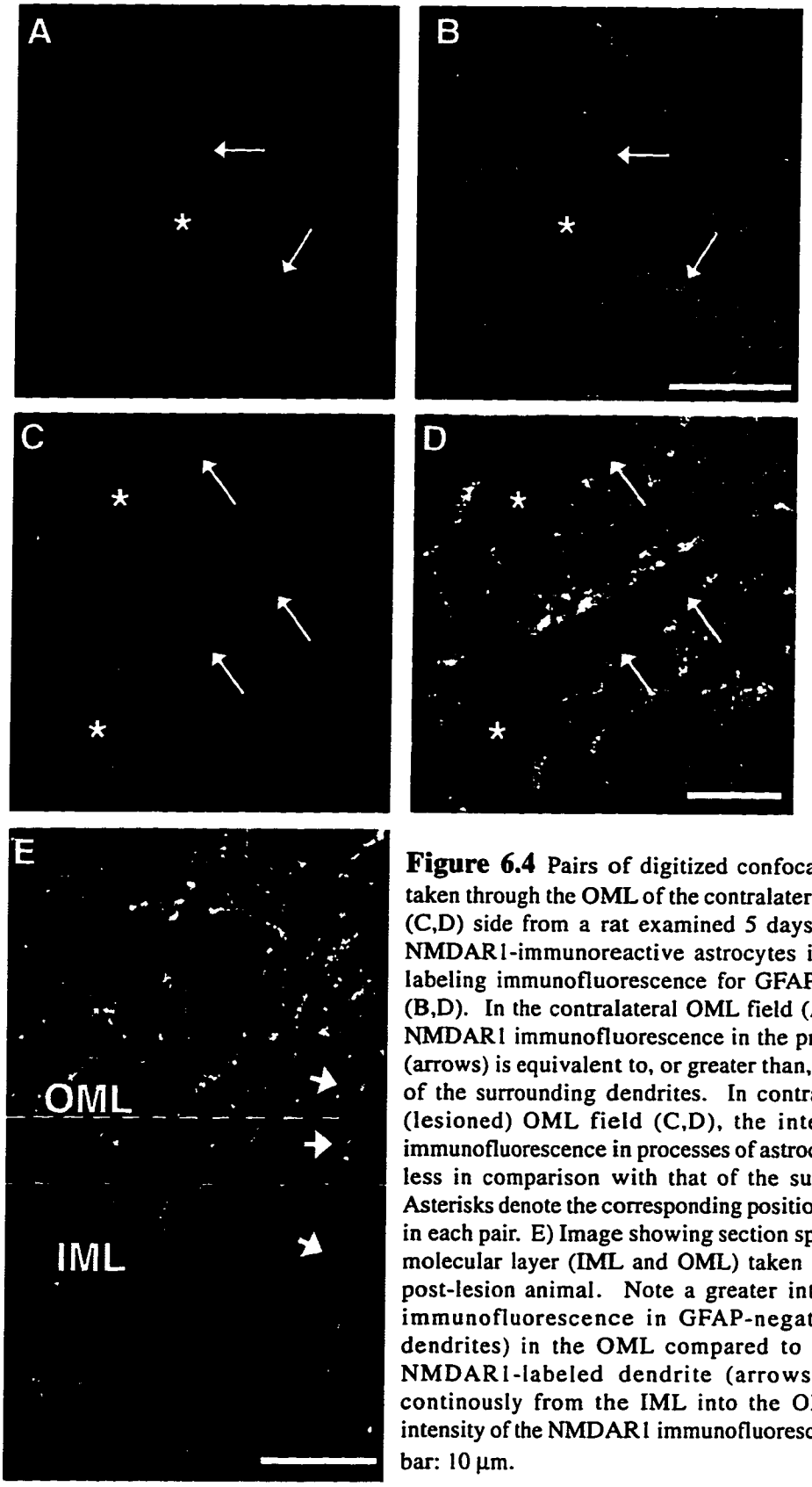

Figure 6.4 Pairs of digitized confocal microscope images taken through the OML of the contralateral (A, B) or ipsilateral (C,D) side from a rat examined 5 days post-lesion showing NMDAR1-immunoreactive astrocytes identified by double-labeling immunofluorescence for GFAP (A,C) or NMDAR1 (B,D). In the contralateral OML field (A,B), the intensity of NMDAR1 immunofluorescence in the processes of astrocytes (arrows) is equivalent to, or greater than, the staining intensity of the surrounding dendrites. In contrast, in the ipsilateral (lesioned) OML field (C,D), the intensity of NMDAR1 immunofluorescence in processes of astrocytes (arrows) is much less in comparison with that of the surrounding dendrites. Asterisks denote the corresponding positions of astrocytic nuclei in each pair. E) Image showing section spanning the ipsilateral molecular layer (IML and OML) taken from the same 5-day post-lesion animal. Note a greater intensity of NMDAR1 immunofluorescence in GFAP-negative processes (i.e. dendrites) in the OML compared to the IML. A single NMDAR1-labeled dendrite (arrows) can be followed continously from the IML into the OML, whereupon the intensity of the NMDAR1 immunofluorescence increases. Scale bar: 10 μm.

but generally less intensely stained than surrounding dendrites (Fig. 6.4C,D). This reveals that any contribution to NMDAR1 immunofluorescence intensity levels by astrocytes would actually decrease the average intensity of the processes in the ipsilateral OML. Thus, the increased intensity of NMDAR1 immunofluorescence detected in the ipsilateral OML of lesioned animals, as compared to the contralateral OML and the OML of control animals, is due primarily to a change that is occurring within dendrites. Consistent with this interpretation, NMDAR1 immunoreactive processes that were GFAP-negative (i.e. dendrites) could be followed from the IML to the OML, where upon crossing this border the immunofluorescence intensity would increase (Fig. 6.4E). Thus, although we have not assessed whether there is an overall change in NMDAR1 immunofluorescence intensity within the astrocytes in response to lesion, we are confident that the intensity alterations we report here are occurring within the granule cell dendrites.

Qualitative Evaluation of NMDAR1 mRNA Hybridization Intensity

In both control and lesioned animals, an intense NMDAR1 mRNA hybridization signal was localized over the somata of the dentate gyrus granule cells and the pyramidal cells of the CA fields, as has been described previously in rat brain (Moriyoshi et al., 1991). In both unoperated and sham-lesioned controls, a very light hybridization signal was observed across the molecular layer of the dentate gyrus and the stratum radiatum of the CA fields, which could be attributed to either very low levels of dendritic mRNA or labeling of astrocytes (Fig. 6.5C). In animals 2 days post-lesion an identical hybridization pattern was evident in both the ipsilateral and contralateral dentate gyrus. At 5 and 9 days post-lesion, however, an increased hybridization signal for NMDAR1 mRNA intensity was apparent over the entire dentate gyrus molecular layer of the side ipsilateral to the lesion (Fig. 6.5B). By contrast, the adjacent stratum radiatum of the CA field (Fig. 6.5B) and the contralateral dentate gyrus molecular layer (Fig. 6.5A) appeared unchanged relative to control animals (Fig. 6.5C). On emulsion dipped slides

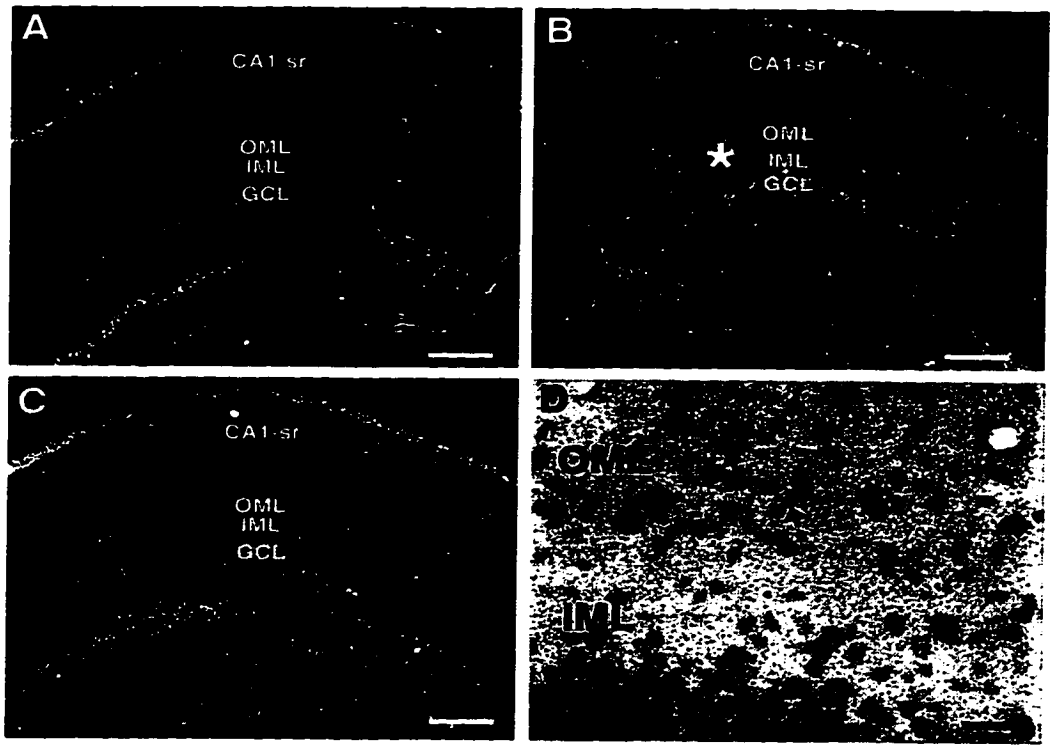

Figure 6.5 Photomicrographs showing cRNA probe hybridization to NMDAR1 mRNA in sections through the contralateral (A) and ipsilateral (B,D) side of the hippocampus in a rat examined 5 days post-lesion, or through one side of a control animal (C). In darkfield images (A-C) note the greater hybridization intensity of both the OML and IML (*) in the ipsilateral side (B) relative to the contralateral side (A) or the control animal (C). (D) Higher magnification brightfield image of a section through the molecular layer, counterstained with cresyl violet. Clustered silver grains overlay darkly Nissl-stained glia (arrows). Silver grains were also diffusely localized throughout the neuropil of the molecular layer, overlying spaces between labeled nuclei. CA1-sr, CA1 stratum radiatum. Scale bars: A-C, 250μm; D, 25 μm

counterstained with cresyl violet, clusters of silver grains indicating the presence of probe hybridized to NMDAR1 mRNA, were concentrated over neurons (identified by their lightly stained nuclei) throughout the granule and pyramidal cell layers. In the dentate gyrus molecular layers of both control and lesioned animals, a small number of darkly stained nuclei, indicative of glial cells, were also overlain by clusters of silver grains (Fig. 6.5D). Additionally, in the dentate gyrus molecular layer ipsilateral to the perforant path lesion, numerous silver grains were present diffusely thoughout the neuropil and were evident in the spaces lying between such darkly Nissl-stained and more lightly stained nuclei (Fig. 6.5D), suggesting that NMDAR1 mRNA is present within dendrites.

To verify the subcellular, and possibly dendritic distribution of NMDAR1 mRNA, in situ hybridization histochemistry was carried out on rat hippocampal neurons grown in culture. When grown at low density, the cell somata and dendrites can be clearly distinguished. In emulsion autoradiograms of cultures hybridized with antisense NMDAR1 mRNA, label was distributed in neuronal somata and throughout dendritic trees (Fig. 6.6A,B). Not every dendritic tree was labeled to the same extent and every branch was not labeled equally. By contrast, label showing hybridization of antisense actin mRNA was confined to neuronal somata (Fig. 6.6C,D). In addition to labeled neurons, both actin and NMDAR1 mRNAs were expressed in astrocytes (data not shown). Sense strand controls showed no label above background.

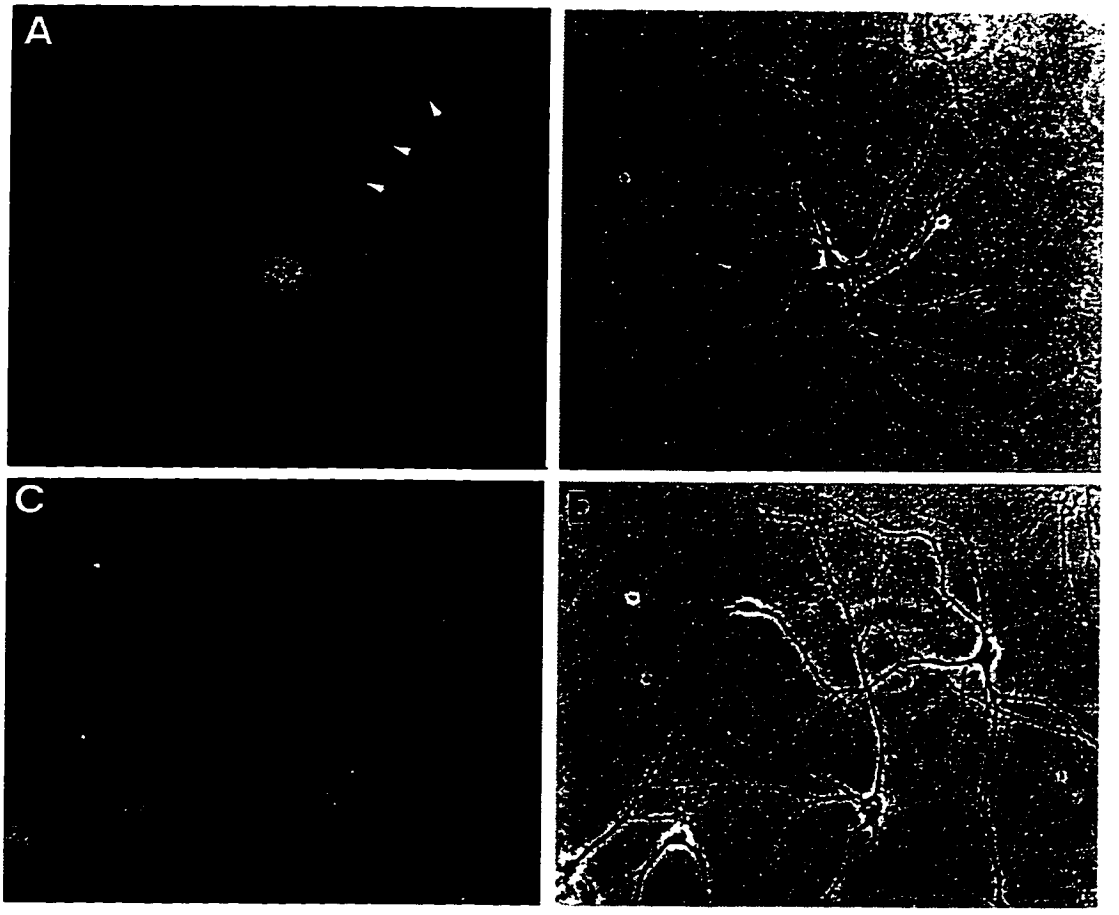

Figure 6.6 Pairs of photomicrographs showing cRNA probe hybridization to NMDAR1 mRNA (A) or actin mRNA (C) in cultured rat hippocampal neurons visualized under darkfield (A,C) or phase contrast optics (B,D). NMDAR1 mRNA hybridization is evident within neuronal somata and along dendritics, one of which is shown by arrow heads. Actin mRNA is confined to the neuronal somata (C). Scale bar: 50 μm

Quantitative Evaluation of NMDAR1 mRNA Hybridization Intensity: Within-Group Comparisons of Ipsilateral vs. Contralateral Regions

Differences in hybridization patterns observed in the film autoradiograms were investigated quantitatively by densitometric analysis. Intensity levels were measured in the dentate gyrus OML, IML and CA1 stratum radiatum (CA1-sr). Somatic layers were not analyzed because hybridization levels frequently exceeded the linear range of the film. Within-group, ipsilateral vs. contralateral molecular layer comparisons revealed an increase in hybridization intensity 5 days post-lesion within both the ipsilateral OML and IML compared to the contralateral OML and IML, respectively. There was no change detected in the CA1-sr at this time point. In contrast to the increases in the ipsilateral IML and OML detected at 5-days post lesion, analysis of both control groups and the 2 and 9 day post-lesion groups revealed no differences in hybridization intensity levels in the OML, IML or CA1-sr between ipsilateral and contralateral sides. However, in the 9 day post-lesion group, there was a trend towards an increased hybridization intensity in the ipsilateral OML and IML relative to the contralateral side.

To further evaluate changes in the OML and IML hybridization intensity between sides, intensity ratios of OML/CA1-sr and IML/CA1-sr were used because the CA1-sr intensity level did not change between sides at any time point (see above), and therefore serves as a non-varying denominator. This analysis confirmed an increase in both the OML and IML of the ipsilateral side as compared to the contralateral side at 5 days post-lesion, with no change in the control groups or the 2 days post-lesion group (Fig. 6.7A,B). However, comparisons of the OML/CA1-sr and IML/CA1-sr ratios between the ipsilateral and contralateral side at 9 days post-lesion revealed a statistically significant increase (Fig. 6.7A,B), suggesting that a change affecting both the OML and IML is indeed occurring 9 days post-lesion. Although there was a non-significant trend toward increased intensity levels of the ipsilateral OML and IML at 9 days when the absolute intensity values of the ipsilateral and contralateral sides were compared

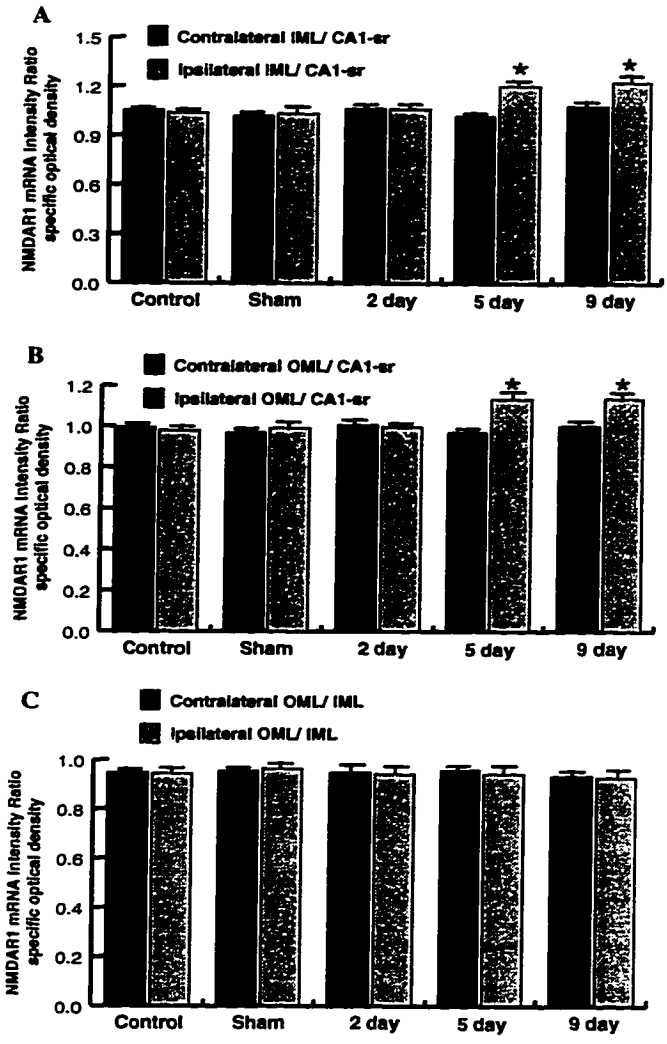

Figure 6.7 Bar graphs comparing ratios of NMDAR1 mRNA hybridization intensity values of the IML/CA1-sr (A), the OML/CA1-sr (B), and the OML/IML (C) for all control and lesioned groups. Statistical comparisons were performed both within-groups (ipsilateral vs. contralateral sides; Student's unpaired t-test) and across-groups (ANOVA and Sheffé's test).Comparisons of either the IML/CA1-sr (A) or the OML/CA1-sr (B) ratios showed that the ipsilateral values at 5 and 9 days (asterisks, $p<0.05$) are increased compared either to the corresponding contralateral side (within-group), or to any of the ipsilateral ratios of the other groups (across-group comparisons). There were no other statistically significant differences, either between contralateral and ipsilateral sides of the same groups, or for comparisons of corresponding sides across groups. Additionally, there were no statistically significant differences in the OML/IML ratios (C) in either within-group or across-group comparisons. Values represent the mean ± SEM for 4 rats

(see above), it is likely that the use of a non-varying denominator in the ratio comparisons decreased the variability and thus revealed a change occurring at 9 days post-lesion.

Quantitative Evaluation of NMDAR1 mRNA Hybridization Intensity: Across-Group Comparisons

To compare NMDAR1 mRNA hybridization intensity levels of the OML and the IML across groups, the OML/CA1-sr and IML/CA1-sr ratios were used. Analysis of the ipsilateral ratios revealed an increase of both the OML/CA1-sr and the IML/CA1-sr ratios at 5 and 9 days post-lesion compared to either control group or to the 2 day post-lesion group (Fig. 6.7A,B). Additionally, the ratios were not significantly different from one another at 5 and 9 days, or among the controls and the 2 day group. A similar

analysis using ratios taken from the side contralateral to the lesion demonstrated no differences across the OML/CA1-sr or the IML/CA1-sr ratios for any of the groups analyzed (Fig. 6.7A,B). Thus, at 5 and 9 days post-lesion, the hybridization intensity of the ipsilateral OML and IML increases compared to both the contralateral OML and IML (see above) and the OML and IML of control animals.

Additional statistical analyses demonstrated no difference in the OML/IML ratios at any post-lesion time point for either within-group comparisons or across-group comparisons (Fig. 6.7C), revealing that post-lesion increases in hybridization intensity levels of the OML and IML were of similar magnitude, and therefore did not produce a differential pattern of hybridization intensity across the molecular layer as was evident for NMDAR1 immunofluorescence.

Discussion

The primary objective of this study was to investigate cellular and molecular mechanisms underlying NMDA receptor plasticity in response to denervation and subsequent synaptic reorganization. There were three principal findings based on quantitative immunofluorescence and *in situ* hybridization methods for localizing the obligatory receptor subunit NMDAR1 to dentate gyrus granule cells following unilateral transection of the perforant path input to the hippocampus. First, changes in NMDAR1 immunofluorescence intensity and mRNA hybridization levels were evident only on the side ipsilateral to the lesion, and occurred with a similar time-course. The earliest detectable changes in both measures were at 5 days post-lesion, and were maintained at least through 9 days post-lesion. Second, perforant path transection induced an overt increase in immunofluorescence intensity that was restricted to dentate gyrus granule cell somata and the portion of their distal dendrites that lay within the denervated OML. Immunoreactive astrocytes did not contribute to such intensity changes. Third, lesion-induced changes in NMDAR1 mRNA hybridization levels were manifested by the novel

appearance of significant mRNA hybridization within the dendrites of dentate gyrus granule cells. These data suggest that NMDAR1 mRNA is a member of a limited population of mRNAs that can be localized within dendrites, in addition to their more customary location in cell somata. However, in comparison with the spatially restricted changes in immunofluorescence within dendritic segments of the OML, the increase in mRNA hybridization was evident throughout the full extent of the dendrites as they traversed both the IML and the OML. Thus, these data indicate that NMDAR1 mRNA and protein exhibit spatially distinct patterns of lesion-induced changes, which occur with a similar time-course. This suggests that while mRNA transport may increase along the entire dendritic extent, cellular mechanisms exist that selectively control the intradendritic parcellation or modification of NMDAR1 protein within a limited region of dendrites whose afferent activity is perturbed. Such mechanisms may include local protein synthesis. Finally, the time-course of such changes suggests that NMDAR1 regulation may be more intimately related to the period of terminal proliferation and synaptogenesis than the earlier period of terminal degeneration.

Localization of NMDAR1 mRNA within Dendrites

The present data suggest that NMDAR1 mRNA is included in a select population of mRNAs that are translocated into dendrites. Other mRNAs of this kind include MAP2 (microtubule-associated protein) (Garner et al., 1988), the α–subunit of CaM kinase II (Ca^{2+}/calmodulin-dependent protein kinase) (Benson et al., 1992; Burgin et al., 1990), Arc (activity-regulated cytoskeleton-associated protein) (Link et al., 1995; Lyford et al., 1995) and the inositol 1,4,5-triphosphate receptor (Ip^3R) (Furuichi et al., 1993). Although a previous single cell PCR study had suggested that NMDAR1 mRNA might be present within dendrites (Miyashiro et al., 1994), previous localization studies have not shown any evidence of a dendritic distribution (Laurie and Seeburg, 1994; Moriyoshi et al., 1991). This discrepancy most likely reflects very low basal levels of dendritic NMDAR1 mRNA, possibly at the limit of detectability by *in situ* hybridization methods,

which become suprathreshold for detectability following perforant path lesion. In the present study, NMDAR1 mRNA was also found within some astrocytes both *in vivo* and *in vitro*. However, the striking increase in NMDAR1 mRNA hybridization levels throughout the full extent of the molecular layer following perforant path transection argues against a major contribution to such increases by reactive astrocytes, since over the time period examined, astrocyte hypertrophy is confined to the OML (Jensen et al., 1994). Furthermore, the increased protein immunoreactivity observed in the present study appeared to be restricted to dendrites and was not observed in the somata or processes of astrocytes. Although most astrocytic glutamate receptors are thought to be non-NMDA receptors, a number of studies support the presence of NMDARs in some astrocytes (Aoki et al., 1994; Gage et al., 1984; Gracy and Pickel, 1995; Ho et al., 1995; Müller et al., 1993). The clear localization of NMDAR1 mRNA in both dendrites and astrocytes in hippocampal cultures strongly suggests that in addition to the potential for localized subunit synthesis near synapses, NMDARs may also mediate glial responses to glutamate. However, the precise physiological function of NMDARs in astrocytes has yet to be fully characterized.

Potential Mechanisms Underlying Protein and mRNA Alterations

Both NMDAR1 protein and mRNA changes were first detected at 5 days post-lesion, which is early in the period of terminal proliferation, but prior to the major onset of new synapse formation (Steward and Vinsant, 1983). Therefore, the initial responses observed may have been induced by axonal sprouting. Terminal proliferation may induce receptor changes through the release of diffusable elements, which could serve to prepare the dendrites for synapse formation. Certain soluble factors produced by CNS tissue have been demonstrated to increase the number of acetylcholine receptors and promote clustering in muscle fibers (Jessell et al., 1979; Schaffner and Daniels, 1982). Although the increases were first demonstrated at 5 days post-lesion, it was maintained through at least 9 days post-lesion during the early period of reactive synaptogenesis. A longer

time-course will be pursued in future studies to evaluate whether receptor levels return to control levels after the majority of synapses have been replaced. A previous autoradiographic study of ligand binding to the NMDAR in the dentate gyrus following entorhinal cortex lesion detected an increase in binding levels in the OML of the ipsilateral side only after 21 days post-lesion, but was not limited to the ipsilateral OML (Ulas et al., 1990). The discrepancy in the time course may represent a difference in the sensitivity of the techniques used and/or differential changes affecting other NMDAR subunits (e.g. 2A-D).

It is also possible that the observed changes in immunofluorescence and hybridization levels may represent a response to denervation, which was either delayed or did not attain a magnitude sufficient to be detected by the techniques used, at 2 days post-lesion. Further time-course studies of animals sacrificed between 2 and 5 days post-lesion are necessary before drawing further conclusions. However, within the context of this model, it is difficult to conclusively distinguish between a response to sprouting or deafferentation because protein and mRNA levels following lesions cannot be assessed in the complete absence of terminal proliferation.

NMDAR1 immunofluorescence visualized within the confocal, cross-sectional profiles of somata and dendritic shafts of granule cells is primarily a reflection of the localization of the cytoplasmic pool of the NMDAR1 subunit protein. Immunoelectron microscopic analyses of NMDAR1 immunolabeling in rat hippocampal neurons and monkey neocortical neurons have revealed dense patches of NMDAR1 labeling throughout the somatodendritic cytoplasm, and is often associated with microtubules, rough endoplasmic reticulum and the Golgi apparatus, suggesting that the cytoplasmic patches of labeling may represent the synthesis and transport pools of the protein (Huntley et al., 1994; Petralia et al., 1994). Given that a previous confocal microscopic investigation has demonstrated that immunofluorescence intensity is a reflection of protein concentration (Good et al., 1992), the increases in NMDAR1

immunofluorescence intensity may represent increases in protein concentration primarily within these cytoplasmic pools. It is likely, although still speculative, that such changes reflect increases in synaptically localized receptors, since previous studies using this lesion paradigm have revealed subsequent increases in NMDAR ligand binding (Geddes et al., 1985).

Previous studies, along with the findings presented in this paper, suggest that the increase in NMDAR1 immunofluorescence within the OML of the lesioned side is at least partially the result of increased local protein synthesis of the NMDAR1 subunit within the denervated dendritic segments of the molecular layer. Electron microscopy has shown that granule cell dendrites contain polyribosomes, which are located predominantly under the base of dendritic spines (Steward and Levy, 1982) and which are in association with membranous cisterns that may represent the functional equivalent of rough endoplasmic reticulum (Steward and Reeves, 1988). A study of synaptodendrosomes, subcellular fractions of pinched-off axon terminals and dendrites, revealed incorporation of radiolabeled amino acids in newly synthesized proteins, some of which become incorporated as components of the synaptic membrane (Rao and Steward, 1991). Interestingly, one such synaptic membrane protein had a molecular weight of 116 kDa, equivalent to that of NMDAR1 found within synaptic plasma membrane fractions (Brose et al., 1993). Most convincingly, Torre and Steward (1996) recently demonstrated that dendrites isolated from their parent cell body can both synthesize and glycosylate proteins, a necessary step in the post-translational processing of membrane-spanning neurotransmitter receptors (Torre and Steward, 1992; Torre and Steward, 1996). Thus, taken together, these data establish the presence of protein synthetic and processing machinery within dendrites.

In view of the close association between polyribosomes and dendritic spines it was suggested that local protein synthesis may be important during synaptic plasticity resulting from alterations in afferent drive (Steward and Levy, 1982). In support of

this, an increased incidence of polyribosomes beneath dendritic spines was identified within the denervated dendritic segments of the dentate gyrus following unilateral entorhinal cortex lesion (Steward, 1983). Additionally, an increase in ribosomal RNA (Philips et al., 1987) and an increase in the incorporation of radiolabeled amino acids (Fass and Steward, 1983; Philips et al., 1987) has been shown to occur exclusively within the denervated OML. These events occur maximally during the period of terminal proliferation and exclusively within the OML, which coincides with the increase in NMDAR1 immunofluorescence observed in the present study, and thus supports the idea that a lamina specific increase in NMDAR1 protein might result in part from increased local protein synthesis. In support of this hypothesis, a recent study demonstrated that growth factor induced synaptic plasticity is dependent upon local protein synthesis (Kang and Schuman, 1996).

Unlike NMDAR1 immunofluorescence, NMDAR1 mRNA hybridization levels increased throughout the full extent of the molecular layer after perforant path transection. Similarly, entorhinal cortex lesions do not differentially affect the distribution across the molecular layer of two other dendritic mRNAs, those encoding MAP2 (Steward and Wallace, 1994) and αCAMKII (Benson et al., 1992; Steward and Wallace, 1994). Likewise, LTP induction in the perforant path induces an increase in dendritic Arc mRNA (Link et al., 1995; Lyford et al., 1995) and αCAMKII mRNA (Thomas et al., 1994b) equally in both the IML and OML. These data suggest that alterations in afferent drive restricted to a specific lamina may induce spatially broad changes in mRNA levels. Thus, while the activation of the protein synthetic machinery may be specific for isolated post-synaptic zones that have been deafferented, the mRNA appears to be non-specifically transported throughout the entire dendrite. Increased levels of mRNA in the dendrites may be the result of an increased rate of dendritic transport or by an alteration in mRNA stability.

In addition to an increase in the local dendritic synthesis of NMDAR1 protein there

may also be an increase in the transport of protein synthesized in the soma, since immunofluorescence intensity increased in ipsilateral granule cell somata as well as within the OML at 5 and 9 days post-lesion. In support of this possibility, there was a trend, although it did not reach statistical significance, of an increase in NMDAR1 immunofluorescence intensity in both the IML and OML 2 days post lesion.

Functional Significance

During the time period in which we have identified increases in NMDAR1 immunofluorescence intensity and mRNA hybridization levels, both physiological (Reeves and Steward, 1988) and behavioral recovery (Loesche and Steward, 1977; Reeves and Smith, 1987) from unilateral entorhinal cortex lesions have been documented. From these studies it was hypothesized that the early phase of physiological recovery, before the major onset of new synapse formation, may be the result of an increase in the number of receptors, producing an increase in the activity of surviving synapses similar to denervation supersensitivity in muscle fibers (Reeves and Steward, 1988). The present data support this hypothesis by suggesting that increases in the concentration of NMDARs, and possibly other glutamate receptor subtypes (Geddes et al., 1985; Ulas et al., 1990), may facilitate this early return of function. Findings suggest that the initial establishment of long-term facilitation in Aplysia involves a redistribution of the reserve pool of excitatory amino acid receptors to supply newly formed synaptic sites, while later stages may require increased protein synthesis of receptors to replenish the reserve pool (Trudeau and Castellucci, 1995). Additionally, in rats receiving bilateral entorhinal cortex lesions, administration of an NMDA receptor antagonist exacerbates spatial learning deficits, suggesting an increased sensitivity of this receptor system during reinnervation (Keseberg and Shmidt, 1995).

The results of this study are consistent with our initial hypothesis that NMDAR1 protein and mRNA levels are modifiable by changes in afferent activity. Thus, the decrease in NMDAR1 immunofluorescence intensity that occurs within the dendrites

of the OML of aged monkeys may indeed be the result of functional changes in the perforant path (see Chapter 4) (Gazzaley et al., 1996b). It is likely that the response of selectively modulating receptor concentrations within the dendrites is not limited to overt experimental manipulations such as lesions, but is a standard, albeit more subtle component of the post-synaptic response to modifications in afferent activity that occur during normal brain functioning and synaptic plasticity. In support of this, we have recently reported that increased estrogen levels in ovariectomized rats, which results in an increased number of spines and synapses on CA1 neurons (Gould et al., 1990; Woolley and McEwen, 1992), also induces an increase in NMDAR1 immunofluorescence intensity within CA1 neurons (see Chapter 5) (Gazzaley et al., 1996c). Greater understanding of the cellular mechanisms of receptor plasticity in mature, non-aged animals may aid in the development of pharmacological interventions directed at averting or correcting functional compromise of specific, receptor-linked circuits that occurs during normal aging, stroke and neurodegenerative processes.

Chapter 7

Discussion

The primary objective of this thesis was to increase our understanding of cellular and molecular alterations associated with age-related memory and learning deficits. In the first study (Chapter 4), we described alterations in NMDAR1 immunofluorescence in the dentate gyrus of aged monkeys compared to young adult and juvenile monkeys. Although direct behavioral correlations were not conducted, considering the important role of both NMDARs and this anatomical region in cognitive processes we suggest that these changes may be associated with age-related learning and memory deficits. Based on these findings, we explored the influence of alterations in estrogen levels (Chapter 5) and synaptic reorganization within the dentate gyrus (Chapter 6) on NMDAR1 protein and mRNA regulation in the hippocampus. These factors were investigated for three reasons; 1) they may be present to some degree in aged monkeys; 2) they may be involved in the formation of age-related memory and learning deficits; and 3) they have been previously demonstrated to alter NMDAR binding levels. Thus, either or both of these factors may have contributed to the alterations in NMDAR1 immunofluorescence described in Chapter 4. Based on the findings of the studies in Chapters 5 and 6, we conclude that fluctuations in estrogen levels and alterations in afferent input from the entorhinal cortex may indeed contribute to the changes we observed in the aged monkeys, and thus may be associated with age-related memory and learning deficits. However, because these studies were the first to investigate the role of alterations in estrogen levels and synaptic reorganization on the cellular mechanisms of NMDAR regulation in the hippocampus, they were performed on young adult rodents, rather than aged primates. This decision was based on the fact that both of these experimental models have been well characterized in rodents and not in monkeys. It was also logical to initiate this study on young adult animals, which would then form

baseline data for comparisons with experimental manipulations in aged animals. Therefore, while certain inferences can be made concerning the involvement of these factors in the generation of the age-related alterations described in Chapter 4, direct correlations are not possible because of species and age differences. Nevertheless, these experiments have served to generate many interesting hypotheses that will be pursued in future experiments on aged rodents and young and aged monkeys.

Implications of Estrogen-Induced GluR Plasticity for Age-Related Memory and Learning Deficits

In Chapter 5 we determined that fluctuations in estrogen levels in young adult rodents modify the intensity levels of NMDAR1 immunofluorescence in the dentate gyrus and the CA1 field of the hippocampus. As discussed in Chapter 5, we suggest that estrogen may be involved in the maintenance of NMDAR levels via an influence on NMDAR1 protein concentration within the cytoplasmic synthesis and transport pools of certain hippocampal neurons. Given that estrogen has been implicated in memory and learning processes, and an important role of the hippocampus and NMDARs in memory and learning has been previously elucidated, the maintenance effect of estrogen on NMDAR1 levels in certain hippocampal neurons (Chapter 5; Results) may play a role in estrogen's involvement in cognitive function. Thus, reductions in estrogen levels during menopause may contribute to age-related memory deficits via a decreased maintenance of NMDAR1 levels within certain hippocampal neurons.

A direct comparison of the data from the studies in Chapters 4 and 5 reveal that although both aging and ovariectomy results in alterations in NMDAR1 immunofluorescence in the dentate gyrus, the effects are not exactly comparable. Ovariectomized rats experienced a decrease in NMDAR1 immunofluorescence intensity in the granule cell bodies, with no detectable decrease in measurements taken from dendrites in the OML, as compared to ovariectomized rats that were treated with estradiol.

Although the IML was not quantitatively evaluated in this study, there was no apparent laminar alterations in NMDAR1 staining intensity across the molecular layer in ovariectomized rats compared to estradiol-treated ovariectomized rats, as was observed in aged monkeys compared to younger monkeys. Thus, ovariectomy of young rodents does not exactly duplicate the NMDAR1 alterations observed in aged monkeys. However, given that estrogen does seem to have a role in the maintenance of NMDAR1 levels in dentate gyrus granule cells, we hypothesize that a reduction in estrogen levels following menopause may make these neurons less able to elicit compensatory modifications in NMDAR1 levels in response to changes that affect these cells during aging, such as alterations in afferent input. An important experiment to test this hypothesis involves the transection of the perforant path in an ovariectomized rat to determine if the compensatory increase in NMDAR1 immunofluorescence that we have described in non-ovariectomized rats (Chapter 6), is altered by changes in estrogen levels. We predict that a perforant path transection in young ovariectomized rats may result in a decrease in NMDAR1 immunofluorescence in the OML relative to the IML, and thus produce a lamina-specific change similar to that observed in aged monkeys.

Implications of Lesion-Induced GluR Plasticity for Age-Related Memory and Learning Deficits

The aged monkey study described in Chapter 4 revealed a decrease in the immunofluorescence intensity of NMDAR1 within the OML of the dentate gyrus, which receives the segregated perforant path input from the entorhinal cortex. The study in Chapter 6 was designed to test the hypothesis that an alteration in the afferent input of the perforant path can modify NMDAR1 immunofluorescence intensity levels selectively within the dendritic segments of the OML. The results of this study are consistent with our initial hypothesis and reveal that cellular mechanisms exist within the dentate gyrus of young adult rodents to selectively control the intradendritic parcellation or

modification of NMDAR1 protein within a limited region of dendrites whose afferent activity is perturbed. Therefore, the decrease in NMDAR1 immunofluorescence intensity that occurs within the dendrites of the OML of aged monkeys may be the result of a functional and/or structural alteration in the perforant path input as suggested, and thus may be involved in age-related memory and learning deficits

Direct comparison of the results of the aging (Chapter 4) and lesion study (Chapter 6) reveal that although they both identify NMDAR1 alterations that occur selectively within the dendritic segments of the OML, the *decrease* in NMDAR1 immunofluorescence intensity within the OML of aged monkeys is in contrast to the *increase* in intensity in the OML of young adult rats following perforant path lesions. Aside from potential species differences, there are several possible reasons for this discrepancy. First, the lesion performed in this study involved the destruction of the majority of perforant path axons to the OML. Thus, this paradigm not only results in an alteration in afferent activity, but also massive synaptic reorganization. It is unclear as to exactly what changes are occurring in the perforant path of aged animals, although the laminar specific alteration identified in the aging monkey study (Chapter 5) suggests that some alteration in this pathway is occurring. In monkeys, there are preliminary results suggesting that there is no change in the number of layer II entorhinal neurons during aging (West et al., 1993), while similar studies have not been performed in rodents. On the other hand, physiological studies have only been performed in rodents and reveal functional changes in the perforant path, although not a straightforward decrease or increase in activity (Barnes, 1994). Thus, we are uncertain to what degree the lesions performed in Chapter 6 mimic changes that actually occur during aging. Additionally, the experimental lesions were induced acutely and are surely of a greater magnitude than changes presumably occurring chronically during aging.

Nevertheless, in young animals, there appear to exist compensatory mechanisms that induce both presynaptic (sprouting) and postsynaptic (NMDAR1

immunofluorescence intensity increase) plasticity responses in the OML following an acute perforant path insult. We hypothesize, that some alteration in the perforant path is occurring during aging, but that the plasticity of the system, either presynaptically and/or postsynaptically, is incapacitated during aging and thus the compensatory response present in young animals is blunted. A plasticity deficit may be the result of hormonal changes, as discussed above, or another as yet unidentified age-induced alteration. We predict that an age-induced plasticity deficit, when coupled with a naturally occurring lesion may result in the decrease in NMDAR1 immunofluorescence that was observed in aged monkeys, and thus may be involved in age-related memory and learning impairments that have been described in primates and rodents. In support of this hypothesis, studies have revealed that there is a decline in the sprouting ability of aged rats in response to lesions (Hoff et al., 1982a; Schauwecker et al., 1996; Scheff et al., 1978) as well as a delay in the process of removal of degenerative debris (Hoff et al., 1982b). However, we cannot yet discount the possibility that the plasticity of the system is preserved during aging, but a physiological alteration in the perforant path, such as an increase in activity, results in a compensatory decrease in NMDAR1 levels in the OML. An important experiment to help clarify these issues involves the transection of the perforant path in aged animals to determine if the ability to upregulate NMDAR1 levels in the OML is preserved during aging. Further experiments designed to explore the exact nature of age-related alterations in the perforant path of both rodents and monkeys would also greatly aid in the interpretation of these studies.

Cellular Mechanisms of Glutamate Receptor Plasticity

Aside from contributing to our understanding of changes associated with age-related memory and learning deficits, the studies presented in this thesis also reveal previously undescribed details of GluR plasticity. Most studies that have investigated GluR alterations in response to various conditions; such as aging, hormonal and

pharmacological manipulations, lesions, kindling and LTP (Bessho et al., 1994; Geddes et al., 1985; Lahtinen et al., 1993'; Magnusson and Cotman, 1993; Maren et al., 1993; Thomas et al., 1994a; Ulas et al., 1990; Weiland, 1992; Wenk and Walker, 1991; Williams et al., 1992), have focused on changes in the number of GluR binding sites to various ligands. While these autoradiographic studies do suggest functional alterations in membrane bound receptor complexes, they do not reveal details of the cellular and molecular mechanisms that may be the basis of physiological and behavioral changes. All the studies described in this thesis used quantitative confocal microscopy to evaluate changes in GluR subunit immunofluorescence intensity (primarily NMDAR1) in discrete neuronal populations and subcellular compartments. As previously discussed, these changes may reflect alterations in NMDAR1 protein concentration within the synthesis and transport pools in the cytoplasm of these cells (Good et al., 1992) (Chapters 4, 5, and 6; Discussion). Other possibilities include changes in antigen conformation, or the binding to the antigenic site by another molecule (i.e. phosphorylation). Nevertheless, the results of the aging and lesion study suggest the existence of cellular mechanisms to generate modifications of NMDAR1 exclusively within specific dendritic segments, in a manner that corresponds with the segregated termination of afferents. Although the dentate gyrus, due its unique anatomy, offers a valuable model to study receptor parcellation within the dendrite, we expect that similar intradendritic control of receptors is present in neurons throughout the nervous system.

Given that the alterations in NMDAR1 immunofluorescence intensity that we have identified in these studies correlate with changes reported in GluR binding studies performed on similar models (Ulas et al., 1990; Weiland, 1992; Wenk and Walker, 1991), it is likely that these alterations reflect changes occurring at the synapse. Additionally, the immunofluorescence intensity changes identified in these studies correlate with predicted behavioral changes, such as alterations in memory abilities (Loesche and Steward, 1977; Luine, 1994; Rapp and Amaral, 1991; Reeves and Smith, 1987; Singh et

al., 1994), that might be expected to result from fluctuations in the concentration of synaptic NMDARs. However, it is important that future studies continue the investigations initiated in this thesis with immunoelectron microscopic techniques designed to evaluate changes in receptor subunit concentration at identifiable synapses.

The mechanism of induction of NMDAR1 immunofluorescence changes may have been related in the two experimental studies performed in this thesis (Chapter 5 and 6). Estradiol replacement increases the number of synapses on CA1 pyramidal cells from the suppressed levels that are initially induced by ovariectomy. The CA1 field is the region where we observed the largest increase in NMDAR1 immunofluorescence (Chapter 5). Similarly, in the lesion study (Chapter 6), we detected an increase in NMDAR1 immunofluorescence in the OML of the dentate gyrus 5 days following transection of the perforant path, during the period of terminal proliferation. Thus, in both studies, an increase in NMDAR1 immunofluorescence intensity levels was associated with the formation of new synapses. We have not, however, proven that these events are causally related or dependent upon synaptic activity. The regulation of NMDAR1 protein may be under the direct control of estrogen itself, or in the case of perforant path lesion, the action of a diffusable factor released during the period of terminal proliferation (Chapters 5 and 6; Discussion).

In addition to investigating changes in immunofluorescence intensity, the studies described in Chapter 5 and 6 also explored changes in NMDAR1 mRNA levels. Although both studies revealed alterations of NMDAR1 immunofluorescence following fluctuations in steroid hormone levels and perforant path transection, only following perforant path transection (Chapter 6) were changes in NMDAR1 mRNA hybridization intensity levels detectable. There are several possible reasons for this discrepancy. Although fluctuations in estrogen levels results in synaptic reorganization, it is of a significantly lower magnitude than the massive synaptic reorganization induced by perforant path lesions. It is thus possible that the lesser degree of synaptic reorganization

following estrogen treatment results in only post-translational NMDAR1 alterations, or very subtle mRNA changes that may have been below the detectability threshold of the quantitative technique used. It is also possible that the immunofluorescence intensity changes identified in the estrogen study were not generated by the synaptic changes at all, but were the result of a direct effect of estrogen on the translational or post-translational machinery driving NMDAR1 protein production.

The lesion study described in Chapter 6 also revealed another important aspect of glutamate receptor plasticity. NMDAR1 mRNA seems to be a member of a limited population of mRNAs that are transported into dendrites, possibly in response to terminal proliferation. However, unlike the induced increase in NMDAR1 immunofluorescence that is selective for the deafferented lamina, NMDAR1 mRNA hybridization increases throughout the dendritic extent of the molecular layer, suggesting a non-specific targeting of mRNA to the dendritic compartment (Chapter 6; Discussion).

Although the studies described in this thesis have contributed to our understanding of the cellular and molecular mechanisms of GluR plasticity in response to aging, hormonal manipulations and acute, massive synaptic reorganization, a more detailed characterization of GluR protein and mRNA regulation remains to be elucidated. This includes a reinvestigation of the studies presented in this thesis with antibodies and molecular probes to the other NMDAR subunits (NMDAR2A-D), the AMPA and kainate subunits and the different subunit splice variants of all the GluR subclasses. This additional information will be necessary in order to understand the full compexity and intracacies of GluR receptor plasticity that we suspect to be operational in hippocampal circuits.

Appendix

Publications

Chapter 4:

Peer-reviewed reports

Gazzaley, A.H., Siegel, S.J., Kordower, J.H., Mufson, E.J., Sladek, J.R. and Morrison, J.H. (1996) Circuit-specific alterations of N-methyl-D-aspartate receptor subunit 1 in the dentate gyrus of aged monkeys. *Proceedings of the National Academy of Science USA* 93:3121-3125

Morrison, J.H., and Gazzaley, A.H. (1996) Age-related alterations of the *N*-methyl-D-aspartate receptor in the dentate gyrus. *Molecular Psychiatry* (In Press)

Morrison, J.H., Siegel, S.J., Gazzaley, A.H., Huntley G.W. (1996) Glutamate receptors: Emerging links between subunit proteins and specific excitatory circuits in primate hippocampus and neocortex. *The Neuroscientist* (In Press)

Abstracts

Gazzaley, A.H., Siegel, S.J., Kordower, J.H., Mufson, E.J., Sladek, J.R. and Morrison, J.H. (1994) Alterations in glutamate receptor distribution in the dentate gyrus of macaque monkeys. *Society of Neuroscience Abstracts* 20:48

Gazzaley, A.H., Siegel, S.J., Kordower, J.H., Mufson, E.J., Sladek, J.R. and Morrison, J.H. (1995) Circuit-specific alterations of NMDA receptors in the hippocampus of aged monkeys. *Society of Neuroscience Abstracts* 21:764

Chapter 5:

Peer-reviewed reports

Gazzaley, A.H., Weiland, N.G., McEwen, B.S. and Morrison, J.H. (1996) Differential regulation of NMDAR1 mRNA and protein by estradiol in the rat hippocampus. *Journal of Neuroscience* (In Press)

Chapter 6:

Peer-reviewed reports

Gazzaley, A.H., Benson, D.L., Huntley G.W. and Morrison J.H. (1996) Differential subcellular regulation of NMDAR1 protein and mRNA in dendrites of dentate gyrus granule cells following perforant path transection. *Journal of Neuroscience* (Submitted)

Abstracts

Gazzaley A.H., Benson D.L., Huntley G.W. and Morrison J.H. (1996) Lamina-specific regulation of NMDAR1 immunoreactivity in dentate gyrus following entorhinal cortex lesions. *Society of Neuroscience Abstracts* (In press)

Benson D.L., Gazzaley A.H., Morrison J.H., Huntley G.W. (1996) Dendritic localization and regulation of NMDAR1 mRNA in hippocampal neurons. *Society of Neuroscience Abstracts* (In press)

References

Albert, M. S. (1990). Cognition and aging. In Principles of Geriatric Medicine and Gerontology, A. McCracken and B. Williams,eds (New York: McGraw Hill), pp. 913-919.

Alvarez, P., Zola, M. S., and Squire, L. R. (1995). Damage limited to the hippocampal region produces long-lasting memory impairment in monkeys. J. Neurosci. *15*, 3796-3807.

Amaral, D. G. (1978). A golgi study of cell types in the hilar region of the hippocampus in the rat. J. Comp. Neurol. *182*, 851-914.

Amaral, D. G., Insausti, D. G., and Cowan, W. M. (1984). The commicural connections of the monkey hippocampal formation. J. Comp. Neurol. *224*, 307-336.

Amaral, D. G., Insausti, R., and Cown, W. M. (1987). The entorhinal cortex of the monkey: I. Cytoarchetectonic Organization. J. Comp. Neurol. *264*, 326-355.

Amaral, D. G., and Witter, M. P. (1989). The three-dimensional organization of the hippocampal foramtion: A review of anatomical data. Neuroscience *31*, 571-591.

Amenta, F., Zaccheo, D., and Collier, W. L. (1991). Neurotransmitters, neuroreceptors and aging. Mech. Ageing and Develop. *61*, 249-273.

Andreasen, M., Lambert, J. D. C., and Jensen, M. S. (1988). Direct demonstration of an N-methyl-D-aspartate receptor mediated componenet of excitatory synaptic transmission in area CA1 of the rat hippocampus. Neurosci. Lett. *93*, 61-66.

Andreasen, M., Lambert, J. D. C., and Jensen, M. S. (1989). Effects of new non-NMDA antagonists on synaptic transmission in area CA1 of the rat hippocampus. J. Physiol. London *414*, 317-336.

Aoki, C., Venkastesan, C., Go, C.-G., Mong, J. A., and Dawson, T. M. (1994). Cellular and subcellular localization of NMDA-R1 subunit immunoreactivity in the visual cortex of adult and neonatal rats. J. Neurosci. *14*, 5202-5222.

Backstrom, T. (1976). Epileptic seizures in women related to plasma estrogen and progesterone during the menstrual cycle. Acta Neurol. Scandinav. *54*, 321-347.

Barnes, C. A. (1994). Normal aging: regionally specific changes in hippocampal synaptic transmission. Trends Neurosci. *17*, 13-18.

Barnes, C. A., and McNaughton, B. L. (1980). Physiological compensation for loss of afferent synapses in rat hippocampal granule cells during senescence. J Physiol *309*, 473-485.

Benson, D. L., Gall, C. M., and Isackson, P. J. (1992). Dendritic localization of type II calcium calmodulin-dependent protein kinase mRNA in normal and reinnervated rat hippocampus. Neuroscience *46*, 851-857.

Berger, T. W., Semple-rowlan, S., and Basset, J. A. (1980). Hippocampal polymorph neurons are the cells of origin for the ipsilateral asscotiation and commissural afferents to the dentate gyrus. Brian Res. *215*, 329-336.

Bessho, Y., Nawa, H., and Nakanishi, S. (1994). Selective up-regulation of an NMDA receptor subunit mRNA in cultured cerebellar granule cells by K^{+}-induced depolarization and NMDA treatment. Neuron *12*, 87-95.

Bettler, B., Boulet, J., Hermans-Borgmeyer, I., O'Shea-Geenfield, A., Deneris, E. S., Moll, C., Borgmeyer, U., Hollmann, M., and Heinemann, S. (1990). Cloning of a novel glutamate receptor subunit GluR5: Expression in the nervous system during development. Neuron *5*, 583-595.

Bliss, T. V. P., and Collingridge, G. L. (1993). A synaptic model of memory: long-term potentiation in the hippocampus. Nature *361*, 31-39.

Bliss, T. V. P., and Lømo, T. (1973). Long-lasting potentiation of synaptic transmission in the dentate area of the anesthetized rabbit following stimulation of the perforant path. J. Physiol. (Lond.) *232*, 331-356.

Borowsky, I. W., and Collins, R. C. (1989). Histochemical changes in enzymes of energy metabolism in the dentate gyrus accompany deafferentation and synaptic reorganization. Neuroscience *33*, 253-262.

Boulter, J., Holmann, M., O'Shea-Greenfield, A., Hartley, M., Deneris, E., Maron.C., and Heinemann, S. (1990). Molecular cloning and functional expression of glutamate receptor subunit genes. Science *249*, 1033-1037.

Bouras, C., Hof, P. R., Giannakopoulos, P., Michel, J.-P., and Morrison, J. H. (1994). Regional distribution of neurofibrillary tangles and senile plaques in the cerebral cortex of elderly patients: A quantitative evaluation of a one-year autopsy population from a geriatric hospital. Cereb. Cortex *4*, 138-150.

Brody, H. (1992). The aging brain. Acta Neurol. Scand. *Suppl. 137*, 40-44.

Brose, N., Gasic, G. P., Vetter, D. E., Sullivan, J. M., and Heinemann, S. F. (1993). Protein chemical characterization and immunocytochemical localization of the NMDA receptor subunit NMDAR1. J. Biol. Chem. *268*, 22663-22671.

Burgin, K. E., Waxham, M. N., Rickling, S., Westgate, S. A., Mobley, W. C., and Kelly, P. T. (1990). *In situ* hybridization histochemistry of Ca/Calmodulin dependent protein kinase in developing rat brain. J. Neurosci *10*, 1788-1798.

Buterbaugh, G. C., and Hudson, G. M. (1991). Estradiol replacement to female rats facilitates dorsal hippocampal but not ventral hippocampal kindled seizure acquisition. Exp. Neurol. *111*, 55-64.

Cabalka, L. M., Hyman, B. T., Goodlett, C. R., Ritchie, T. C., and W., V. H. G. (1992). Alteration in the pattern of nerve terminal protein immunoreactivity in the perforant pathway in Alzheimer's disease and in rats after entorhinal lesions. Neurobiol Aging *13*, 283-91.

Caceres, A., and Steward, O. (1983). Dendritic reorganization in the rat denervated dentate gyrus of the rat following entorhinal cortical lesions: A Golgi and electron microscopic analysis. J. Comp. Neurol. *214*, 387-403.

Clairborne, B. J., Amaral, D. G., and Cown, W. M. (1990). Quantitative three-dimensional analysis of granule cell dendrites in the rat dentate gyrus. J. Comp. Neurol. *302*, 206-219.

Collingridge, G. L. (1987). The role of NMDA receptors in learning and memory. Nature *330*, 604-605.

Collingridge, G. L., and Bliss, T. V. P. (1987). NMDA receptors- their role in long term potentiation. Trends Neurosci. *10*, 289-293.

Coons, A. A., Creech, H. J., Jones, R. N., and Berliner, E. (1942). The demonstration of pneumococcal antigen in tissues by the use of fluorescent antibody. J. Immunol. *45*, 159-170.

Cotman, C. W., Monaghan, D. T., Ottersen, O. P., and Storm-Mathisen, J. (1987). Anatomical organization of excitatory amino acid receptors and their pathways. Trends Neurosci. *10*, 273-280.

Craik, F. I. M. (1977). Age differences in human memory. In Handbook of the psychology of aging, J. E. Birren and K. W. Schaie,eds (New York: Van Nostrand Reinhold) , pp. 384-420.

Davis, L., Vinsant, S. L., and Steward, O. (1988). Ultrastructural characterization of synapses of the crossed temporodentate pathway in rats. J. Comp. Neurol. *267*, 190-202.

Dodge, D. E., Rucker, R. B., Singh, G., and Plopper, C. G. (1993). Quantitative comparison of intracellular concentration and volume of Clara cell 10 KD protein in rat bronchi and bronchioles based in laser scanning confocal microscopy. J. Histochem. Cytochem. *41*, 1171-1183.

Don Carlos, L. L., Monroy, E., and Morrell, J. (1991). Distribution of estrogen receptor-immunoreactive cells in the forebrain of the female guinea pig. J. Comp. Neurol. *305*, 591-612.

Duffy, C. J., and Rakic, P. (1983). Differentiation of granule cell dendrites in the dentate gyrus of the rhesus monkey: A quantitative golgi study. J. Comp. Neurol. *214*, 224-237.

Ehlers, M. D., Tingley, W. G., and Huganir, R. L. (1995). Regulated subcellular distribution of the NR1 subunit of the NMDA receptor. Science *269*, 1734-1737.

Fambrough, D. M. (1979). Control of acetylcholine receptors in skeletal muscle. Physiol. Rev. *59*, 165-227.

Fass, B., and Steward, O. (1983). Increases in protein-precursor incorporation in the denervated neuropil of the dentate gyrus during reinnervation. Neuroscience *3*, 653-664.

Flicker, C., Bartus, T. H., Crook, T. H., and Ferris, S. H. (1984). Effects of aging and dementai upon recent visuospatial memory. Neurobiol. Aging *5*, 275-283.

Flood, D. G., Buell, S. J., Horwitz, G. J., and Coleman, P. D. (1987). Dendritic extent in human dentate gyrus granule cells in normal aging and senile dementia. Brain Res. *402*, 205-216.

Follesa, P., and Ticku, M. K. (1995). Chronic ethanol treatment differentially regulates NMDA receptor subunit mRNA expression in rat brain. Mol. Brain Res. *29*, 99-106.

Follesa, P., and Ticku, M. K. (1996). NMDA receptor upregulation: molecular studies in cultured mouse cortical neurons after chronic antagonist exposure. J. Neurosci. *16*, 2172-2178.

Frank, E., and Fischbach, G. D. (1979). Early events in neuromuscular junction formation in vitro. J. Cell Biol. *83*, 143-158.

Frank, E., Gautvik, K., and Sommerschild, H. (1975). Cholinergic receptors at denervated mammalian motor end-plates. Acta. Physiol. Scand. *95*, 66-76.

Friedman, L. K., Pellegrini-Giampietro, D. E., Sperber, E. F., Bennet, M. V. L., Moshe, S. L., and Zukin, S. R. (1994). Kainate-induced status epilepticus alters glutamate and $GABA_A$ receptor gene expression in adult rat hippocampus: an *in situ* hybridization study. J. Neurosci. *14*, 2697-2707.

Frotscher, M., Kraft, J., and Zorn, U. (1988). Fine structure of identified neurons in the primate hippocampus: a combined Golgi/EM study in the baboon. J Comp Neurol *275*, 254-270.

Frotscher, M., Seress, L., Schwerdtfeger, W. K., and Buhl, E. (1991). The mossy cells of the fascia dentata: a comparative study of their fine structure and synaptic connections in rodents and primates. J Comp Neurol *312*, 145-163.

Furuichi, T., Samon-Chazottes, D., Fujino, I., Yamada, N., Hasegawa, M., Miyawaki, A., Yoshikawa, S., Guenet, J.-L., and Mikoshiba, K. (1993). Widespread expression of inositol 1,4,5-triphosphate receptor type 1 gene (*Insp3r1)* in the mouse central nervous system. Receptors Channels *1*, 11-24.

Gage, F. H., Dunnett, S. B., and Bjorklund, A. (1984). Spatial learning and motor deficits in aged rats. Neurobiol. Aging *5*, 43-48.

Gall, J. G., and Pardue, M. (1969). Formation and detection of RNA-DNA hybrid molecules in cytological preparations. Proc. Natl. Acad. Sci. (USA) *63*, 378.

Gallagher, M., and Burwell, R. D. (1989). Relationship of age-related decline across several behavioral domains. Neurobiol. Aging 691-708.

Garner, C. C., Tucker, R. P., and Matus, A. (1988). Selective localization of messenger RNA for the cytoskeletal protein protein MAP2 in dendrites. Nature *336*, 674-677.

Gazzaley, A. H., Benson, D. L., Huntley, G. W., and Morrison, J. H. (1996a). Differential subcellular regulation of NMDAR1 protein and mRNA in dendrites of dentate gyrus granule cells following perforant path transection. J. Neurosci. Submitted.

Gazzaley, A. H., Siegel, S. J., Kordower, J. H., Mufson, E. J., and Morrison, J. H. (1996b). Circuit-specific alterations of *N*-methyl-D-aspartate receptor subunit 1 in the dentate gyrus of aged monkeys. Proc. Natl. Acad. Sci. USA *93*, 3121-3125.

Gazzaley, A. H., Weiland, N. G., McEwen, B. S., and Morrison, J. H. (1996c). Differential regulation of NMDAR1 mRNA and protein by estradiol in the rat hippocampus. J. Neurosci. In press.

Geddes, J. W., Monaghan, D. T., Cotman, C. W., Lott, I. T., Kim, R. C., and Chui, H. C. (1985). Plasticity of hippocampal circuitry in Alzheimer's disease. Science *230*, 1179-1181.

Geffen, L. B., Livett, B. G., and Rush, R. A. (1969). Immunhistochemical localization of protein components of chatecholamine synthesis and degradation. J. Physiol.,London *204*, 593-605.

Geinisman, Y., de Toledo-Morrell, L., Morrell, F., Persina, I. S., and Rossi, M. (1992). Age-related loss of axospinous synapses formed by two afferent systems in the rat dentate gyrus as revealed by the unbiases stereological dissector technique. Hippocampus *2*, 437-444.

Geinisman, Y., Morrell, F., and de Toledo-Morrell, L. (1987). Axospinous synapses with segmented postsynaptic densities: a morphologically distinct synaptic subtype contributing to the number of profiles of 'perforated' synapses visualized in random sections. Brain Res *423*, 179-88.

Gilbert, M. E. (1988). The NMDA-receptor antagonist, MK-801, suppresses limbic kindling and kindled sizures. Brain Res. *463*, 90-99.

Gold, S. J., Hennegriff, M., Lynch, G., and Gall, C. M. (1996). Relative concentrations and seizure-induced changes in mRNAs encoding three AMPA receptor subunits in hippocampus and cortex. J. Comp. Neurol. *365*, 541-555.

Goldwitz, D., White, W. F., Steward, O., Cotman, C., and Lynch, G. (1975). Anatomical evidence for a projection from the entorhinal cortex to the contralateral dentate gyrus of the rat. Exp. Neurol. *47*, 433-441.

Golomb, J., deLeon, M. J., Kluger, A., George, A. E., Tarshish, C., and Ferris, S. H. (1993). Hippocampal atrophy in normal aging. Arch Neurol *50*, 967-973.

Golomb, J., Kluger, A., deLeon, M. J., Ferris, S. H., Convit, A., Mittleman.M.S., Cohen, J., Rusinek, H., De Santi, S., and George, A. E. (1994). Hippocampal formation size in normal human aging: A correlate of delayed secondary memory performance. Learning & Memory *1*, 45-54.

Good, M. J., Hage, W. J., Mummery, C. L., De Latt, S. W., and Boonstra, J. (1992). Localization and quantification of epidermal growth factor receptors on single cells by confocal laser scanning microscopy. J. Histochem. Cytochem. *40*, 1353-1361.

Gore, A. C., Wu, T. J., Rosenberg, J. J., and Roberts, J. L. (1996). Gonadotropin-releasing hormone and NMDA receptor gene expression and colocalization change during puberty in female rats. J. Neurosci. *16*, 5281-5289.

Goslin, K., and Banker, G. (1991). Rat hippocampal neurons in low density culture. In Culturing Nerve Cells, G. Banker and K. Goslin,eds (Cambridge: MIT Press), pp. 251-282.

Gould, E., Woolley, C. S., Frankfurt, M., and McEwen, B. S. (1990). Gonadal steroids regulate dendritic spine density in hippocampal pyramidal cells in adulthood. J. Neurosci. *4*, 1286-1291.

Gracy, K. N., and Pickel, V. M. (1995). Comparative ultrastructural localization of the NMDAR1 glutamate receptor in the rat basolateral amygdala and bed nucleus of the stria terminalis. J. Comp. Neurol. *362*, 71-85.

Halasy, K., and Somogyi, P. (1993). Subdivisions in the multiple GABAergic innervation of granule cells in the dentate gyrus of the rat hippocmpus. Eur. J. Neurosci. *5*, 411-429.

Ho, A., Gore, A. C., Shannon Weickert, C., and Blum, M. (1995). Glutamate regulation of GDNF gene expression in the striatum and primary striatal astrocytes. Neuroreport *6*, 1326-1330.

Hof, P., and Morrison, J. H. (1994). The cellular basis of cortical disconnection in Alzheimer's disease and related dementing conditions. In Alzheimer's disease, R. D. Terry, R. Katzman and K. L. Bick,eds (New York: Raven Press), pp. 197-229.

Hoff, S. F., Sheff, S. W., Bernardo, L. S., and Cotman, C. W. (1982a). Lesion-induced synaptogenesis in the dentate gyrus of aged rats: I Loss and reaquisition of normal synaptic density. J. Comp. Neurol. *205*, 246-252.

Hoff, S. F., Sheff, S. W., and Cotman, C. W. (1982b). Lesion-induced synaptogenesis in the dentate gyrus of aged rats: II Demonstration of an impaired degeneration cleaning response. J. Comp. Neurol. *205*, 253-259.

Hollmann, M., and Heinemann, S. (1994). Cloned glutamate receptors. Annu. Rev. Neurosci. *17*, 31-108.

Hollmann, M., O'Shea-Greenfield, A., Rogers, S. W., and Heinemann, S. (1989). Cloning by functional expression of a member of the glutamate receptor family. Nature *342*, 643-648.

Honer, W. G., Dickson, D. W., Gleeson, J., and Davies, P. (1992). Regional synaptic pathology in Alzheimer's disease. Neurobiol Aging *13*, 375-382.

Huber, G., and Matus, A. (1984). Differences in the cellular distributions of two microtubule-associated proteins, MAP1 and MAP2, in rat brain. J. Neurosci. *4*, 151-160.

Huntley, G. W., Rogers, S. W., Moran, T., Janssen, W., Archin, N., Vickers, J. C., Cauley, K., Heinemann, S. F., and Morrison, J. H. (1993). Selective distribution of kainate receptor subunit immunoreactivity in the monkey neocortex revealed by a monoclonal antibody that recognizes glutamate receptor subunits GluR 5/6/7. J. Neurosci. *13*, 2965-2981.

Huntley, G. W., Vickers, J. C., Janssen, W., Brose, N., Heinemann, S. F., and Morrison, J. H. (1994). Distribution and synaptic localization of immunocytochemically identified NMDA receptor subunit proteins in sensory-motor and visual cortices of monkey and human. J. Neurosci. *14*, 3603-3619.

Hyman, B. T., Penney, J. D. J., Blackstone, C. B., and Young, A. B. (1994). Localization of non-N-methyl-D-apartate glutamate receptors in normal and Alheimer hippocampal formation. Ann. Neurol. *35*, 31-37.

Hyman, B. T., Van, H. G. W., Kromer, L. J., and Damasio, A. R. (1986). Original Articles: Perforant Pathway Changes and the Memory Impairment of Alzheimer's Disease. Annals of Neurology *20*, 472-481.

Hyman, B. T., Van Hoesen, G. W., Damasio, A. R., and Barnes, C. L. (1984). Alzheimer's disease: Cell-specific pathology isolates the hippocampal formation. Science *225*, 1168-1170.

Jensen, M. B., Gonzalez, B., Castellano, B., and Zimmer, J. (1994). Microglial and astrogial reactions to anterograde axonal degeneration: A histochemical and immunocytochemical study of the adult rat fascia dentata after entorhinal perforant path lesions. Exp. Brain Res. *98*, 245-260.

Jessell, T. M., Siegel, R. E., and Fishbach, G. D. (1979). Induction of acetylcholine receptor on cultured skeletal muscle by a factor extracted from the serum and spinal cord. Proc. Natl. Acad. Sci. USA *76*, 5397-5401.

Kamphuis, W., De Rijk, T. C., Talamini, L. M., and Lopes da Silva, F. H. (1994). Rat hippocampal kindling induces changes in the glutamate receptor mRNA expression patterns in the dentate granule neurons. Eur. J. Neurosci. *6*, 1119-1127.

Kang, H., and Schuman, E. M. (1996). A requirement for local protein synthesis in neurotrophin-induced hippocampal synaptic plasticity. Science *273*, 1402-1406.

Keinanen, K., Wisden, W., Sommer, B., Werner, P., Herb, A., Verdoorn, T. A., Sakmann, B., and Seeburg, P. H. (1990). A family of AMPA-selective glutamate receptors. Science *248*, 556-560.

Keseberg, U., and Shmidt, W. J. (1995). Low-dose challenge by the NMDA receptor antagonist dizocilipine exacerbates the spatial learning deficit in entorhinal cortex-lesioned rats. Behav. Brain Res. *67*, 255-261.

Kleiman, R., Banker, G., and Steward, O. (1990). Differential subcellular localization of particular mRNAs in hippocampal neurons in culture. Neuron *5*, 821-830.

Klein, W. L., Sullivan, J., Skorupa, A., and Aguilar, J. S. (1989). Plasticity of neuronal receptors. FASEB *3*, 2132-2140.

Lahtinen, H., Castren, E., Miettinen, R., Ylinen, A., Paljarvi, L., and Riekkinen, P. J. S. (1993). NMDA-sensitive [^{3}H]glutamate binding in the epileptic rat hippocampus: an autoradiographic study. Neuroreport *4*, 45-48.

Lambert, J. D. C., and Jones, R. S. G. (1990). A reevaluation of excitatory amino acid-mediated synaptic transmission in rat dentate gyrus. J. Neurophysiol. *64*, 119-132.

Laping, N. J., Morgan, T. E., Nichols, N. R., Rozovsky, I., Young-Chan, C. S., Zarow, C., and Finch, C. E. (1994). Transforming growth factor-β1 induces neuronal and astrocytic genes: Tubulin α1, glial fibrillary acidic protein and clusterin. Neuroscience *58*, 563-572.

Laurie, D. J., and Seeburg, P. H. (1994). Regional and developmental heterogeneity in splicing of the rat brain NMDAR1 mRNA. J. Neurosci. *14*, 3180-3194.

Link, W., Konietzko, U., Kauselmann, G., Krug, M., Schwanke, B., Frey, U., and Kuhl, D. (1995). Somatodendritic expression of an immediate early gene is regulated by synaptic activity. Proc. Natl. Acad. Sci. USA *92*, 5734-5738.

Lippa, C. F., Hamos, J. E., Pulaski-Salo, D., Degennaro, L. J., and Drachman, D. A. (1992). Alzheimer's disease and aging: Effects on perforant pathway perikarya and synapses. Neurobiol. Aging *13*, 405-411.

Loesche, J., and Steward, O. (1977). Behavioral correlates of denervation and reinnervation of the hippocampal formation of the rat: recovery of alternation performance following unilateral entorhinal cortex lesions. Brain Res. Bull. *2*, 31-39.

Lømo, T., and Rosenthal, J. (1972). Control of Ach sensitivity by muscle activity in the rat. J. Physiol. *221*, 493-513.

Loy, R., Gerlach, J. L., and McEwen, B. S. (1988). Autoradiographic localization of estradiol-binding neurons in the rat hippocampal formation and entorhinal cortex. Dev. Brain Res. *39*, 2 45-251.

Luine, V. N. (1994). Steroid hormone influences on spatial memory. Ann. N Y. Acad. Sci. *14*, 201-211.

Lyford, G. L., Yamagata, K., Kaufmann, W. E., Barnes, C. A., Sanders, L. K., Copeland, N. G., Gilbert, D. J., Jenkins, N. A., Lanahan, A. A., and Worley, P. F. (1995). Arc, a growth factor and activity-regulated gene, encodes a novel cytoskeleton-associated protein that is enriched in neuronal dendrites. Neuron *14*, 433-445.

Lynch, G., Gall, C., and Cotman, C. (1977). Temporal parameters of axon "sprouting" in the brain of the adult rat. Exp. Neurol. *54*, 179-183.

Magnusson, K. R., and Cotman, C. W. (1993). Age-related changes in excitatory amino acid receptors in two mouse strains. Neurobiol. Aging *14*, 197-206.

Maren, S., Georges, T., Standley, S., Baudry, M., and Thompson, R. (1993). Postsynaptic factors in the expression of long-term potentiation (LTP): Increased glutamate receptor binding following LTP induction *in vivo*. Proc. Natl. Acad. Sci. USA *90*, 9654-9658.

Marrack, J. (1934). Nature of antibodies. Nature *133*, 292-293.

Masliah, E., Fagan, A. M., Terry, R. D., DeTeresa, R., Mallory, M., and Gage, F. H. (1991). Reactive synaptogenesis assessed by synaptophysin immunoreactivity is associated with GAP-43 in the dentate gyrus of the adult rat. Exp. Neurol. *113*, 131-142.

Masliah, E., Mallory, M., Hansen, L., DeTeresa, R., and Terry, R. D. (1993). Quantitative synaptic alterations in the human neocortex during normal aging. Neurology *43*, 192-197.

Matthews, D. A., Cotman, C., and Lynch, G. (1976a). An electron microscopic study of lesion-induces synaptogenesis in the dentate gyrus of the adult rat. I. Magnitude and time course of degeneration. Brain Res. *115*, 1-21.

Matthews, D. A., Cotman, C., and Lynch, G. (1976b). An electron microscopic study of lesion-induces synaptogenesis in the dentate gyrus of the adult rat. II. Reappearance of morphologically normal synaptic contacts. Brain Res. *115*, 23-41.

McEwen, B. S., Gould, E., Orchinik, M., Weiland, N. G., and Woolley, C. S. (1995). Oestrogens and the structural and functional plasticity of neurons: implications for memory, ageing and neurodegenerative processes. In Non-Reproductive Actions of Sex Steroids (Ciba Foundation Symposium), R. B. Gregory and J. A. Goode,eds (Chichester: Wiley & Sons), pp. 52-73.

Merlie, J. P., Isenberg, K. E., Russell, S. D., and Sanes, J. R. (1984). Denervation supersensitivity in skeletal muscle: analysis with a cloned cDNA probe. J. Cell Bio. *99*, 332-335.

Meunier, M., Bachevalier, J., Mishkin, M., and Murray, E. A. (1993). Effects on visual recognition of combined and separate ablations of the entorhinal and perirhinal cortex in rhesus monkeys. J. Neurosci. *13*, 5418-5432.

Miledi, R., and Potter, L. T. (1971). Acetylcholine receptors in muscle fibres. Nature *233*, 599-603.

Miyashiro, K., Dichter, M., and Eberwine, J. (1994). On the nature and differential distribution of mRNAs in hippocampal neurites: Implications for neuronal functioning. Proc. Natl. Acad. Sci. USA *91*, 10800-10804.

Monaghan, D. T., and Cotman, C. W. (1982). The distribution of [^{3}H] kainic acid binding sites in rat CNS as determined by autoradiography. Brain Res. *252*, 91-100.

Monaghan, D. T., Holets, V. R., Toy, D. W., and Cotman, C. W. (1983). Anatomical distributions of four pharmnacologically distinct [^{3}H]-L-glutamate binding sites. Nature *306*, 176-179.

Monyer, H., Sprengel, R., Schoepfer, R., Herb, A., Higuchi, M., Lomeli, H., Burnashev, N., Sakmann, B., and Seeburg, P. H. (1992). Heteromeric NMDA receptors: Molecular and functional distinction of subtypes. Science *256*, 1271-1221.

Moriyoshi, K., Masu, M., Takahiro, I., Shigemoto, R., Mizuno, N., and Nakanishi, S. (1991). Molecular cloning and characterization of the rat NMDA receptor. Nature *354*, 31-37.

Morris, R. G. M., Anderson, E., Lynch, G. S., and Baudry, M. (1986). Selective impairment of learning and blockade of long-term potentiation by an *N*-methyl-D-aspartate receptor antagonist, AP5. Nature *319*, 774-776.

Morris, R. G. M., Garrud.P., Rawlins, J. N. P., and O'Keefe, J. (1982). Place-navigation in rats with hippocampal lesions. Nature *297*, 681-683.

Mufson, E. J., Benzing, W. C., Cole, G. M., Emerich, D. F., Sladek, J. R. J., Morrison, J. H., and Kordower, J. H. (1994). Apolipoprotein E-immunoreactivity in aged rhesus monkey cortex: Colocalization with amyloid plaques. Neurobiol. Aging *15*, 621-627.

Müller, T., Grosche, J., Ohlemeyer, C., and Kettenmann, H. (1993). NMDA-activated currents in Bergmann glial cells. NeuroReport *4*, 671-674.

Nakanishi, N., Schneider, N. A., and Axel, R. (1990). A family of glutamate receptor genes: Evidence for the formation of heteromultimeric receptors with distinct channel properties. Neuron *5*, 569-581.

Nakanishi, S. (1992). Molecular diversity of glutamate receptors and implications for brain function. Science *258*, 597-603.

Nicoletti, V. G., Condorelli, D. F., Dell'Albani, P., Ragusa, N., and Giuffrida Stella, A. M. (1995). AMPA-selective glutamate receptor subunits in the rat hippocampus during aging. J Neurosci Res *40*, 220-224.

Orchinik, M., Weiland, N. G., and McEwen, B. S. (1994). Adrenalectomy selectively regulates GABAA receptor subunit expression in the hippocampus. Mol. Cell. Neurosci. *5*, 451-458.

Parnavelas, J. G., Lynch, G., Brecha, N., Cotman, C. W., and Globus, A. (1974). Spine loss and regrowth in the hippocampus following deafferentation. Nature *248*, 71-73.

Perlmutter, M., Metzger, R., Nexworski, T., and Miller, K. (1981). Spatial and temporal memory in 20 and 60 year olds. J. Gerontol. *36*, 59-65.

Peters, A. (1991). Aging in monkey cerebral cortex. In Cerebral cortex - Volume 9: Normal and altered states of function, A. Peters and E. G. Jones,eds (New York: Plenum Press), pp. 485-510.

Petersen, R. C., Smith, G., Kokmen, E., Ivnik, R. J., and Tangalos, E. G. (1992). Memory function in normal aging. Neurology *42*, 396-401.

Petralia, R. S., Yokotani, N., and Wenthold, R. J. (1994). Light and electron microscope distribution of the NMDA receptor subunit NMDAR1 in the rat nervous system using a selective anti-peptide antibody. J. Neurosci. *14*, 667-696.

Philips, L., Nostrandt, S. J., Chikaraishi, D. M., and Steward, O. (1987). Increases in ribosomal RNA within the denervated neuropil of the dentate gyrus during reinnervation: Evaluation by *in situ* hybridization using cDNA probes complementary to ribosomal RNA. Mol. Brain Res. *2*, 251-261.

Philips, S. M., and Sherwin, B. B. (1992a). Variations in memory function and sex steroid hormones across the menstrual cycle. Psychoneuroendocrinology *17*, 497-506.

Philips, S. M., and Sherwin, B. B. (1992b). Effects of estrogen on memory function in surgically menopausal women. Psychoneuroendocrinology *17*, 485-495.

Poon, L. W. (1985). Differences in human memory with aging: nature, causes, and clinical implications. In Handbook of the Psychology of Aging, J. E. Birren and K. W. Shaie,eds (New York: Van Nostrand Reinhold), pp. 427-462.

Press, G. A., Amaral.D.G., and Squire, L. R. (1989). Hippocampal abnormalities in the amnesic patients revealed by high-resolution magnetic resonance imaging. Nature *341*, 54-57.

Price, J. L., Davis, P. B., Morris, J. C., and White, D. L. (1991). The distribution of tangles, plaques and related immunohistochemical markers in healthy aging and Alzheimer's disease. Neurobiol. Aging *12*, 295-312.

Rao, A., and Steward, O. (1991). Evidence that protein constituents of postsynaptic membrane specializations are locally synthesized: Analysis of proteins synthesized within synaptosomes. J. Neurosci. *11*, 2881-2895.

Rapp, P. R., and Amaral, D. G. (1991). Recognition memory deficits in a subpopulation of aged monkeys resemble the effects of medial temporal lobe damage. Neurobiol. Aging *12*, 481-486.

Rapp, P. R., and Amaral, D. G. (1992). Individual differences in the cognitive and neurobiological consequences of normal aging. Trends Neurosci *15*, 340-545.

Reeves, T. M., and Smith, D. C. (1987). Reinnervation of the dentate gyrus and recovery of alternation behavior following entorhinal cortex lesions. Behav. Neurosci. *101*, 179-186.

Reeves, T. M., and Steward, O. (1988). Changes in the firing properties of neurons in the dentate gyrus with denervation and reinnervation: Implications for behavioral recovery. Exp. Neurol. *107*, 37-49.

Reinikainen, K. J., Koivisto, K., Mykkanen, L., Hanninen, T., Laakso, M., Pyorala, K., and Reinikainen, P. J. (1990). Age-associated memory impairment in aged population: an epidemiological study. Neurology *40 (Suppl. 1)*, 177.

Rosene, D., and Van Hoesen, G. W. (1987). The hippocampal formation of the primate brain: A review of some comparative aspects of cytoarchitecture and connections. In Cerebral Cortex - Volume 6: Further aspects of cortical function, including hippocampus, E. G. Jones and A. Peters, eds (New York: Plenum Press), pp. 345-456

Rowe, J., and Kahn, R. (1987). Human aging: usual and successful. Science *10*, 143-149.

Ruth, R. E., Collier, T. J., and Routtenberg, A. (1982). Topography between the entorhinal cortex and the dentate septotemporal axis in rats: I. Medial and intermediate entorhianl projecting cells. J. COmp. Neurol. *209*, 69-78.

Sato, K., Morimot, K., Hiramatsu, M., Mori, A., and Otsuki, S. (1989). Effect of a noncompetitive antagonist (MK-801) of NMDA receptors on convulsions and brain amino acid level in E1 mice. Neurochem. Res. *14*, 741-744.

Schaffner, A. E., and Daniels, M. P. (1982). Conditioned medium from cultures of embryonic neurons contains a high molecular weight factor which induces acetylcholine aggregation on cultured myotubules. J. Neurosci. *2*, 623-632.

Schauwecker, P. E., Cheng, H.-W., Serquinia, R. M. P., Mori, N., and McNeill, T. H. (1996). Lesion-induced sprouting of commissural/associational axons and induction of GAP-43 mRNA in hilar and CA3 pyramidal neurons in the hippocampus are diminished in aged rats. J. Neurosci. *15*, 2462-2470.

Scheff, S. W., Bernardo, L. S., and Cotman, C. W. (1978). Decrease in adrenergic axon sprouting in the senescent rat. Science *202*, 775-778.

Schuetze, S. M., and Role, L. W. (1987). Developmental regulation of nicotinic acetylcholine receptors. Annu. Rev. Neurosci. *10*, 403-457.

Seress, L., and Mrzljak, L. (1987). Basal dendrites of granule cells are normal fearutes of the fetal and adult dentate gyrus of both monkey and human hippocampal formations. Brain Res. *405*, 169-174.

Shatz, C. J. (1990). Impulse activity and the patterning of connections during CNS development. Neuron *5*, 745-756.

Siegel, S. J., Janssen, W. G., Gasic, G. P., Jahn, R., Heinemann, S. F., and Morrison, J. H. (1994). Regional, cellular and ultrastructural distribution of N-methyl-D-aspartate receptor subunit 1 in monkey hippocampus. Proc. Natl. Acad. Sci. USA *91*, 564-568.

Siegel, S. J., Janssen, W. G., Tullai, J. W., Rogers, S. W., Moran, T., Heinemann, S. F., and Morrison, J. H. (1995). Distribution of the excitatory amino acid receptor subunits GluR2(4) in monkey hippocampus and colocalization with subunits GluR5-7 and NMDAR1. J. Neurosci *15*, 2707-2719.

Singh, M., Meyer, E. M., Millard, W. J., and Simpkins, J. W. (1994). Ovarian steroid deprivation results in reversible learning impairment and compromised cholinergic function in female Sprague-Dawley rats. Brain Res. *644*, 305-312.

Skelton, R. W., and McNamara, R. K. (1992). Bilateral knife cuts to the perforant path disrupt spatial learning in the Morris water maze. Hippocampus *2*, 73-80.

Sommer, B., Keinanen, K., Verdoorn, T. A., Wisden, W., Burnashev, N., Herb, A., Kohler, M., Takagi, T., Sakmann, B., and Seeburg, P. H. (1990). Flip and flop: a cell-specific functional switch in glutamate-operated channels of the CNS. Science *249*, 1580-1585.

Steward, O. (1976). Topographic organization of the projections from the entorhinal area to the hippocampal formation of the rat. J. Comp. Neurol. *167*, 285-314.

Steward, O. (1983). Alterations in polyribosomes associated with dendritic spines during the reinnervation of the dentate gyrus of the adult rat. J. Neurosci. *3*, 177-178.

Steward, O., Cotman, C., and Lynch, G. (1976). A quantitative autoradiographic and electrophysiological study of the reinnervation of the dentate gyrus by the contralateral entorhinal cortex following ipsilateral entorhinal lesions. Brain Res. *114*, 181-200.

Steward, O., Cotman, C. W., and Lynch, G. (1974). Growth of a new fiber projection in the brain of the adult rat: Reinnervation of the dentate gyrus by the contralateral entorhinal cortex following ipsilateral entorhinal lesion. Exp. Brain Res. *20*, 45-66.

Steward, O., and Levy, W. B. (1982). Preferential localization of polyribosomes under the base of dendritic spines in granule cells of the dentate gyrus. J. Neurosci. *2*, 284-291.

Steward, O., and Reeves, T. M. (1988). Protein synthetic machinery beneath postsynaptic sites on CNS neurons; association between polyribosomes and other organelles at the synaptic site. J. Neurosci. *8*, 176-184.

Steward, O., and Vinsant, S. L. (1983). The process of reinnervation in the dentate gyrus of adult rats: A quantitative electron microscopic analysis of terminal proliferation and reactive synaptogenesis. J. Comp. Neurol. *214*, 370-386.

Steward, O., and Wallace, C. S. (1994). mRNA distribution within dendrites: relationship to afferent innervation. J. Neurobiol. *26*, 447-458.

Sucher, N. J., Brose, N., Dietcher, D. L., Awobuluyi, M., Gassic, G. P., Bading, H., Cepko, C. L., Greenberg, M. E., Jahn, R., Heinemann, S. F., and Lipton, S. A. (1993). Expression of endogenous NMDAR1 transcripts without receptor protein suggests post-transcriptional control in PC12 cells. J. Biol. Chem. *30*, 22299-22304.

Sugiyama, H., Ito, I., and Hirono, C. (1987). A new type of glutamte receptor linked to inositol phospholipid matabolism. Nature *325*, 531-533.

Tamura, M., Yoned, Y., Ogita, K., Shimizu, J., and Nagata, Y. (1991). Age-related decreases of the N-methyl-D-apartate receptor complex in the rat cerebral cortex and hippocampus. Brain Res. *542*, 83-90.

Terasawa, E., and Timiras, P. S. (1968). Electrical activity during the estrous cycle of the rat: cyclic changes in limbic structures. Endocrinology *83*, 203-216.

Thomas, K. L., Davis, S., Laroche, S., and Hunt, S. P. (1994a). Regulation of the expression of NRI NMDA glutamate receptor subunits during hippocampal LTP. NeuroReport *6*, 119-123.

Thomas, K. L., Laroche, S., Errington, M. L., Bliss, T. V. P., and Hunt, S. P. (1994b). Spatial and temporal changes in signal transduction pathways during LTP. Neuron *13*, 737-745.

Tigges, J., Herndon, J. G., and Rosene, D. L. (1995). Mild age-related changes in the dentate gyrus of adult rhesus monkeys. Acta. Anat. *153*, 39-48.

Torre, E. R., and Steward, O. (1992). Demonstration of local protein synthesis within dendrites using a new cell culture system that permits the isolation of living axons and dendrites from their cell bodies. J. Neurosci *12*, 762-772.

Torre, E. R., and Steward, O. (1996). Protein synthesis within dendrites: Glycosylation of newly synthesized proteins in dendrites of hippocampal neurons in culture. J. Neurosci. In press.

Trevisan, L., Fitzgerald, L. W., Brose, N., Gasic, G. P., Heinemann, S. F., Duman, R. S., and Nestler, E. J. (1994). Chronic ingestion of ethanol up-regulates NMDAR1 receptor subunit immunoreactivity in rat hippocampus. J. Neurochem. *62*, 1635-1638.

Trudeau, L.-E., and Castellucci, V. F. (1995). Postsynaptic modifications in long-term facilitation in Aplysia: Upregulation of excitatory amino acid receptors. J. Neurosci. *15*, 1275-1284.

Ulas, J., Monagahn, D. T., and Cotman, C. W. (1990). Plastic response of hippocampal excitatory amino acid receptors to deafferentation and reinnervation. Neuroscience *34*, 9-17.

Van Hoesen, G. W., and Hyman, B. T. (1990). Hippocampal formation: anatomy and patterns of pathology in Alzheimer's disease. Prog. Brain Res. *83*, 445-457.

Vnek, N., Gleason, T. C., Kromer, L. F., and Rothblat, L. A. (1995). Entorhinal-hippocampal connections and object memory in the rat: Acquisition versus retention. J. Neurosci. *15*, 3193-3199.

Weiland, N. G. (1992). Estradiol selectively regulates agonist binding sites on the N-methyl-D-aspartate receptor complex in the CA1 region of the hippocampus. Endocrinology *131*, 662-668.

Weiland, N. G., Orikasa, C., Hayashi, S., and McEwen, B. S. (1996). Localization of estrogen receptors in the hippocampus of male and female rats. Soc. Neurosci. Abs. *In Press*,

Wenk, G. W., and Walker, L. C. (1991). Loss of NMDA, but not GABA-A, binding in the brains of aged rats and monkeys. Neurobiol. Aging *12*, 93-98.

Wenthold, R. J., Yokatani, N., Doi, K., and Wada, K. (1992). Immunochemical characterization of the non-NMDA glutamate receptor using subunit-specific antibodies. J. Biol. Chem. *267*, 501-507.

West, M. J. (1993). Regionally specific loss of neurons in the aged human hippocampus. Neurobiol. Aging *14*, 287-293.

West, M. J., Amaral, D. J., and Rapp, P. R. (1993). Preserved hippocampal cell number in aged monkeys with recognition memory deficits. Soc. Neurosci. Abstr. *19*, 599.

Wiedenmann, B., and Franke, W. W. (1985). Identification and localization of synaptophysin, an integral membrane glycoprotein of M_r 38,000 characteristic of presynaptic vesicles. Cell *41*, 1017-1028.

Williams, K., Dichter, M. A., and Molinoff, P. B. (1992). Up-regulation of N-methyl-D-aspartate receptors on cultured cortical neurons after exposure to antagonists. Mol. Pharmacol. *42*, 147-151.

Witter, M. (1989). Connectivity of the rat hippocampus. In The Hippocampus-New Vistas, (New York: Alan R. Liss), pp. 53-69.

Witter, M. P., and Amaral, D. G. (1991). Entorhinal cortex of the monkey: V. Projections to the dentate gyrus, hippocampus, and subicular complex. J Comp Neurol *307*, 437-459.

Witter, M. P., and Groenewegen, H. J. (1984). Laminar oragin and septotemporal distribution of entorhinal and perirhianl projections to the hippocampus in the cat. J. Comp Neurol. *224*, 371-385.

Witter, M. P., Van Hoesen, G. W., and Amaral, D. G. (1989). Topographical organization of the entorhinal projection to the dentate gyrus of the monkey. J. Neurosci. *9*, 216-228.

Wong, M., and Moss, R. L. (1992). Long-term and short-term electrophysiological effects of estrogen on the synaptic properties of hippocampal CA1 neurons. J. Neurosci. *12*, 3217-3225.

Wong-Riley, M. T. T. (1979). Changes in the visual system of monocularly sutured or enucleated kittens demonstrable with cytochrome oxidase histochemistry. Brain Res. *171*, 11-28.

Woolley, C. S., and McEwen (1993). Roles of estradiol and progesterone in regulation of hippocampal dendritic spine density during the estrous cycle in the rat. J. Comp. Neurol. *336*, 293-306.

Woolley, C. S., and McEwen, B. S. (1992). Estradiol mediates fluctuations in hippocampal synapse density during the estrous cycle in the adult rat. J. Neurosci. *12*, 2549-2554.

Woolley, C. S., and McEwen, B. S. (1994). Estradiol regulates hippocampal dendritic spine density via and N-methyl-D- aspartate receptor-dependent mechanism. J. Neurosci. *14*, 7680-7687.

Woolley, C. W., Gould, E., Frankfurt, M., and McEwen, B. S. (1990). Naturally occurring fluctuations in dendritic spine density on adult hippocampal pyramidal neurons. J. Neurosci. *10*, 4035-4039.

Zimmer, J. (1973). Extended commissural and ipsilateral projections in postnatally deentorhinated hippocampus and fascia dentata demonstrated in rats by silver impregnation. Brain Res. *64*, 293-311.

Zola, M. S., Squire, L. R., and Amaral, D. G. (1986). Human amnesia and the medial temporal lobe region: enduring memory impairment following a bilateral lesion limited to the field CA1 of the hippocampus. J. Neurosci. *6*, 2950-2967.

Zola, M. S., Squire, L. R., and Amaral, D. G. (1989). Lesions of the hippocampal formation but not lesions of the fornix or the mamillary nuclei produce long-lasting memory impairment in monkeys. J. Neurosci. *9*, 898-913.

Zola, M. S., Squire, L. R., Rempel, N. L., Clower, R. P., and Amaral, D. G. (1992). Enduring memory impairment in monkeys after ischemic damage to the hippocampus. J. Neurosci. *12*, 2582-2596.

Zukin, R. S., and Bennett, M. V. L. (1995). Alternatively spliced isoforms of the NMDAR1 receptor subunit. Trends Neurosci. *18*, 306-316.